DISTRIBUTION AND CONTAMINATION ASSESSMENT OF SELECTED HEAVY METALS AND RARE EARTH ELEMENTS IN SOIL OF PENANG ISLAND, MALAYSIA

FATIMAH AZ ZAHRA' BT ABDUL HAMID

FACULTY OF SCIENCE
UNIVERSITY OF MALAYA
KUALA LUMPUR

2018

DISTRIBUTION AND CONTAMINATION ASSESSMENT OF SELECTED HEAVY METALS AND RARE EARTH ELEMENTS IN SOIL OF PENANG ISLAND, MALAYSIA

FATIMAH AZ ZAHRA' BT ABDUL HAMID

DISSERTATION SUBMITTED IN FULFILMENT OF THE REQUIREMENTS FOR THE DEGREE OF MASTER OF SCIENCE

DEPARTMENT OF GEOLOGY
FACULTY OF SCIENCE
UNIVERSITY OF MALAYA
KUALA LUMPUR

2018

UNIVERSITY OF MALAYA

ORIGINAL LITERARY WORK DECLARATION

Name of Candidate: FATIMAH AZ ZAHRA' BT ABDUL HAMID

Matric No: SGR 150068

Name of Degree: Master of Science

Title of Project Paper/Research Report/Dissertation/Thesis ("this Work"):

DISTRIBUTION AND CONTAMINATION ASSESSMENT OF SELECTED HEAVY METALS AND RARE EARTH ELEMENTS IN SOIL OF PENANG ISLAND, MALAYSIA

Field of Study: Applied Geology

I do solemnly and sincerely declare that:

(1) I am the sole author/writer of this Work;
(2) This Work is original;
(3) Any use of any work in which copyright exists was done by way of fair dealing and for permitted purposes and any excerpt or extract from, or reference to or reproduction of any copyright work has been disclosed expressly and sufficiently and the title of the Work and its authorship have been acknowledged in this Work;
(4) I do not have any actual knowledge nor do I ought reasonably to know that the making of this work constitutes an infringement of any copyright work;
(5) I hereby assign all and every rights in the copyright to this Work to the University of Malaya ("UM"), who henceforth shall be owner of the copyright in this Work and that any reproduction or use in any form or by any means whatsoever is prohibited without the written consent of UM having been first had and obtained;
(6) I am fully aware that if in the course of making this Work I have infringed any copyright whether intentionally or otherwise, I may be subject to legal action or any other action as may be determined by UM.

Candidate's Signature Date:

Subscribed and solemnly declared before,

Witness's Signature Date:

Name:

Designation:

Witness's Signature Date:

Name:

Designation:

DISTRIBUTION AND CONTAMINATION ASSESSMENT OF SELECTED HEAVY METALS AND RARE EARTH ELEMENTS IN SOIL OF PENANG ISLAND, MALAYSIA

ABSTRACT

This study focused on the distribution and contamination assessment of selected heavy metals and rare earth elements (REE) in top soil of Penang Island. Four heavy metals (As, Pb, Cd and Ni) and seven REE (La, Ce, Nd, Eu, Tb, Dy and Er) have been analysed in 31 soil samples using Inductively Coupled Plasma-Mass Spectrometry (ICP-MS). The descending order of highest mean concentration of these elements was Pb > As > Ce > La > Nd > Ni > Dy > Er > Tb > Cd > Eu. Results of heavy metal concentrations showed that As content ranged from 67.9 to 2942.1 mg/Kg with mean value of 366.6 mg/Kg, Pb content ranged from 42.1 to 7019.6 mg/Kg with mean value of 422.9 mg/Kg, Ni content ranged from 6.5 mg/Kg to 1049.2 mg/Kg with mean value of 51.7 mg/Kg and Cd content ranged from 0.2 to 16.7 mg/Kg with mean value of 1.6 mg/Kg. REE concentration results showed that La content ranged from 34.0 to 218.9 mg/Kg with mean value of 82.1 mg/Kg, Ce content ranged from 70.1 to 602.3 mg/Kg with mean value of 191.2 mg/Kg, Nd content ranged from 28.8 to 201.9 mg/Kg with mean value of 72.9 mg/Kg, Eu content ranged from 0.14 to 5.86 mg/Kg with mean value of 1.16 mg/Kg, Tb content ranged from 0.77 to 6.23 mg/Kg with mean value of 2.01 mg/Kg, Dy content ranged from 3.12 to 24.20 mg/Kg with mean value of 8.57 mg/Kg and Er content ranged from 0.99 to 12.63 mg/Kg with mean value of 4.16 mg/Kg. In spatial distribution analysis, George Town, Batu Ferringhi, Jelutong and Bandar Air Itam were identified as high concentration areas of heavy metals whereas Teluk Bahang, Bandar Air Itam, George Town and Balik Pulau were identified as high concentration areas of REE. In contamination level assessment, Bandar Air Itam, George Town, Batu Ferringhi, Jelutong, Teluk Bahang, Tanjung Bunga and Balik Pulau

were determined as high CF, I_{geo} and CI value of heavy metals and REE. The result of statistical analysis represented that the relationship among heavy metals was showed by Pb and Cd whereas the relationships among REE were represented by division of LREE and HREE. Between heavy metals and REE, the relationships were represented by As with Eu and Tb. The relationships between heavy metals and REE with soil physicochemical properties were represented by Cd and OM with positive correlation and, Nd and OM with negative correlation.

Keywords: heavy metals, REE, soil, Penang Island.

TABURAN DAN PENILAIAN PENCEMARAN BAGI UNSUR LOGAM BERAT DAN UNSUR NADIR BUMI TERTENTU DALAM TANAH DI PULAU PINANG, MALAYSIA

ABSTRAK

Kajian ini telah difokuskan kepada taburan dan penilaian pencemaran bagi unsur logam berat dan unsur nadir bumi tertentu dalam bahagian atas tanah di Pulau Pinang. Empat unsur logam berat (As, Pb, Cd dan Ni) dan tujuh unsur nadir bumi, (La, Ce, Nd, Eu, Tb, Dy and Er) telah dipilih untuk dianalisa kadar konsentrasinya di dalam 31 sampel tanah dengan menggunakan Plasma Ganding Induktif-Spektrofotometer (ICP-MS). Turutan purata tertinggi bagi kadar konsentrasi unsur logam berat dan unsur nadir bumi adalah Pb > As > Ce > La > Nd > Ni > Dy > Er > Tb > Cd > Eu. Keputusan kadar konsentrasi logam berat menunjukkan bahawa kandungan As menunjukkan julat antara 67.9 hingga 2942.1 mg/Kg dengan purata 366.6 mg/Kg, kandungan Pb menunjukkan julat antara 42.1 hingga 7019.6 mg/Kg dengan purata 422.9 mg/Kg, kandungan Ni menunjukkan julat antara 6.5 mg/Kg hingga 1049.2 mg/Kg dengan purata 51.7 mg/Kg dan kandungan Cd menunjukkan julat antara 0.2 hingga 16.7 mg/Kg dengan purata 1.6 mg/Kg. Keputusan kadar konsentrasi REE menunjukkan bahawa kandungan La menunjukkan julat antara 34.0 hingga 218.9 mg/Kg dengan purata 82.1 mg/Kg, kandungan Ce menunjukkan julat antara 70.1 hingga 602.3 mg/Kg dengan purata 191.2 mg/Kg, kandungan Nd menunjukkan julat antara 28.8 hingga 201.9 mg/Kg dengan purata 72.9 mg/Kg, kandungan Eu menunjukkan julat antara 0.14 hingga 5.86 mg/Kg dengan purata 1.16 mg/Kg, kandungan Tb menunjukkan julat antara 0.77 hingga 6.23 mg/Kg dengan purata 2.01 mg/Kg, kandungan Dy menunjukkan julat antara 3.12 hingga 24.20 mg/Kg dengan nilai purata 8.57 mg/Kg dan Er menunjukkan julat antara 0.99 hingga 12.63 mg/Kg dengan nilai purata 4.16 mg/Kg. Dalam analisa taburan spasial, George Town, Batu Ferringhi, Jelutong dan Bandar Air Itam telah dikenal pasti sebagai kawasan yang

mempunyai konsentrasi unsur logam berat yang tinggi manakala Teluk Bahang, Bandar Air Itam, George Town dan Balik Pulau telah dikenal pasti sebagai kawasan yang mempunyai konsentrasi unsur nadir bumi yang tinggi. Dalam penilaian tahap pencemaran, Bandar Air Itam, George Town, Batu Ferringhi, Jelutong, Teluk Bahang, Tanjung Bunga and Balik Pulau telah dikenal pasti sebagai nilai CF, I_{geo} dan CI yang tinggi bagi unsur logam berat dan unsur nadir bumi. Keputusan analisa statistik telah menunjukkan bahawa perhubungan antara unsur logam berat telah ditunjukkan oleh Pb dan Cd manakala perhubungan antara unsur nadir bumi telah ditunjukkan dengan pembahagian antara kumpulan unsur nadir bumi ringan dan kumpulan unsur nadir bumi berat. Antara unsur logam berat dan unsur nadir bumi, perhubungan telah ditunjukkan oleh As dengan Eu dan Tb. Perhubungan antara unsur logam berat dan unsur nadir bumi dengan ciri fizik kimia tanah telah ditunjukkan oleh Cd dan OM dengan perhubungan positif dan, Nd dan OM dengan perhubungan negatif.

Kata kunci: Unsur logam berat, unsur nadir bumi, tanah, Pulau Pinang.

ACKNOWLEDGEMENTS

Alhamdulillah, praise be to Allah for His Benevolence made it possible for me to complete my research. My deepest appreciation to both my supervisors, Dr. Ahmad Farid bin Abu Bakar and Dr. Ng Tham Fatt, for their vital support and encouragements, words could not express how their guidance and sharing of valueable experiences helped me throughout my studies.

I would like to thank everyone whom had always given support and du'a during my studies especially my beloved husband, Abdul Latif bin Saad and my beloved parents, Abdul Hamid bin Sulaiman and Faridah Zainal. A big thank you to Shuhada Md. Rifin, whom had supported me with great advice when I first started this journey.

Finally, I would like to acknowledge and extent my heartfelt gratitude to everyone who helped me throughout my research especially Prof. Dr. Azman Bin Abd Ghani, Allahyarham Dr. Mohamad Tarmizi Bin Mohamad Zulkifley, Mr. Mat Nazri Mat Nasir, Mr. Zaharudin Md Salleh, Mr. Zamrut Daunar, Miss. Nusyahira Ismail, Mr. Shahrom Said, Mr. Saharuddin Zainal, Azlan Shah Nerwan Shah, Long Xiang Quek, Muhammad Hatta Roselee, Galih Yudha, Mohd Amiruddin Amran, Mohd Zulfadhlie Fithol and my fellow RA collegues. Thank you very much.

TABLE OF CONTENTS

LIST OF FIGURES

LIST OF TABLES

LIST OF SYMBOLS AND ABBREVIATIONS

Al	:	Aluminium
As	:	Arsenic
B_i	:	Background values
Cd	:	Cadmium
Ce	:	Cerium
CEC	:	Cation Exchange Capacity
CF	:	Contamination Factor
CI	:	Contamination index
cm	:	centimetre
°C	:	Degree Centigrade
Dy	:	Dysprosium
E	:	East
Eu	:	Europium
Er	:	Erbium
Fe	:	Ferum
FOREGS	:	Forum of European Geological Surveys
g	:	gram
g/cm^3	:	gram per cubic centimetre
GPS	:	Global Positioning System
HREE	:	Heavy Rare Earth Elements
I_{geo}	:	Geo-accumulation index
ICP-MS	:	Inductively Coupled Plasma Mass Spectrometry
km^2	:	square kilometre
La	:	Lanthanum

LOI	:	Loss on ignition
LREE	:	Light Rare Earth Elements
m^2	:	square metre
MAD	:	Median Absolute Deviation
meq/g	:	milliequivalents per gram
mg/Kg	:	milligram per kilogram
mg/ml	:	milligram per milliliter
ml	:	milliliter
mm	:	millimetre
Mn	:	Manganese
µm	:	micrometre
N	:	North
Nd	:	Neodymium
Ni	:	Nickel
OM	:	Organic Matter
PLI	:	Pollution load index
Pb	:	Lead
PCA	:	Principal component analysis
pH	:	Power of hydrogen
ppb	:	parts per billion
ppm	:	parts per million
REE	:	Rare Earth Elements
Tb	:	Terbium
USDA	:	United States Department of Agriculture

LIST OF APPENDICES

CHAPTER 1: INTRODUCTION

1.1 Introduction

Massive urbanisation and development in many places throughout the world have led to changes of the natural environment including the element concentrations in soils (Mirsal, 2008; Meuser, 2010). Many studies showed that the contamination of heavy metals in soil of urban areas are related to various human activities (Birke & Rauch, 2000; Zhengyu et al., 2006; Wei & Yang, 2010; Brioschi et al., 2013; Zong et al., 2016; Nannoni & Protano, 2016; Gulan et al., 2017; Ungureanu et al., 2016). However, the study of rare earth elements (REE) contamination in soil of urban areas is still new as compared to the study of heavy metal contamination, but it had been revealed in some studies (Kabata-Pendias & Mukherjee, 2007; Figueiredo et al., 2009; Brioschi et al., 2013; Ramos et al., 2016).

Soil is generally described as unconsolidated body of mineral and organic constituent produced by weathering of solid material, and become the habitat for many organisms and living medium for plants (Mirsal, 2008). Soil is originated from physical and chemical breakdown of solid rock by weathering processes (Skinner et al., 2004). Soil texture can be classified according to proportions of different size of particles which influence the soil ability to retain and transmit water and air (Tarbuck & Lutgens, 2009). Soil contains abundant of trace elements which can be derived from lithogenic and anthropogenic sources (Kabata-Pendias & Mukherjee, 2007). The lithogenic source of trace elements can be derived from various types of parent materials whereas the anthropogenic source of trace elements is mainly derived from human activities which emit the trace elements into the soil (Kabata-Pendias & Mukherjee, 2007). The anthropogenic changes such as cut and fill can affect the bedrock and parent materials and may increase the level of certain trace elements in the soil. Deposition of dust from industries in dry condition also can contributes to the increasing of contamination level

of elements in the soils due to suspension of the particulate matter on the top soil (Meuser, 2010).

Heavy metal is a group of metals and metalloids that has relatively high atomic mass (> 5 g/cm^3) (Alloway, 2013). The examples of heavy metal elements are arsenic (As), cadmium (Cd), chromium (Cr), cobalt (Co), copper (Cu), mercury (Hg), lead (Pb), manganese (Mn), nickel (Ni), selenium (Se), zinc (Zn), antimony (Sb), barium (Ba), gold (Au), molybdenum (Mo), silver (Ag), thallium (Tl), tin (Sn), tungsten (W), uranium (U) and vanadium (V) (Alloway, 2013). The examples of parent rocks that contain high heavy metals content are black shales, limestones, phosphorites, ultramafic rocks, sedimentary ironstones and metalliferous ores (Alloway, 2013). Some heavy metals may give many benefits to other organisms. For example, the importance of cobalt, chromium, copper, iron, potassium, magnesium, manganese, sodium, nickel and zinc when in appropriate concentrations, they become micronutrients in several vital processes such as redox-processes, stabilization of molecules through electrostatic interactions, acting as components of various enzymes and regulation of osmotic pressure (Mirsal, 2008).

The unnecessary heavy metals such as silver (Ag), cadmium (Cd), gold (Au), lead (Pb) and mercury (Hg) are non-beneficial in biological needs and harmful to organism (Bruins et al., 2000). Heavy metals may impact human health when they exceed a certain threshold (Sherameti & Varma, 2010). Heavy metals are also cannot be degraded or destroyed and they might become toxic and poisonous even at low concentration (Berkowitz et al., 2008). Several diseases could be affected from high heavy metals consume such as cell membranes damage, alteration of enzyme specificity, cellular function disruption and damage of the DNA structure (Bruins et al., 2000).

REE, another potentially harmful elements, are become highly demanded nowadays, in the making of most technology equipments as these elements are used to have unique physical and chemical properties (Ramos et al., 2016). Recently, China is the major REE supplier in the world which produces nearly 90 % of global REE supply (Wubbeke, 2015). There are 17 elements in REE group such as scandium (Sc), yttrium (Y), lanthanum (La), cerium (Ce), praseodymium (Pr), neodymium (Nd), promethium (Pm), samarium (Sm), europium (Eu), gadolinium (Gd), terbium (Tb), dysprosium (Dy), holmium (Ho), erbium (Er), thulium (Tm), ytterbium (Yb) and lutetium (Lu). REE have very small differences in solubility and can be derived naturally from minerals (Voncken, 2016). REE can be divided into two groups which are light rare earth element (LREE) and heavy rare earth element (HREE). The elements of LREE are La, Ce, Pr, Nd, Pm, Sm and Eu and the rest are classified under HREE (Zhengyi et al., 2006). Granite is one of parent rocks that contains highest REE concentrations, followed by basalt and sandstone (Ramos et al., 2016).

Like heavy metals, REE are also hazardous to human health. In study of toxicological evaluations of REE by Korea occupational safety and health, workers that have been exposed to low-dose REE in long term are potentially accumulating REE in their bone structure, bone tissue impact and increase of bone marrow micronucleus (MN) rate (Kyung et al., 2013).

1.2 Problem statement

Heavy metals and REE are harmful elements to human and ecosystem when they exceed a certain level (Sherameti & Varma, 2010; Brioschi et al., 2013; Ramos et al., 2016). Heavy metals are very useful tracers of environmental pollution especially in urban areas (Manta et al., 2002). Study of REE pollution in urban environment become concern nowadays as the use of REE become increasingly worldwide (Brioschi et al., 2013; Ramos et al., 2016). Heavy metals and REE pollutants in the soil may retained

within the soil body and transported by soil solution, or undergo alteration, transformation and initiation of chemical changes within the soil (Mirsal, 2008).

Penang Island is a rapid urbanization area in Peninsular Malaysia that may exposed to various human activities such as industrialization, traffic emissions and agricultural activities where the soil in this area could be polluted with heavy metals and REE. Development of Penang Island had started since the end of 18th century (Shamsuddin et al., 2012). Many reports have revealed the contamination of heavy metals and REE in urban soils (Wong et al., 2006; Zhengyu et al., 2006; Rogan Šmuc et al., 2012; Brioschi et al., 2013; Cidu et al., 2013; Zong et al., 2016; Nannoni & Protano, 2016; Gulan et al., 2017). According to Meuser (2010), the accumulation of contaminants could increase in top soils gradually. Due to continuous urbanization in development area, the soils may continuously receive a significant amount of pollutants from anthropogenic sources (Birke & Rauch, 2000; Wei & Yang, 2010).

In this study, four potentially harmful heavy metals were selected for analysis. Arsenic (As), lead (Pb), nickel (Ni) and cadmium (Cd) were among the hazardous chemical elements which can contaminate urban soils (Birke & Rauch, 2000; Zhengyu et al., 2006; Wei & Yang, 2010; Lu & Bai, 2010; Simasuwannarong et al., 2012; Brioschi et al., 2013; Zong et al., 2016; Nannoni & Protano, 2016; Ungureanu et al., 2016; Gulan et al., 2017; Mehr et al., 2017). In urban areas, common anthropogenic sources of As can be dust from ores smelting, pesticides manufacturing, coal combustion, geothermal power plants, sulphide ore roasting and smelting, wood preserving agents, and pig and poultry sewage (Kabata-Pendias & Mukherjee, 2007; Buttafuoco et al., 2016). The common anthropogenic sources of Pb in urban areas are industrial emissions, high-temperature processes in smelters, lead-acid batteries, previously used leaded petrol, erosion and chemical weathering of tailings in mining areas (Simasuwannarong et al., 2012; Ağca, 2015). Nickel contamination in urban soil

can be sourced from thermal power plant, metal processing operation, combustion of coal and oil, sewage sludges, phosphate fertilizers and municipal sludges (Alloway, 2013; Özkul, 2016). Contamination of Cd in urban soil can be originated from the use of phosphate fertilizers, a by-product in mining and refining of zinc (Zn), battery production, stabilizers for various plastics and traffic emissions (Hamzeh et al., 2011; Ağca, 2015; Huang et al., 2018).

Seven potentially harmful REE were selected for analysis in this study. Lanthanum (La), cerium (Ce), neodymium (Nd), europium (Eu), terbium (Tb), dysprosium (Dy) and erbium (Er) are among REE that could potentially contaminate urban soils (Kabata-Pendias & Mukherjee, 2007; Figueiredo et al., 2009; Brioschi et al., 2013; Sadeghi et al., 2013; Ramos et al., 2016; Yuan et al., 2017). Lanthanum, Ce, Nd, Eu and Tb are among the worldwide contents of REE reported for major phosphate fertilizers and other particular agricultural inputs (Ramos et al., 2016). The example of agricultural products that containing La, Ce, Nd, Eu and Tb is thermophosphate, phosphoric acid and apatite concentrate (Ramos et al., 2016). High amount of La, Ce, Nd, Eu, Tb, Dy and Er are also can be found in sewage sludge and manure (Kabata-Pendias & Mukherjee, 2007). In industry, La, Ce, Ne, Eu, Tb, Dy and Er are elements that commonly used in glass production, sophisticated electronic devices, catalytic converters, metallic alloys, rechargeable batteries and radars (Kabata-Pendias & Mukherjee, 2007).

1.3 Objectives

The objectives of this research are to:

- Identify concentration levels of four selected heavy metals, As, Pb, Ni and Cd and, seven selected REE, La, Ce, Nd, Eu, Tb, Dy and Er in top soils of Penang Island.
- Analyse spatial distribution of selected heavy metals and REE in the top soils of Penang Island.

- Assess the contamination level of selected heavy metals and REE in top soils of Penang Island.
- Identify the relationship between selected heavy metals, selected REE and the physicochemical properties of top soil samples through statistical analysis.

1.4 Outline of the thesis

This dissertation consists of five chapters and represented as follows:

Chapter 1 describes the details about the research including the problem statement and objectives. The problem statement highlights the importance of this research. The objectives used to explain the aim of this research.

Chapter 2 reviews about heavy metals and REE distribution assessments in other urban areas.

Chapter 3 describes the methodology and materials applied in this research. This chapter also explains how this research was developed. The methodologies were applied according to the standard methods.

Chapter 4 describes the results and the interpretation from the analysis. The concentration level of selected heavy metals and REE were compared with other studies. The high concentration areas of selected heavy metals and REE were identified from the generated spatial distribution maps and prediction of contamination source from type of land use and geology of the area. Contamination level assessments of selected heavy metals and REE in the top soils of Penang Island were done and compared between each other. The relationships between heavy metals, REE and soil physicochemical properties were determined from statistical analysis and compared with previous studies.

Chapter 5 concludes all of the research outcomes.

CHAPTER 2: LITERATURE REVIEW

2.1 Introduction

This chapter summarises and discusses published work and reports by scholars and researchers related to the research. The review includes the methods to investigate and evaluate the distribution of elements in soils in other study areas, analyses that have been applied and their results.

2.2 Studies of heavy metals and REE in Malaysia and regional areas.

There are inadequacy studies of heavy metals and REE distributions in urban soils in Malaysia and the regional areas. Many studies had used different type of sample media in their analysis such as sediment, river soil and river water. In Penang Island, no any evidence of study of heavy metals and REE distributions in top soils was found. Example of the study of heavy metals in Penang Island was represented by Ong et al. (2016) which surface sediments of Penang river estuary was used as media examined. Another studies of heavy metals in Penang Island used river water for analysis (Mohd Saad et al., 2000; Lim et al., 2017).

In Malaysia, except in Penang Island, only one study of heavy metals in urban soil was found which in Perlis, Malaysia (Mat Ripin et al., 2014). Many studies of heavy metals and REE in Malaysia were use sediment, river soil and river water as sample examined. For example, study of Cu, Pb and Zn in sediments of Ibai Estuary, Kuala Terengganu (Noor Azhar et al., 2003), study of heavy metal in tropical microtidal river in Chukai-Kemaman river, Terengganu (Kamaruzzaman et al., 2002), study of heavy metals in surfical sediment in Setiu Lagoon, Terengganu (Ong et al., 2009), study of heavy metals in mangrove sediment in Bebar, Pahang (Kamaruzzaman et al., 2004), study of heavy metals in surface sediment in Tanjung Lumpur mangrove forest, Kuantan (Kamaruzzaman et al., 2011), heavy metal distribution in surface sediment of exclusive economic zone of east cost of Peninsular Malaysia (Shaari et al., 2015), study

of heavy metals in surface sediment in Bidong Island, east coast of Peninsular Malaysia (Ong et al., 2015), study of REE in rocky shore ecosystem at West Coast of Peninsular Malaysia (Kamaruzzaman et al., 2017), study of REE in sediment of ex-mining area (Masood Khan et al., 2017) and study of REE in sediment, soil and surface water of Terengganu River Basin (Sultan & Noor Azhar, 2009).

In regional area, a heavy metals distribution study in soil and sediment samples of industrial, residential and nature reserve areas in Singapore was found to be outdated (Zhou et al., 1997). Another study of heavy metals in Singapore was done in marine sediments sample (Goh & Chou, 1997). In Thailand, many studies of heavy metals distribution in soil were focused on the agriculture land and river sediment instead of urban area. For example, study of heavy metals in agriculture soil in Thailand (Zarcinas et al., 2004), study of heavy metals contamination in soil from paddy fields in north and west of Bangkok (Chinoim & Sinbuathong, 2010) and study of heavy metals contamination in sediment of Chao Phraya River estuary (Polprasert, 1982). In Indonesia, many studies of heavy metals were concerned on agriculture area and sediment. For example, study of heavy metals content in cocoa plantation soil in East Kolaka (Arham et al., 2017) and study of heavy metals in coastal marine sediment (Arifin et al., 2012). Many studies of REE in Thailand had focused on the agriculture areas and rocks. For instance, study of REE in paddy soils from the central region of the Mekong River (Egashira et al., 1997) and study of REE geochemistry of Southern Thailand granites (Wu & Ishihara, 1994). In Indonesia, a study of REE found related to the geochemistry of the granitic rocks in Sulawesi Island (Maulana et al., 2014).

Table 2.1: Studies of heavy metals and REE in Malaysia and regional areas.

Study area	Research title	Finding	Reference
Penang	Distribution of Heavy Metals and Rare Earth Elements in the Surface Sediments of Penang River Estuary, Malaysia	• Sediment size showed a positive correlation with REE and Mn.	Ong et al. (2016)

Table 2.1, continued

Study area	Research title	Finding	Reference
Penang, Malaysia	Distribution of Heavy Metals and Rare Earth Elements in the Surface Sediments of Penang River Estuary, Malaysia	• Enrichment factor and geoaccumulation index showed that most of the elemental sources were natural especially REE. • Pollution load index revealed the higher levels of Cr, Cd, Zn and Pb indicating anthropogenic sources.	Ong et al. (2016)
Penang, Malaysia	Identification of pollution sources within the Sungai Pinang river basin	• Water quality of Sungai Pinang River Basin classified as very polluted.	Mohd Saad et al. (2000)
Penang Island, Malaysia	Characteristics of water quality of rivers related to land-use in Penang Island, Malaysia.	• Results show that total organic carbon (TOC) increases generally as the rivers flow towards the river mouths. • Characteristics of water quality in Penang Island are highly affected by land-use surrounding the rivers.	Lim et al. (2017)
Perlis, Malaysia	Analysis and pollution assessment of heavy metal in soil, Perlis.	• Concentration of Cu, Cr, Ni, Cd and Pb in the soil samples ranged from 0.38 to 240.59, 0.642 to 3.921, 0.689 to 2.398, 0-0.63 and 0.39 to 27.47 mg/Kg respectively. • Decreasing trend of concentration: Cu>Pb>Cr>Ni>Cd.	Mat Ripin et al. (2014)
Terengganu, Malaysia	Study on the distribution of some heavy metals and pollution status of a tropical microtidal river: the Chukai-Kemaman River, Terengganu, Malaysia.	Concentration levels of Co, Mn and Cu in Chukai river and Fe, Ni, Cr, Ti, Zn and Cu in Kemaman river in surface sediment showed no evidence of recent anthropogenic input of metals.	Kamaruzzaman et al. (2002)
Setiu Lagoon, Terengganu, Malaysia	Geochemical studies of Setiu Lagoon, Terengganu, Malaysia	The concentration of Pb, Co and Cu at present is not widespread enough as to have much influence on pollution of that area.	Ong et al. (2009)

Table 2.1, continued

Study area	Research title	Finding	Reference
Hutan Paya Bakau Bebar, Pahang	Study of sediment accretion rate and concentration of selected heavy metals on the surface sediment in Hutan Paya Bakau Bebar, Pahang.	The elements Cr, Cu, Pb and Zn showed considerable spatial variation with a lower average concentration near the estuary and relatively higher concentration at the area away from the estuary.	Kamaruzzaman et al. (2004)
Tanjung Lumpur Mangrove Forest, Kuantan, Malaysia	Heavy metal concentration in the surface sediment of Tanjung Lumpur Mangrove Forest, Kuantan, Malaysia.	• Average concentrations of Pb, Cu, Co and Mn were 44.41 µg/g dry weight, 32.79 µg/g dry weight, 5.79 µg/g dry weight and 117.73 µg/g dry weight, respectively. • Co and Mn can be considered to have the terigeneous in sources while Pb and Cu are considered to have anthropogenic input.	Kamaruzzaman et al. (2011)
East coast of Peninsular Malaysia	Spatial distribution of selected heavy metalsin surface sediments of the EEZ of the east coast of Peninsular Malaysia.	• Results showed heavy metal concentrations ranged between 207.58 and 491.33 µg/g for Mn, 36.13 and 125.93 µg/g for Zn, 14.49 and 22.33 µg/g for Cu, 2.00 and 11.12 µg/g for Co, 6.20 and 8.95% for Fe, and 0.94 and 6.62% for Al. • Enrichment factor (EF) and geo-accumulation index results represented that the surface sediment trace metal levels in the study area might be enriched by anthropogenic sources.	Shaari et al. (2015)
Bidong Island, Malaysia	Heavy metals concentration in surficial sediments of Bidong Island, South China Sea off the East Coast of Peninsular Malaysia.	The geochemistry of the sediment of Bidong Island was influenced by both natural and anthropogenic inputs to the catchment.	Ong et al. (2015)
West Coast of Peninsular Malaysia	Rare earth elements behaviour at West Coast of Peninsular Malaysia rocky shore ecosystem using *Saccostrea Cucullata* as bioindicator.	Filter feeder *S. cucullata* is considered to be highly potential as a bioindicator for REEs. Results showed that the values are considerably below the safety limit, with the exception of Ce and Nd in the soft tissue of *S. cucullata*.	Kamaruzzaman et al. (2017)

Table 2.1, continued

Study area	Research title	Finding	Reference
Kinta River, Malaysia	Erratum to: assessing anthropogenic levels, speciation, and potential mobility of rare earth elements (REEs) in ex-tin mining area.	• The total concentration of REEs in the ex-mining lake water samples and sediments were found to be 3685 mg/l and 14159 mg/Kg, respectively. • Total concentration of REEs in Kinta River water sample was found to be 1224 mg/l. • Based on potential mobility, REEs could be released and subsequently pollute the environment.	Masood Khan et al. (2017)
Terengganu River Basin, Malaysia	Rare earth elements in tropical surface water, soil and sediments of the Terengganu River Basin, Malaysia.	• The REE patterns in sediments reflected the soil REE patterns with an overall order of abundance: LREE>>MREE>HREE. • The chondrite normalized REE patterns of river water carried strong signature of local geology.	Sultan & Noor Azhar (2009)
Singapore	Soil lead and other metal levels in industrial, residential and nature reserve areas in Singapore.	• Five measured metal loading on the surface soils was in the order: industrial area > residential area > nature reserve area. • The trace metal concentrations in surface soil from areas of heavy traffic are higher than residential areas. • Vehicular exhaust and industrial activities are the main source of metal pollution.	Zhou et al. (1997)
Singapore	Heavy metal levels in marine sediments of Singapore.	Levels of heavy metals in marine sediment was largely dependant on sediment particle size.	Goh & Chou (1997)
Thailand	Heavy metals in soils and crops in Southeast Asia. 2. Thailand	Results showed that concentrations of heavy metals varied widely among the different regions of Thailand.	Zarcinas et al. (2004)

Table 2.1, continued

Study area	Research title	Finding	Reference
Thailand	Heavy metal contamination of soils from organic paddy fields in Thailand. Paper presented at the 19th World Congress of Soil Science, Soil Solutions for a Changing World.	Heavy metal concentrations measured in the soil samples ranged from 0 to 0.0727 mg/Kg for Cd, 0 to 1.92 mg/Kg for Cr, 0.186 to 1.39 mg/Kg for Pb, 0.372 to 2.57 mg/Kg for Ni, 0.698 to 2.90 mg/Kg for Cu, and 0.987 to 14.4 mg/Kg for Zn.	Chinoim & Sinbuathong (2010)
Chao Phraya River estuary, Thailand	Heavy metal pollution in the Chao Phraya River estuary, Thailand.	Thai people may ingest Hg and Pb in fish in the Chao Phraya River estuary at quantities more than those reported for other countries.	Polprasert (1982)
East Kolaka, Indonesia	Heavy metal content of cocoa plantation soil in East Kolaka, Indonesia.	• The existence of Pb and Cd in plantation soil have been exceeded the WHO permissible. • Ni, Cu, and Zn is still within the permissible limits.	Arham et al. (2017)
Indonesia	Heavy metal contamination in Indonesian coastal marine ecosystems: a historical perspective.	• An elevated heavy metal contamination has been mostly recorded in the northern coast of Java Island and the eastern coast of Sumatra Island. • The concentration of heavy metals in water and biota is very low.	Arifin et al. (2012)
Mekong River, Laos	Rare earth element and clay minerals of paddy soils from the central region of the Mekong River, Laos.	REE as the chondrite-normalized curve of the plot of Ce/Eu against Eu/Sm were found to be useful for grouping soils according to their origins.	Egashira et al. (1997)
Thainland	REE geochemistry of the Southern Thailand granites.	Based on total REE concentration, granites of the area can be divided into three groups as follows: Group I, having low to intermediate REE contents; Group II, showing variable REE abundances; and Group III, possessing exceptionally high REE contents (500–700 ppm).	Wu & Ishihara (1994)
Sulawesi Island, Indonesia	Geochemistry of rare earth elements (REE) in the weathered crusts from the granitic rocks in Sulawesi Island, Indonesia.	Weathered profiles show that the total REE increased from the parent rocks to the horizon B but significantly decrease toward the upper part (horizon A).	Maulana et al. (2014)

2.3 Heavy metals concentration in urban soils

In study of heavy metals contamination in Perlis, Malaysia, 18 top soil samples were collected to analyse total concentration of Cu, Cr, Ni, Cd and Pb. The results showed that the descending order of highest mean concentration of heavy metals was Cu > Pb > Cr > Ni > Cd. The highest mean concentration of heavy metals was presented by Cu with the concentration ranges from 38 to 240.59 mg/Kg (Mat Ripin et al., 2014).

In Indonesia, 168 top soil samples were collected for study of Pb distribution in Yogyakarta City. The result showed that the concentration of Pb ranged from 16 to 95.20 mg/Kg with mean value of 65.4 mg/Kg (Budianta, 2012).

In a study of heavy metals distribution in 83 top soil samples of Isfahan Province, Iran, the total concentration of As, Cd, Co, Cr, Cu, Ni, Pb and Zn in soil samples were determined using inductively coupled plasma-mass spectrometer (ICP-MS). The results showed that the descending order of highest mean concentration of heavy metals in top soils was Zn > Pb > Cu > Cr > Ni > As > Co > Cd. The highest mean concentration of heavy metals, Zn was showed the range concentration from 68.80 to 6554.60 mg/Kg with mean value of 470.36 mg/Kg (Mehr et al., 2017).

In a study of spatial distribution of heavy metals in 359 top soil samples of Tampere, Finland, total concentrations of 40 geochemical elements were analysed in the soil samples using inductively coupled plasma atomic emission spectroscopy (ICP-AES) and inductively coupled plasma mass spectrometry (ICP-MS). The results showed that the highest mean concentration of heavy metal was Ba which the concentration ranged from 28.50 to 810.00 mg/Kg with mean value of 118.63 mg/Kg (Buttafuoco et al., 2017).

In north east of Vaslui County, Romania 193 soil samples were collected for study of heavy metal spatial distribution. Eight selected heavy metals, As, Cd, Co, Cr, Cu, Ni, Pb

and Zn were analysed in the soil samples using x-ray fluorescence analysis (ED-XRF). The results showed that the highest mean concentration among heavy metals was Zn which showed range from 31.00 to 192.00 mg/Kg with mean value of 68.22 mg/Kg. The descending order of highest mean concentration of heavy metals was represented as Zn > Cr > Ni > Cu > Pb > Co > As > Cd (Ungureanu et al., 2016).

In Xinjiang, China, 56 top soil samples were collected to analyse concentrations of Cu, Zn, Cd, Pb, Cr, As and Ni. The selected elements of heavy metals were analysed using Inductively Coupled Plasma Optical Emission Spectroscopy (ICP-OES) (ICAP 6300, Thermo Fisher Scientific, Massachusetts, United States). The highest mean concentration was Zn which showed concentration ranges between 84.73 to 233.49 mg/Kg with mean value of 123.32 mg/Kg. The results also showed the descending order of highest mean concentration of heavy metals was Zn > Cr > Cu > Ni > Pb > As > Cd (Wang et al., 2016).

In Rayong Province, Thailand, Cu, Pb, Zn, As and Cd were measured on 130 surface soil samples using Inductively Coupled Plasma Atomic Emission Spectroscopy (ICP-AES) (Horiba, Jobin Yvon 2000 emission). The highest mean concentration among these heavy metals was represented by Cu which the range was from 4.52 to 265.00 mg/Kg and the mean was 40.68 mg/Kg.Among the heavy metals, the descending order of highest mean concentration was Cu > Zn > As > Pb > Cd (Simasuwannarong et al., 2012).

2.4 REE concentration in urban soils

In São Paulo, Brazil, study of REE concentration in urban top soils was done in fourteen public parks. Concentration of eight selected REE, La, Ce, Nd, Sm, Eu, Tb, Yb and Lu were measured in the soil samples using instrumental neutron activation analysis (INAA). The results showed that the highest mean concentration of REE was

represented by Ce in Rodrigo de Gáspari public park which the concentration ranged from 85 to 222 mg/Kg with mean value of 144.8 ± 38.9 mg/Kg. The descending order of highest mean concentration of REE for all public parks was represented as Ce > La > Nd > Sm > Yb > Eu > Tb > Lu. Rodrigo de Gáspari public parks was the highest mean concentration of La, Ce, Nd, Sm and Eu. The highest mean concentration of Tb area was represented by Guarapiranga public park while Trianon public park represented as the highest concentration of Yb area. The highest mean concentration of Lu area was represented by Ibirapuera public park. (Figueiredo et al., 2009).

In London, concentration of La, Ce, Nd, Sm, Yb, Sc and Y were measured in 6467 top soil samples using wavelength dispersive X-ray fluorescence (XRF) spectrometry. According to the results, the highest mean concentration of REE was represented by Ce which the concentration ranged from 18.0 to 238.0 mg/Kg with mean value of 50.9 mg/Kg. The descending order of highest mean concentration of REE was represented as Ce > La > Nd > Y > Sc > Sm > Y (Yuan et al., 2017).

In Sweden, 51 top soil samples were collected to analyse the concentration of 14 REE, such as La, Ce, Nd, Pr, Sm, Eu, Gd, Tb, Dy, Ho, Er, Tm, Yb and Lu, using inductively coupled plasma-mass spectrometer (ICP-MS). The highest mean concentration among REE was represented by Ce which the range of concentration was from 13.80 to 83.00 mg/Kg with mean value of 37.67 mg/Kg. The descending order of highest mean concentration of REE was represented as Ce > La > Nd > Pr > Gd > Sm > Dy > Yb > Er > Eu > Ho > Tb > Lu > Tm (Sadeghi et al., 2013).

2.5 Heavy metals and REE spatial distributions in urban soils

Study of spatial distributions analysis of element in soil may helps to visualize the pattern of element distribution in the selected area. In north eastern part of Vaslui County, Romania, 193 top soil samples were collected for the study of spatial distributions of As, Cd, Co, Cr, Cu, Ni, Pb and Zn (Ungureanu et al., 2016). Total of 56

top soil samples were collected for study of spatial distributions of Cu, Zn, Cd, Pb, Cr, Ni and As in Xinjiang, China (Wang et al., 2016). In Lianyuan, China, 6078 surface soil samples were collected around a coal mine city in order to determine spatial distribution of Zn, Cd, Cu, Hg, Pb, Sb, As, Mo, V, Mn, Fe and Cr in this area (Liang et al., 2017).

The distribution of elements in top soils were mapped to observe the distribution pattern of the selected elements (Simasuwannarong et al., 2012; Guo et al., 2012; Benhaddya & Hadjel, 2013; Sadeghi et al., 2013; Wang & Liang, 2015; Wang et al., 2016; Unguraenu et al., 2016). In the major industrial region in Algeria, Hassi Messaoud city, the spatial distribution map of heavy metals in top soils showed that Pb and Zn concentration patterns decreasing from the centre of the city to the suburb. Cu concentration displayed two hot-spot areas in the north western of the city which associated with industrial areas and main roads with heavy traffic (Benhaddya & Hadjel, 2013).

In urban area of Xinjiang China, Cu, Zn, Cd and Pb spatial distributions showed high concentrations in the southern and northern parts of the area. The southern part of the study area is residential region whereas the northern part is industrial region. Spatial distribution of As and Cr showed highest concentrations in residential area. The source of high As contamination was also expected to be derived from coal combustion because coal was the main energy source for heating activities in the study area. The spatial distribution of Ni showed highest concentration in northeast part, which suspected to be influenced by weathering of parent rock and smelting activities (Wang et al., 2016).

Table 2.2: Range (R) and mean (M) concentrations of heavy metals (mg/Kg) in top soils of different urban areas.

Location	Cu	Ni	Pb	Zn	As	Cd	Cr	Co	Ba	Reference
Perlis, Malaysia	R: 0.38 to 240.59 M: 22.42	R: 0.689 to 2.398 M: 1.57	R: 0.39 to 27.47 M: 2.58	-	-	R: 0 to 0.63 M: 0.06	R: 0.642 to 3.921 M: 1.43	-	-	Mat Ripin et al. (2014)
Yogyakarta, Indonesia	-	-	R: 16 to 95.20 M: 65.4	-	-	-	-	-	-	Budianta (2012)
Isfahan Province, Iran.	-	R: 26.40 to 125.60 M: 61.65	R: 18.54 to 1929.86 M: 179.97	-	R: 5.00 to 178.90 M: 16.17	R: 0.25 to 74.72 M: 2.17	-	-	-	Mehr et al. (2017)
Tampere, Finland	R: 4.80 to 232.00 M: 26.98	R: 3.20 to 38.80 M: 18.52	R: 2.50 to 198.00 M: 16.42	R: 21.00 to 251.00 M: 90.01	R: 1.65 to 15.10 M: 63.05	R: 0.03 to 0.59 M: 0.17	R: 6.70 to 141.00 M: 39.85	R: 2.10 to 23.80 M: 10.16	R: 28.50 to 810.00 M: 118.63	Buttafuoco et al. (2017)
North east of Vaslui County, Romania	R:14.00 to 300.00 M:29.83	R:24.00 to 73.00 M: 47.36	R: 16.00 to 84.00 M: 25.27	R:31.00 to 192.00 M:68.22	R: 6.70 to 16.30 M: 10.14	R:0.02 to 0.80 M: 0.32	R:27.00 to 93.00 M:62.05	R:2.50 to 18.40 M:10.83	-	Ungureanu et al. (2016)
Xinjiang, China	R:52.60 to 90.90 M:64.22	R: 6.15 to 60.51 M: 42.70	R: 10.48 to 126.61 M: 32.56	R:84.73 to 233.49 M:123.32	R: 12.37 to 31.01 M: 20.65	R:0.07 to 1.74 M: 0.74	R: 100.37 to 141.59 M: 117.86	-	-	Wang et al. (2016)
Rayong Province, Thailand	R:4.52 to 265.00 M:40.68	-	R: 0.06 to 134.77 M: 19.97	R:3.61 to 409.27 M:35.53	R: 0.12 to 94.41 M: 26.23	R:0.03 to 12.60 M: 3.56	-	-	-	Simasuwannarong et al. (2012)

Table 2.3: Range (R) and mean (M) concentrations of REE (mg/Kg) in top soils of different urban areas.

Location	La	Ce	Nd	Sm	Eu	Gd	Tb	Dy	Er	Yb	Lu	Pr	Sc	Ho	Tm	Y	Reference
Rodrigo de Gáspari public park, São Paulo, Brazil.	R: 48 to 85 M: 67.5 ± 11.9	R: 85 to 222 M: 144.8 ± 38.9	R: 34 to 68 M: 53.8 ± 12.0	R: 5.3 to 11.8 M: 8.8 ± 1.8	R: 1.04 to 2.72 M: 1.99 ± 0.46	-	R: 0.61 to 1.01 M: 0.76 ± 0.12	-	-	R: 1.1 to 2.3 M: 1.57 ± 0.39	R: 0.27 to 0.52 M: 0.35 ± 0.08	-	-	-	-	-	Figueiredo et al. (2009)
Guara-piranga public park, São Paulo, Brazil	R: 22 to 73 M: 50.4 ± 19.6	R78 to 181 M: 130 ± 32	R: 18 to 75 M: 47.0 ± 18.3	R: 3.9 to 12.3 M: 8.05 ± 2.65	R: 0.37 to 2.2 M: 1.09 ± 0.65	-	R: 0.56 to 2.04 M: 1.27 ± 0.50	-	-	R: 1.7 to 7.8 M: 4.24 ± 1.82	R: 0.30 to 0.80 M: 0.535 ± 0.174	-	-	-	-	-	Figueiredo et al. (2009)
Trianon public park, São Paulo, Brazil	R: 16.6 to 35 M: 20.9 ± 8.3	R: 31 to 174 M: 66.2 ± 55.4	R: 12 to 62 M: 24.5 ± 19.3	R: 2.5 to 13.4 M: 5.2 ± 4.3	R: 0.44 to 1.00 M: 0.615 ± 0.206	-	R: 0.18 to 1.00 M: 0.80 ± 0.79	-	-	R: 2.5 to 9.0 M: 7.0 ± 2.4	R: 0.38 to 1.00 M: 0.535 ± 0.233	-	-	-	-	-	Figueiredo et al. (2009)
Ibirapuera public park, São Paulo, Brazil	R: 25 to 46 M: 33.5 ± 7.2	R: 55 to 102 M: 72.9 ± 18.1	R: 12.0 to 46.5 M: 29.4 ± 9.0	R: 3.0 to 7.1 M: 4.85± 1.21	R: 0.43 to 1.15 M: 0.60 ± 0.23	-	R: 0.62 to 1.10 M: 0.81 ± 0.19	-	-	R: 3.0 to 5.7 M: 4.27 ± 1.01	R: 0.47 to 0.90 M: 0.65 ± 0.15	-	-	-	-	-	Figueiredo et al. (2009)
London	R: 3.0 to 130.0 M: 25.2	R: 18.0 to 238.0 M: 50.9	R: 0.5 to 122.8 M: 22.3	R: 0.1 to 25.8 M: 3.6	-	-	-	-	-	R: 0.1 to 8.8 M: 1.9	-	-	R: 0.2 to 33.3 M: 8.3	-	-	R: 4.8 to 132.9 M: 21.1	Yuan et al. (2017)
Sweden	R: 6.92 to 34.30 M:17.42	R: 13.80 to 83.00 M: 37.67	R: 6.71 to 31.80 M: 15.14	R:1.37 to 6.01 M:2.98	R: 0.24 to 1.29 M: 0.65	R:1.15 to 6.40 M:3.07	R: 0.22 to 1.08 M: 0.49	R: 1.48 to 6.18 M: 2.95	R: 0.95 to 3.96 M: 1.88	R:1.08 to 4.19 M:2.01	R: 0.17 to 0.58 M: 0.30	R: 1.64 to 8.16 M: 4.10	-	R: 0.28 to 1.34 M: 0.61	R: 0.13 to 0.57 M: 0.28	-	Sadeghi et al. (2013)

In north eastern part of Vaslui County, Romania, spatial distribution maps of Pb and Zn in top soils displayed high values in vicinity of areas inhabited by humans and near major road of large amounts of traffic. Spatial distribution of Cu in top soils showed high value in area of vines plantation. However, spatial distribution of Cr, As, Ni and Co presented less variability and concentrations in the area (Unguraenu et al., 2016).

In Athens, Greece, the spatial distribution maps of top soils showed high concentrations of Cu, Pb and Zn in road verge soil compared to other land use categories. Concentrations of Pb, Cu, Zn, Sb and Sn showed higher in the older parts of the city whereas Arsenic concentration showed higher in parks and woodland areas. Chromium and Co concentrations were expected to be derived from weathering process because their distribution amounts are too low to reach contamination level (Argyraki & Kelepertzis, 2014).

Spatial distribution map of REE in top soils of Sweden displayed light REE (LREE) higher enrichment than heavy REE (HREE) in soils developed on the Archean rocks in northern Sweden, Archean and Palaeoproterozoic basement rocks in Jämtland and Västerbotten, and younger granites in Bohuslan (Sadeghi et al., 2013).

In London, spatial distribution of selected REE, La, Ce, Nd, Sm, Sc, Yb and Y showed similar distribution pattern which displaying elevated values in the northwest, northeast and south parts. The distribution of Sc showed slightly elevated concentration in the central area. The low concentrations of REE were located along the both sides of River Thames. The large areas of elevated and low concentrations of REE were expected to be influenced by natural factors. However, high concentration of La, Ce, Nd, Yb and Y in parks, wetlands and agriculture lands which located in Hillingdon, Hounslow and Enfield were expected to be influenced by fertilizer application. In Redbridge, Newham, Barking, Dagenham and Rainham, REE high concentrations in these areas were predicted to be influenced by landfill, metal recycling and cement

plants. High concentrations of REE in central part of London especially La, Ce, Nd and Y were expected to be influenced by vehicular emission (Yuan et al., 2017).

Table 2.4: Spatial distribution of heavy metals and REE in different study areas.

Study area	Spatial distribution pattern	Reference
Hassi Messaoud city, Algeria.	▪ Pb and Zn concentrations decreasing from the centre of the city to the suburb. ▪ Cu high concentration areas associated with industrial areas and main roads with heavy traffic.	Benhaddya and Hadjel (2013)
Xinjiang, China	▪ Cu, Zn, Cd and Pb spatial distributions showed high concentrations in the southern (residential area) and northern (industrial) parts of the area. ▪ Spatial distribution of As and Cr showed highest concentrations in residential area. ▪ The spatial distribution of Ni showed highest concentration in northeast part which related to weathering of parent rock and smelting activities	Wang et al. (2016)
North eastern part of Vaslui County, Romania.	▪ Pb and Zn distributions displayed high values in vicinity of areas inhabited by humans and near major road of large amounts of traffic. ▪ Cu distribution showed high value in area of vines plantation. ▪ Cr, As, Ni and Co distributions presented less variability.	Unguraenu et al. (2016)
Athens, Greece	▪ High concentrations of Cu, Pb and Zn in road verge soil compared to other land use categories. ▪ Concentrations of Pb, Cu, Zn, Sb and Sn showed higher in the older parts of the city. ▪ Arsenic concentration showed higher in parks and woodland areas. ▪ Chromium and Co concentrations were expected to be derived from weathering process because their distributions amounts are too low to reach contamination level.	Argyraki and Kelepertzis (2014)
Sweden	▪ Light REE (LREE) showed higher enrichment than heavy REE (HREE) in soils developed on the Archean rocks in northern Sweden, Archean and Palaeoproterozoic basement rocks in Jämtland and Västerbotten, and younger granites in Bohuslan.	Sadeghi et al. (2013)
London	▪ La, Ce, Nd, Sm, Sc, Yb and Y showed similar distribution pattern, elevated values in the northwest, northeast and south parts. ▪ The large areas of elevated and low concentrations of REE were expected to be influenced by natural factors. ▪ High concentrations of La, Ce, Nd, Yb and Y in parks, wetlands and agriculture lands which located in Hillingdon, Hounslow and Enfield were expected to be influenced by fertilizer application. ▪ REE high concentrations in Redbridge, Newham, Barking, Dagenham and Rainham were predicted to be influenced by landfill, metal recycling and cement plants. ▪ High concentrations of REE in central part of London especially La, Ce, Nd and Y were expected to be influenced by vehicular emission.	Wang and Liang (2015)

Table 2.4, continued

Study area	Spatial distribution pattern	Reference
Xinjiang, China	▪ Cu, Zn, Cd and Pb spatial distributions showed high concentrations in the southern (residential area) and northern (industrial) parts of the area. ▪ Spatial distribution of As and Cr showed highest concentrations in residential area. ▪ The spatial distribution of Ni showed highest concentration in northeast part which related to weathering of parent rock and smelting activities.	Wang et al. (2016)
North eastern part of Vaslui County, Romania.	▪ Pb and Zn distributions displayed high values in vicinity of areas inhabited by humans and near major road of large amounts of traffic. ▪ Cu distribution showed high value in area of vines plantation. ▪ Cr, As, Ni and Co distributions presented less variability.	Unguraenu et al. (2016)
Athens, Greece	▪ High concentrations of Cu, Pb and Zn in road verge soil compared to other land use categories. ▪ Concentrations of Pb, Cu, Zn, Sb and Sn showed higher in the older parts of the city. ▪ Arsenic concentration showed higher in parks and woodland areas. ▪ Chromium and Co concentrations were expected to be derived from weathering process because their distributions amounts are too low to reach contamination level.	Argyraki and Kelepertzis (2014)
Sweden	▪ Light REE (LREE) showed higher enrichment than heavy REE (HREE) in soils developed on the Archean rocks in northern Sweden, Archean and Palaeoproterozoic basement rocks in Jämtland and Västerbotten, and younger granites in Bohuslan.	Sadeghi et al. (2013)
London	▪ La, Ce, Nd, Sm, Sc, Yb and Y showed similar distribution pattern, elevated values in the northwest, northeast and south parts. ▪ The large areas of elevated and low concentrations of REE were expected to be influenced by natural factors. ▪ High concentrations of La, Ce, Nd, Yb and Y in parks, wetlands and agriculture lands which located in Hillingdon, Hounslow and Enfield were expected to be influenced by fertilizer application. ▪ REE high concentrations in Redbridge, Newham, Barking, Dagenham and Rainham were predicted to be influenced by landfill, metal recycling and cement plants. ▪ High concentrations of REE in central part of London especially La, Ce, Nd and Y were expected to be influenced by vehicular emission.	Wang and Liang (2015)

2.6 Heavy metals and REE contamination level assessment in urban soils

Assessment of heavy metals contamination level in Perlis, Malaysia, showed that highest mean pollution index (PI) value was represented by Cu with value of 0.84 and followed by Cd, Pb, Ni and Cr. The high PI values of heavy metals were also found in heavy traffic and industrial areas (Mat Ripin et al., 2014).

In Xinjiang, China, average value potential ecological risk index of Cd showed higher than Cu, Zn, Pb, Cr, As and Ni which the values are between 18.66 to 434.46 and average of 185.05. The descending order of highest average potential ecological risk index was Cd > As > Cu > Pb > Cr > Ni, Zn. Spatial map of potential ecological risk of Cd showed similar distribution pattern to the spatial distribution of Cd concentration (Wang et al., 2016).

In Niger Delta, Nigeria, heavy metal contamination factor (CF) assessment of top soils showed moderately contaminated level was represented by Cd whereas Cr, Ni, Pb and Zn indicated low degree of contamination levels. In pollution load index (PLI) assessment, all heavy metals indicated unpolluted level in top soils (Benson et al., 2016).

In assessment of heavy metals contamination in urban top soils of Isfahan Province, Iran, the mean I_{geo} of Pb and Zn were classified as moderately polluted level. Both mean I_{geo} for Cd and Cu showed levels of unpolluted to moderately polluted. However, mean I_{geo} of As showed unpolluted level. In CF assessment, very high contamination levels were represented by As content from 1.20 % of the total samples, Cd content from 9.64 % of the total samples, Cu content from 6.02 % of the total samples, Pb content from 16.86 % of the total samples and Zn content from 12.06 % of the total samples (Mehr et al., 2017).

Assessment of heavy metals pollution in top soils in Hassi Messaoud, the major industrial region in Algeria showed that enrichment factor (EF) assessment of Pb and Zn presented highest average EF values. In this assessment, Pb content was classified as significant enrichment level whereas Zn content was classified as moderate enrichment level. In I_{geo} assessment, the result showed that the study area was moderately contaminated by Pb and Zn (Benhaddya & Hadjel, 2013).

In Katanga, Democratic Republic of the Congo, assessment of trace metals and REE contamination was done in soil and sediment around abandoned and active mine area. In enrichment factor (EF) assessment, the highest values of EF were represented by Co and Cu which were classified as extremely severe enrichment. Three samples were classified as extremely severe enrichment for Pb concentration and one sample was classified as extremely severe enrichment for Zn concentration. Most samples showed U concentration at moderate enrichment level. No enrichment levels were represented by other trace metals and REE in all samples. In I_{geo} assessment, Mo, Th, U, Eu, Ho and Tm concentrations were classified as moderately polluted and/or unpolluted levels whereas other trace metals and REE were classified as extremely polluted levels (Atibu et al., 2016).

In study of spatial distribution and risk assessment of As, Cd, Cu, Pb, and Zn in top soils of Rayong Province, Thailand, distributions of hazard index (HI) of each element were mapped. The order of highest total of HI was As > Pb > Cu > Cd > Zn. All heavy metals showed maximum HI less than one which indicate no adverse health effects level. In the distribution of HI map, high HI of As was located in the eastern part of the study area which consists of agriculture area and also in the south western part of the study area which consists of industrial area (Simasuwannarong et al., 2012).

Table 2.5: Contamination level assessment of heavy metals and REE in urban soils.

Elements	Study area	Contamination level result	Reference
Cu, Cd, Pb, Ni and Cr	Perlis, Malaysia	Pollution index (PI) assessment: ▪ Value was represented by Cu with value of 0.84 and followed by Cd, Pb, Ni and Cr. ▪ The high PI values of heavy metals were also found in heavy traffic and industrial areas (Mat Ripin et al., 2014).	Mat Ripin et al. (2014)
Cd and As	Xinjiang, China	Potential ecological risk index assessment: ▪ Average value of Cd showed higher than Cu, Zn, Pb, Cr, As and Ni which the values are between 18.66 to 434.46 and average of 185.05. ▪ The descending order of highest average potential ecological risk index was Cd > As > Cu > Pb > Cr > Ni, Zn. ▪ Spatial map of potential ecological risk of Cd showed similar distribution pattern to the spatial distribution of Cd concentration.	Wang et al. (2016)
Cd, Cr, Ni, Pb and Zn	Niger Delta, Nigeria.	CF assessment: ▪ Cd showed moderately contaminated level. ▪ Cr, Ni, Pb and Zn indicated low degree of contamination levels. PLI assessment: ▪ All heavy metals indicated unpolluted level.	Benson et al. (2016)
Pb, Zn, Cd, Cu and As	Isfahan Province, Iran.	I_{geo} assessment: ▪ Mean I_{geo} of Pb and Zn were classified as moderately polluted level. ▪ Mean I_{geo} of Cd and Cu showed unpolluted to moderately polluted levels. ▪ Mean I_{geo} of As showed unpolluted level. CF assessment: ▪ 1.20 % of the total samples showed very high contamination levels of As. ▪ 9.64 % of the total samples showed very high contamination levels of Cd. ▪ 6.02 % of the total samples showed very high contamination levels of Cu, ▪ 16.86 % of the total samples showed very high contamination levels of Pb. ▪ 12.06 % of the total samples showed very high contamination levels of Zn.	Mehr et al. (2017)

Table 2.5, continued

Elements	Study area	Contamination level result	Reference
Pb and Zn	Hassi Messaoud, Algeria.	EF assessment: ▪ Pb and Zn showed highest average EF values. ▪ Pb was classified as significant enrichment level. ▪ Zn was classified as moderate enrichment level. I_{geo} assessment: ▪ The study area was moderately contaminated by Pb and Zn.	Benhaddya and Hadjel (2013)
Co, Ni, Cu, Zn, As, Mo, Pb Th, U, La, Ce, Pr, Nd, Sm, Eu, Gd, Tb, Dy, Ho, Er, Tm, Yb and Lu	Katanga, Democratic Republic of the Congo.	EF assessment: ▪ The highest values of EF were represented by Co and Cu and classified as extremely severe enrichment level. ▪ Three samples were classified as extremely severe enrichment for Pb concentration. ▪ One sample was classified as extremely severe enrichment for Zn concentration. ▪ Most samples showed U concentration at moderate enrichment level. ▪ No enrichment levels were represented by other trace metals and REE in all samples. I_{geo} assessment: ▪ Mo, Th, U, Eu, Ho and Tm were classified as moderately polluted and/or unpolluted levels. ▪ Other trace metals and REE were classified as extremely polluted levels.	Atibu et al. (2016)
As, Pb, Cu, Cd and Zn	Rayong Province, Thailand.	HI assessment: ▪ The order of highest total of HI was As> Pb > Cu > Cd > Zn. ▪ All heavy metals showed maximum HI less than one which indicate no adverse health effects. ▪ In HI map, high HI of As was located in the eastern part of the study area which consists of agriculture area and also in the south western part of the study area which consists of industrial area.	Simasuwannarong et al. (2012)

2.7 Factors contributing heavy metals and REE contamination in urban soils

In study of heavy metals spatial distribution in urban areas of Isfahan Province, Iran, the highest concentration of As was found in surface soils of both Kelishad and Abrisham cities. The high content of As was expected to be derived from Pb-Zn mine which may also contribute to the high Pb, Cd and Zn concentrations in both cities. However, the high concentration of Cu in Najafabad, Khomeynishahr and Isfahan cities was suggested to be connected with intense anthropogenic activities and dense traffic as these cities are the largest populated and industrialized cities in Isfahan Province. Other than that, Ni and Cr concentrations in the samples collected from Shahinshahr city were expected to be related to the Shahinshahr refinery. Concentration of Cr in soils also was predicted to be affected by Dehsorkh municipal waste dump site (Mehr et al., 2017).

In spatial distribution study of heavy metals in top soils of Rayong Province, Thailand, the concentration of Cd decreased from north to south across the province. The concentration of Cd was expected to be derived from agriculture as it is the main land use type in the northern part. The high concentration of Zn was found in urban area in south of province. Both Cd and Zn were also predicted to be derived from metal-working industry. The concentration of Zn in Rayong Province also was related to mineralogy of the bedrock as mentioned from the previous research (Simasuwannarong et al., 2012).

In study of spatial distribution of heavy metals in soils of north east area of Vaslui County, Romania, vehicle emissions, human activities and agricultural materials were identified to become an important source of Zn, Pb and Cu contaminations in this area. Concentrations of As, Ni and Co were suspected to be originated from geogenic and pedogenic sources. Contamination of Pb and Zn which found highly concentrated in high traffic area was predicted originated from traffic emission. Fertilizers or

copperbased fungicides that used in vineyards were expected to become source of Cu contamination in the soils (Ungureanu et al., 2016).

In São Paulo city, Brazil, spatial distribution analysis of selected REE, La, Ce, Nd, Sm, Eu, Tb, Yb and Lu was done to investigate the influence of traffic emission to the concentration of REE in the soils. The results showed that the enrichment of REE in soils were not clearly related to vehicular traffic as the REE concentrations were highly associated with the natural geological composition of the soils. The parent rock of the area, sedimentary rocks of the Tertiary Basin of São Paulo become the main source of REE concentrations in the soils (Figueiredo et al., 2009).

In Jharia coal field, Dhanbad, India, selected REE concentrations, La, Ce, Pr, Nd, Sm, Eu, Gd, Tb, Dy, Ho, Er, Tm, Yb, Lu, Sc and Y were determined in the soil samples around the area. The coal mining activities were identified to become a source of REE enrichment in the nearby soils (Masto et al., 2011).

A study of REE spatial distribution was done in area near to the thermal power plant in Plomin, Crotia. The results showed that the high level of REE in soils were predicted to be originated from the recent ashes, resulting from combustion of imported coal that used in the thermal power plantfrom 1990's onwards (Fiket et al., 2016).

2.8 Statistical analysis of heavy metals, REE and soil physicochemical properties

Pearson correlation analysis and principal component analysis (PCA) are among selected statistical analysis that commonly applied in the study of element distribution and contamination (Guo et al., 2012; Sadeghi et al., 2013; Unguraenu et al., 2016). The coefficient of Pearson correlation, r in the analysis represents the strength of the relationship between two variables where the relationships between the selected elements can provide important information on the element sources and pathways (Manta et al., 2002). Principal component analysis (PCA) is used to reduce high

dimensionality of the complex dataset by transforming the data into orthogonal components that are linear combinations of the original variables (Slavkovic´ et al., 2004; Ağca, 2015). The relationship showed between selected elements in both principal component analysis (PCA) and Pearson correlation analysis can be used to predict the sources of contamination (Benhaddya & Hadjel, 2013; Ağca, 2015).

In study of heavy metals distribution in urban top soils of Xinjiang, China, Pearson correlation analysis showed the relationships between Cu and Zn, Cu and Cd, Cu and Pb, Zn and Cd, Zn and Pb, Zn and Cr, Cd and Pb, and, Cr and As with positive correlations. In PCA, the correlations were showed by Cd-Cu-Pb-Zn and As-Cr. However, Ni showed different extracted component with other elements (Wang et al., 2016).

Results of Pearson correlation test of heavy metals distribution in top soil of north eastern part of Vaslui County, Romania showed Co was correlated with Ni, Zn and As with positive correlations, Cr was correlated with Cd with negative correlation, Cr was correlated with As with positive correlation, Ni was correlated with Zn, Cd and As with positive correlations, Cu was correlated with Pb with positive correlation, Zn was correlated with Cd, Pb and As with positive correlations and Pb was correlated with As with positive correlation. In PCA, relationships were showed by Co-Ni-As, Zn-Pb and Cr-Cd with positive correlations (Unguraenu et al., 2016).

In the study of spatial distribution of REE in top soil of Sweden, results of Pearson correlation analysis showed among light REE (LREE), La was correlated with Ce, Pr, Nd and Sm with positive correlations, Ce was correlated with Pr and Nd with positive correlations, Pr was correlated with Nd and Sm with positive correlations and Nd was correlated with Sm with positive correlation. Among heavy REE (HREE), Gd was correlated with Tb, Dy and Ho with positive correlations, Tb was correlated with Dy,

Ho and Er with positive correlations, Dy was correlated with Ho, Er, Tm and Yb with positive correlations, Ho was correlated with Er, Tm, Yb and Lu with positive correlations, Er was correlated with Tm, Yb and Lu with positive correlations, Tm was correlated with Yb and Lu with positive correlations and Yb was correlated with Lu with positive correlation. Between LREE and HREE, Pr was correlated with Gd with positive correlation, Nd was correlated with Gd and Tb with positive correlations, Sm was correlated with Gd and Tb with positive correlations. In PCA, first and second extracted components showed contrast between LREE and HREE, first and third extracted components showed three distinct clusters which represented by one comprising most REE, one for Ce and one for Eu. In plot of loadings diagram, three distinct clusters were represented by one comprising most REE, one for Ce and one for Eu (Sadeghi et al., 2013).

In the study of spatial distribution of heavy metals in top soils of industrial area in Southern Turkey, the relationships between heavy metals and physicochemical properties of soils in Pearson correlation analysis were represented by Fe and sand with positive correlation, Fe and organic matter (OM) with positive correlation, Mn and sand with negative correlation, Mn and silt with positive correlation, Mn and clay with positive correlation, Ni and silt with positive correlation and, Zn and OM with positive correlation (Ağca, 2015).

In Northern Ghorveh, Western Iran, Pearson correlation analysis of As and Cd distribution in top soils showed that As was correlated with sand with negative correlation, As was correlated with silt and clay with positive correlations, Cd was correlated with calcium carbonate, OM, silt, clay and cation exchange capacity (CEC) with negative correlations and Cd was correlated with sand with positive correlation (Nezhad et al., 2011).

In Mashhad plain, north eastern Iran, Pearson correlation analysis of the distribution of heavy metals in surface soils represented pH was correlated with Ni, Pb and Zn with negative correlations, sand was correlated with Fe and Ni with positive correlations, silt was correlated with Fe, Ni and Zn with negative correlations, calcium carbonate was correlated with Fe, Ni and Zn with negative correlations, calcium sulphate was correlated with Ni, Pb and Zn with negative correlations and soil organic carbon (SOC) was correlated with Ni, Pb and Zn with positive correlations (Karimi et al., 2017).

Table 2.6: Statistical analysis for selected element concentrations and soil physicochemical properties in other studies.

Study area	**Pearson correlation analysis**	**PCA**	**Reference**
Xinjiang, China	▪ Cu correlated with Zn, Cd and Pb with positive correlations. ▪ Zn correlated with Cd, Pb and Cr with positive correlation. ▪ Cd correlated with Pb with positive correlation. ▪ Cr correlated with As with positive correlations.	▪ Correlations were showed by Cd-Cu-Pb-Zn, and As-Cr. However, Ni showed different extracted component with other elements.	Wang et al. (2016)
North eastern part of Vaslui County, Romania	▪ Co correlated with Ni, Zn and As with positive correlations. ▪ Cr correlated with Cd with negative correlation. ▪ Cr correlated with As with positive correlation. ▪ Ni correlated with Zn, Cd and As with positive correlations. ▪ Cu correlated with Pb with positive correlation. ▪ Zn correlated with Cd, Pb and As with positive correlations. ▪ Pb correlated with As with positive correlation.	▪ Relationships were showed by Co-Ni-As, Zn-Pb and Cr-Cd with positive correlations.	Unguraenu et al. (2016)
Sweden	Among LREE: ▪ La correlated with Ce, Pr, Nd and Sm with positive correlations. ▪ Ce correlated with Pr and Nd with positive correlations. ▪ Pr correlated with Nd and Sm with positive correlations. ▪ Nd correlated with Sm with positive correlation.	▪ First and second extracted components showed contrast between LREE and HREE, first and third extracted components showed three distinct clusters which represented by one comprising most REE, one for Ce and one for Eu.	Sadeghi et al. (2013)

Table 2.6, continued

Study area	Pearson correlation analysis	PCA	Reference
Sweden	Among HREE: ▪ Gd correlated with Tb, Dy and Ho with positive correlations. ▪ Tb correlated with Dy, Ho and Er with positive correlations. ▪ Dy correlated with Ho, Er, Tm and Yb with positive correlations. ▪ Ho correlated with Er, Tm, Yb and Lu with positive correlations. ▪ Er correlated with Tm, Yb and Lu with positive correlations. ▪ Tm correlated with Yb and Lu with positive correlations. ▪ Yb correlated with Lu with positive correlation. Between LREE and HREE: ▪ Pr correlated with Gd with positive correlation. ▪ Nd correlated with Gd and Tb with positive correlations. ▪ Sm correlated with Gd and Tb with positive correlations.	▪ In plot of loadings diagram, three distinct clusters were represented by one comprising most REE, one for Ce and one for Eu.	Sadeghi et al. (2013)
Industrial area, Southern Turkey.	Positive correlation: ▪ Fe & sand. ▪ Fe & OM. ▪ Mn & silt. ▪ Mn & clay. ▪ Ni & silt. ▪ Zn & OM. Negative correlation: ▪ Mn & sand with negative correlation.		Ağca (2015)
Northern Ghorveh, Western Iran.	Positive correlation: ▪ As & silt. ▪ As & clay. ▪ Cd & sand. Negative correlation: ▪ As & sand. ▪ Cd & calcium carbonate. ▪ Cd & OM. ▪ Cd & silt. ▪ Cd & clay. ▪ Cd & CEC.		Nezhad et al. (2011)

Table 2.6, continued

Study area	Pearson correlation analysis	PCA	Reference
Northern Ghorveh, Western Iran.	Positive correlation: ▪ As & silt. ▪ As & clay. ▪ Cd & sand. Negative correlation: ▪ As & sand. ▪ Cd & calcium carbonate. ▪ Cd & OM. ▪ Cd & silt. ▪ Cd & clay. ▪ Cd & CEC.		Nezhad et al. (2011)
Mashhad plain, northeastern Iran.	Positive correlation: ▪ Sand & Fe. ▪ Sand & Ni. ▪ SOC & Ni. ▪ SOC & Pb. ▪ SOC & Zn. Negative correlation: ▪ pH & Ni. ▪ pH & Pb. ▪ pH & Zn. ▪ Silt & Fe. ▪ Silt & Ni. ▪ Silt & Zn. ▪ Calcium carbonate & Fe. ▪ Calcium carbonate & Ni. ▪ Calcium carbonate **&** Zn. ▪ Calcium sulphate & Ni. ▪ Calcium sulphate & Pb. ▪ Calcium sulphate & Zn.		Karimi et al. (2017)

2.9 Summary

Based on the previous studies, the concentration of selected element was measured using many types of equipments. For this study, ICP-MS will be used to measure the concentration of selected heavy metals and REE. Like spatial distribution analysis from other studies, heavy metals and REE concentrations in this study will be mapped to observe the concentration distribution pattern in Penang Island. Contamination assessment such as CF and I_{geo} will be used to determine the level of heavy metals and REE contamination in top soils of Penang Island. Statistical analysis such as Pearson

correlation analysis and PCA will be applied to identify the relationship among the selected elements and also the relation between the selected elements with soil physicochemical properties.

CHAPTER 3: METHODOLOGY

3.1 Introduction

This chapter explains the methods and techniques employed to assess the distribution of selected heavy metals and REE in top soils of Penang Island.

3.2 Study area

3.2.1 Location and history

The location for this research, Penang Island is shown in **Figure 3.1** and it covers an area about 297 km^2. Penang Island is situated at North-West of Peninsular Malaysia at about 5° 15' N to 5° 30' N of latitudes and 100° 10' E to 100° 20' E of longitudes. The average rainfall of Penang Island is from 2254 to 2903 mm annually and has relative humidity at 70 % to 90 %. Elevation of terrain in Penang Island ranges from 0 to 820 m above sea level and has slope gradient ranges from 0° to 87° (Tay et al., 2014).

Development of Penang Island started at the end of 18^{th} century when George Town became the first British port town and also the oldest British colonial town in South East Asia (Shamsuddin et al., 2012). In 7 July 2008, UNESCO (United Nations Educational, Scientific and Cultural Organization) has recognized George Town as a heritage site in 32^{th} meeting of UNESCO World Heritage Committee in Quebac, Canada (Mustafa et al., 2015). Since 1970s, Penang undergoes rapid urbanisation and industrialization which has resulted in drastic changes to the physical and social landscapes of the old rural villages. In 1972, 974 acres of land surrounding Bayan Lepas which is located in southwest district was made for industrial, housing and town centre developments. The city has expended even further to Batu Maung in the southwest (Ghazali, 2013).

3.2.2 Land use

Land use map of Penang Island is shown in **Figure 3.2**. Penang Island is an important economic area in Malaysia which comprises many urban activities such as industrial activity (7.5 %), business activity (11 %), mining sector (1.3 %) and, agricultural and farm activities (48 %) (Town and Country Planning Department of Penang, 2015). Penang Island is subdivided into two districts which is northeast district and southwest district. Residential area of Penang Island (70 %) is located mostly at northeast district compared to southwest district. However, agricultural and farming are the major activities at southwest district compared to northeast district (Town and Country Planning Department of Penang, 2015). According to Department of Statistics Malaysia (2013), northeast district was accommodated by 535.2 thousand inhabitants whereas southwests district was accommodated by 205.9 thousand inhabitants.

3.2.3 Geology

Geology map of Penang Island is shown in **Figure 3.3**. Penang Island is mainly underlain by granitic bedrock and Quaternary deposits present in low-lying areas. The types of granitic rocks are fine to coarse grained biotite granite and fine to coarse grained megacrystic biotite granite. This granitic rock is separated into two groups which is the North Penang Pluton and South Penang Pluton. The North Penang Pluton is divided into Ferringhi Granite, Tanjung Bungah Granite and Muka Head micro granite. The South Penang Pluton is divided into Batu Maung Granite and Sungai Ara Granite (Ahmad et al., 2006).

According to Hassan (1990), Quaternary stratigraphy of Penang Island is divided into Simpang Formation, Gula Formation and Beruas Formation. They generally made up of sand, silt, clay and gravel and also small amount of peat intercalations. Gula Formation comprises group of Bagan Datoh Member, Teluk Intan Member, Port Weld Member, Parit Buntar Member and Matang Gelugor Member. Simpang Formation is

Pleistocene sediment deposited in terrestrial environment. Both Gula Formation and Beruas Formation are Holocene sediments. The difference between them is Gula Formation is made up of marine sediments whereas Beruas Formation is made up of terrestrial sediments.

Figure 3.1: Map of Penang Island and its location in Peninsular Malaysia. (Source: Google Earth).

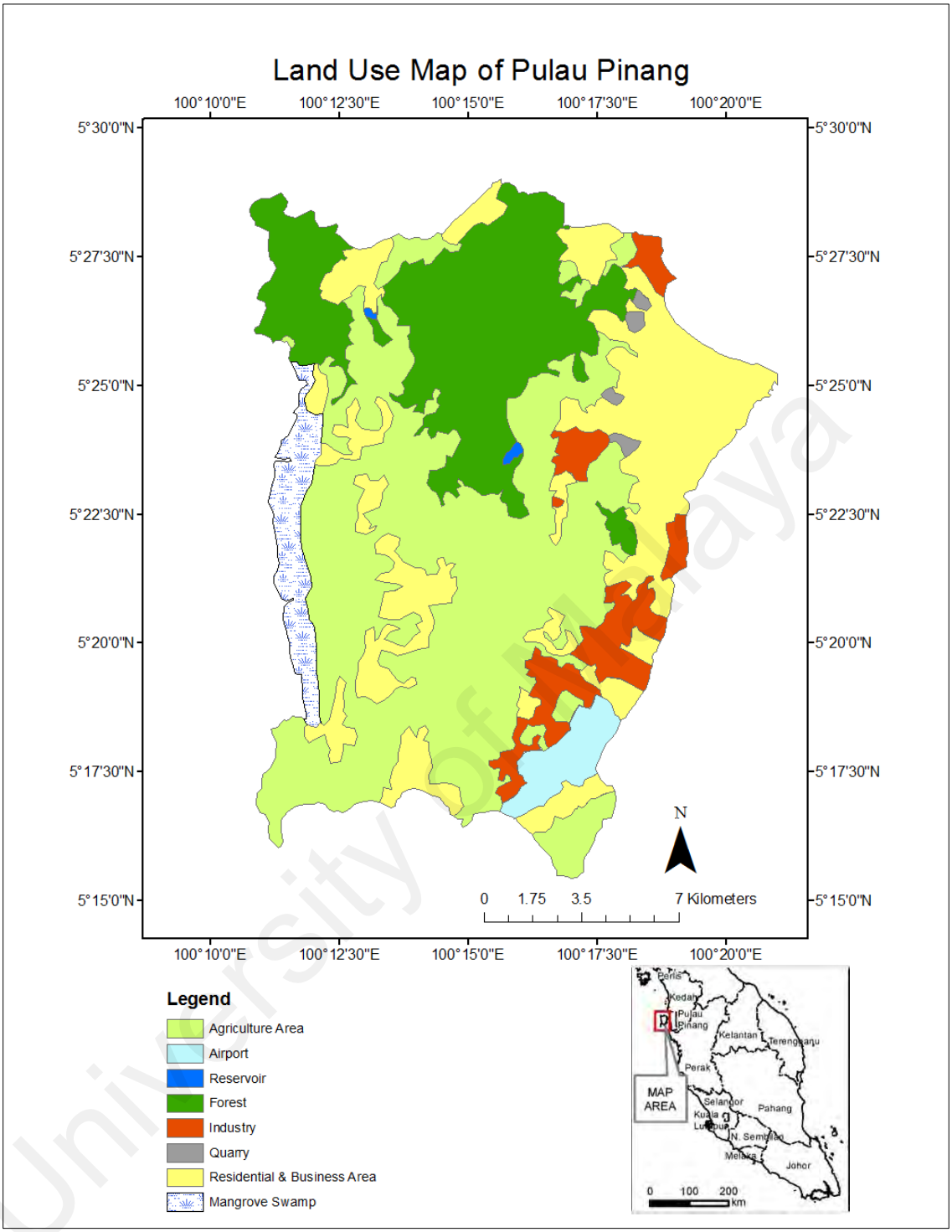

Figure 3.2: Land use map of Penang Island. The map was digitized using ArcGIS from original map sourced from Department of Agriculture Malaysia.

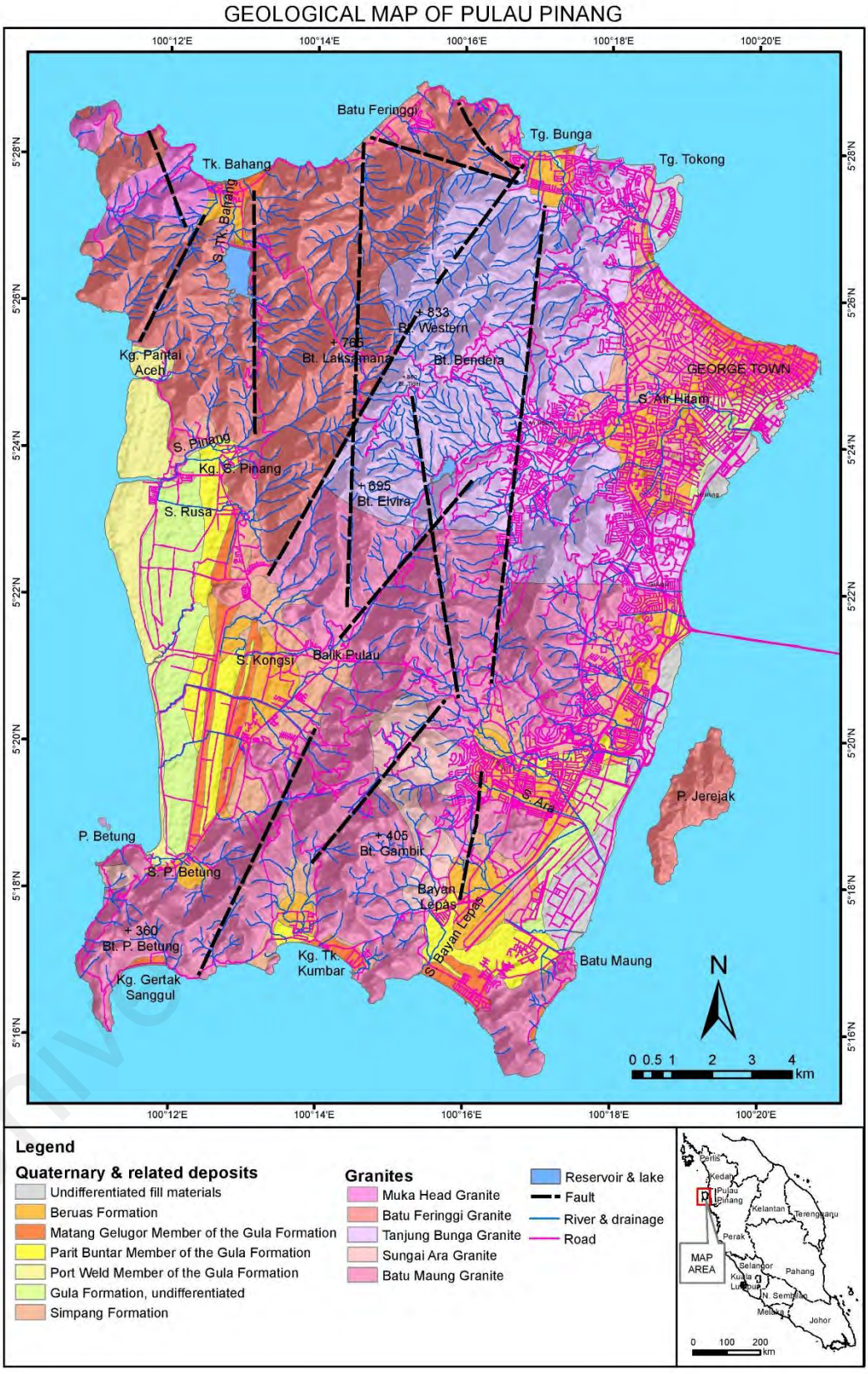

Figure 3.3: Geological map of Penang Island. The map was generated using ArcGIS with data obtained from Hassan (1990) and Ahmad et al. (2006).

3.3 Soil sampling procedure

A total of thirty-one top soil samples which comprised different types of land use and geology were collected at approximately a 0 to 20 cm in depth around the Penang Island for spatial distribution analysis of selected heavy metals and REE. All of the sampling locations were marked on the land use map in **Figure 3.4**.

All of the soil samples were collected using hand auger. The hand auger was cleaned after every sampling session to prevent the soil samples contamination. The soil samples were stored in polyethylene bags, labelled and tied tight to preserve moisture content before placed in a cool box. The details such as coordinate of the location, soil colour, type of soil (granite residual soil or Quaternary deposit) and type of land use were recorded during sampling campaign. The colour of each soil sample was classified according to Munsell soil colour chart. A global positioning system (GPS) device was used to determine the coordinate of the sampling location. All of 31 soil samples descriptions were represented in **Table 3.1**.

3.4 Laboratory analysis

Laboratory analysis includes the determination of soil physicochemical properties and total concentration analysis. The soil physicochemical properties that were measured include pH, organic matter (OM) content, cationic exchange capacity (CEC) and particle size distribution. Total concentration of four selected heavy metals, As, Pb, Ni and Cd and, seven selected REE, La, Ce, Nd, Eu, Tb, Dy and Er were determined. Quality control and assurance were also included in the laboratory practices (see section 3.4.3).

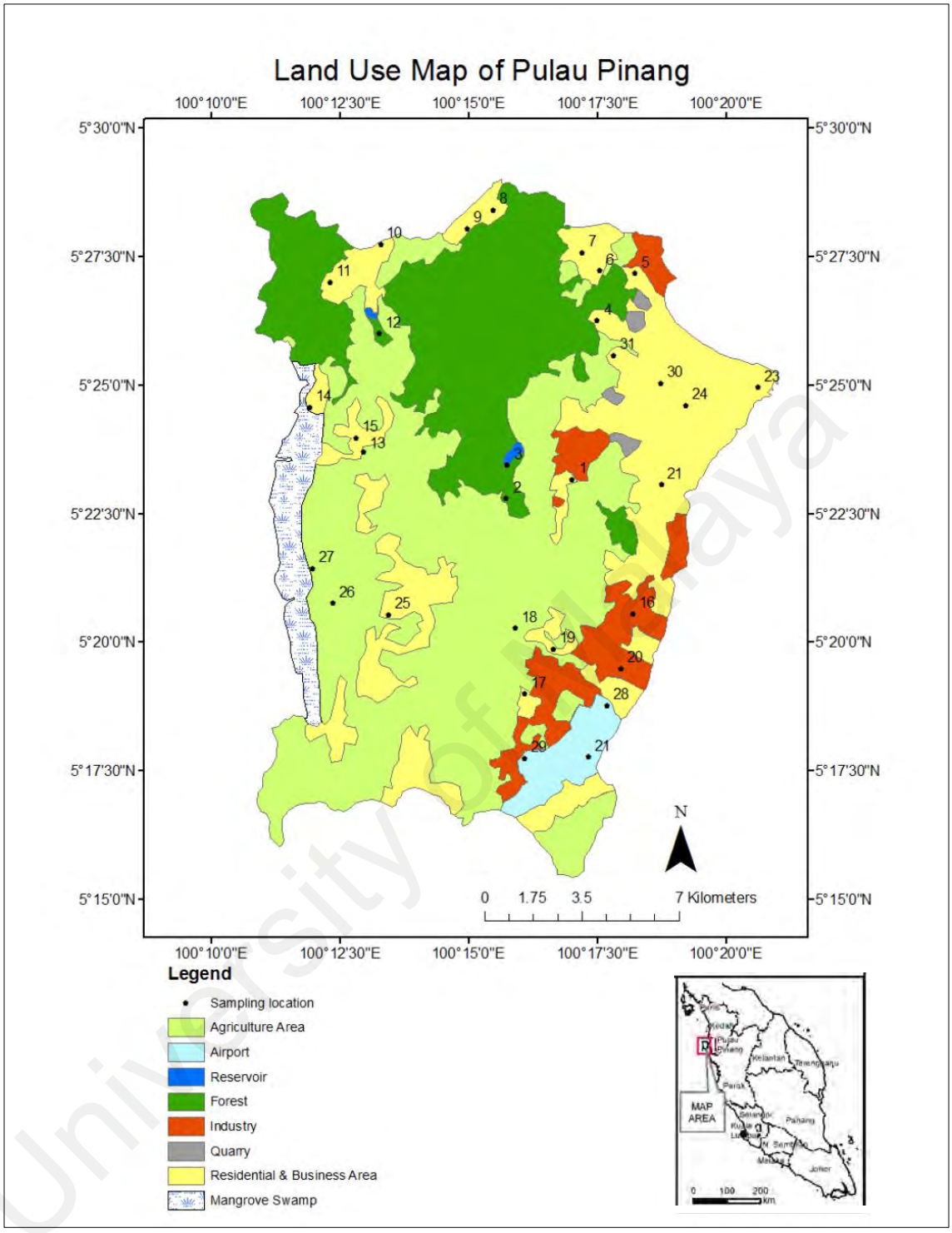

Figure 3.4: Land use map of Penang Island with the soil sampling locations (n=31).

Figure 3.5: Collection of soil sample using a hand auger in the field.

Figure 3.6: Soil colour determination by using Munsell chart.

Table 3.1: Soil samples descriptions.

Sample name	Latitude	Longitude	Sampling time	Weather	Land use type	Soil geology type	Soil particle type
1A	5.38611	100.2834	7/5/2016	Not rain within 12 hours	Residential & business areas	Granite residual	Sand
2A	5.37989	100.2621	7/5/2016	Not rain within 12 hours	Forest	Granite residual	Sand
3A	5.39072	100.2624	7/5/2016	Not rain within 12 hours	Forest	Granite residual	Sand
6A	5.43747	100.2915	7/5/2016	Not rain within 12 hours	Residential & business areas	Granite residual	Sand
7A	5.45284	100.3037	7/5/2016	Not rain within 12 hours	Residential & business areas	Quaternary deposit	Sand
8A	5.45375	100.2923	7/5/2016	Not rain within 12 hours	Residential & business areas	Granite residual	Sand
9A	5.45959	100.2865	5/6/2016	Not rain within 10 hours	Residential & business areas	Granite residual	Sand
11A	5.47343	100.2577	5/6/2016	Not rain within 10 hours	Residential & business areas	Granite residual	Sand
12A	5.46742	100.2494	7/5/2016	Not rain within 2 hours	Residential & business areas	Granite residual	Sand
13A	5.46225	100.2214	7/5/2016	Not rain within 2 hours	Residential & business areas	Quaternary deposit	Sand
15A	5.44992	100.205	7/5/2016	Not rain within 2 hours	Residential & business areas	Quaternary deposit	Sand
16A	5.43328	100.221	7/5/2016	Not rain within 5 hours	Forest	Granite residual	Sand
17A	5.394844	100.2159	7/5/2016	Not rain within 5 hours	Agriculture area	Quaternary deposit	Sand
18A	5.40952	100.1984	7/5/2016	Not rain within 5 hours	Residential & business areas	Quaternary deposit	Silty clay
19A	5.399599	100.2133	7/5/2016	Not rain within 6 hours	Residential & business areas	Quaternary deposit	Sand
21A	5.34261	100.3032	8/5/2016	Not rain within 8 hours	Residential & business areas	Quaternary deposit	Sand

Table 3.1, continued

Sample name	Latitude	Longitude	Sampling time	Weather	Land use type	Soil geology type	Soil particle type
23A	5.31667	100.2679	8/5/2016	Not rain within 8 hours	Residential & business areas	Quaternary deposit	Sand
25A	5.33789	100.2651	8/5/2016	Not rain within 8 hours	Agriculture area	Granite residual	Sand
26A	5.33121	100.2773	8/5/2016	Not rain within 8 hours	Residential & business areas	Quaternary deposit	Sand
27A	5.32478	100.2993	8/5/2016	Not rain within 10 hours	Industry	Quaternary deposit	Sand
28A	5.29625	100.2888	8/5/2016	Not rain within 10 hours	Industry	Quaternary deposit	Sand
29A	5.38436	100.3123	8/5/2016	Not rain within 10 hours	Residential & business areas	Quaternary deposit	Sand
30A	5.415886	100.3435	8/5/2016	Not rain within 12 hours	Residential & business areas	Granite residual	Sand
33A	5.41	100.3201	8/5/2016	Not rain within 12 hours	Residential & business areas	Quaternary deposit	Sand
35A	5.34222	100.2238	4/6/2016	Not rain within 24 hours	Residential & business areas	Granite residual	Sand
36A	5.346	100.2059	4/6/2016	Not rain within 24 hours	Agriculture area	Quaternary deposit	Silty clay
37A	5.35733	100.1993	4/6/2016	Not rain within 24 hours	Agriculture area	Quaternary deposit	Silty clay
38A	5.31286	100.2949	4/6/2016	Not rain within 24 hours	Industry	Quaternary deposit	Sand
39A	5.29578	100.2681	4/6/2016	Not rain within 24 hours	Airport	Quaternary deposit	Sand
40A	5.417323	100.3121	9/7/2016	Not rain within 12 hours	Residential & business areas	Quaternary deposit	Sand
41A	5.426306	100.2969	9/7/2016	Not rain within 12 hours	Residential & business areas	Quaternary deposit	Sand

3.4.1 Soil physicochemical properties analysis

3.4.1.1 Particle size distribution

Particle size distribution analysis was done in compliance to British Standard 1377 method (BS 1377-2, 1990). British Standard 1377 method was prepared according to the Road Engineering Standards Policy Committee which comprise of many methods for soil testing including general requirements and sample preparations, soil classification tests and, chemical and electro-chemical tests (BS 1377-1, 1990; BS 1377-2, 1990; BS 1377-3, 1990).

In the sieving test, the soil samples were dried up in the oven at 105 °C for three days to remove water content except for mud soil samples. The dried soil samples were disaggregated before being sieved. The test sieves are complied with BS 410 with the pan size of 5 mm, 3.35 mm, 2 mm, 1.18 mm, 600 μm, 425 μm, 300 μm, 212 μm, 150 μm and 63 μm (BS 1377-2, 1990). The mass of the soils left on each pan were determined and recorded after processed in mechanical sieve shaker.

The percentage of silt and clay particles (< 63 μm) from the sieve test and other mud soil sample were determined by using laser particle size analyser, Malvern Mastersizer, and the results were merged with those obtained from sieving. The percentage of silt and clay particles in mud soil sample was also determined by using laser particle-measure instrument, Malvern (Pansu & Gautheyrou, 2006).

The variability of particle size distribution can be characterized statistically in terms of mean (average size), median (mid-point of grain size distribution), kurtosis (degree of flatness of the grains relative to the average) and standard deviation (the sorting of the sizes around the average) (Lucian, 2017). Median corresponds to the 50 % percentile diameter or 50 % of the total frequency on the cumulative curve (Lucian, 2017). Mean, kurtosis, standard deviation of particle size distribution of this study was calculated according to Folk and Ward in 1957 with following equations (Lucian, 2017):

$$\emptyset_m = \frac{\emptyset_{16} + \emptyset_{50} + \emptyset_{84}}{3} \qquad (1)$$

$$K = \frac{\emptyset_{95} - \emptyset_5}{244(\emptyset_{75} - \emptyset_{25})} \qquad (2)$$

$$S = \frac{\emptyset_{84} - \emptyset_{16}}{4} + \frac{\emptyset_{95} - \emptyset_5}{6.6} \qquad (3)$$

Where,

$\emptyset_x$ = The grain diameter in phi units at the cumulative percentile value of x.

$\emptyset_m$ = Mean grain size.

K = Kurtosis.

S = Standard deviation.

The ∅ (phi) unit was calculated as following equation (Lucian, 2017):

$$\emptyset = -\left[\frac{Log_{10} d}{Log_{10} 2}\right] \qquad (4)$$

Where,

$\emptyset$ = Particle size in Ø units.

D = Diameter of particle in mm.

The result of mean, kurtosis and standard deviation will determine the characteristics of the soil samples which the classification is represented in **Table 3.2**. Percentage of sand, silt and clay for each soil sample result was plotted on the United States Department of Agriculture (USDA) soil triangle diagram as shown in **Figure 3.7** to classify the type of the soil sample particle distribution (Pansu & Gautheyrou, 2006).

Table 3.2: Classifications of mean, standard deviation and kurtosis values of soil in phi unit (Lucian, 2017).

Mean		Standard deviation		Kurtosis	
Value	**Classification**	**Value**	**Classification**	**Value**	**Classification**
-12 to -8	Boulder	Under 0.35	Very well sorted	Under 0.67	Very platykurtic
-8 to -6	Cobble	0.35 to 0.50	Well sorted	0.67 to 0.90	Platykurtic
-6 to -2	Pebble	0.50 to 0.71	Moderately well sorted	0.90 to 1.11	Mesokurtic
-2 to -1	Granular	0.71 to 1.0	Moderately sorted	1.11 to 1.50	Leptokurtic
-1 to 0	Very coarse grained	1.0 to 2.0	Poorly sorted	1.50 to 3.00	Very leptokurtic
0 to 1.0	Coarse grained	2.0 to 4.0	Very poorly sorted	Over 3.00	Extremely leptokurtic
1.0 to 2.0	Medium grained	Over 4.0	Extremely poorly sorted		
2.0 to 3.0	Fine grained				
3.0 to 4.0	Very fine grained				
5.0 to 6.0	Medium silt				
6.0 to 7.0	Fine silt				
7.0 to 8.0	Very fine silt				
Over 8.0	Clay				

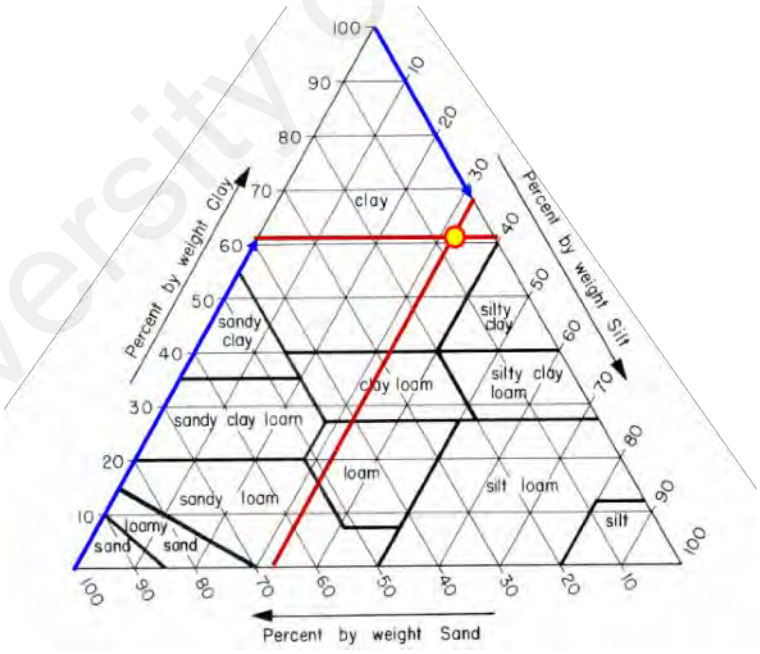

Figure 3.7: United States Department of Agriculture (USDA) soil triangle diagram.

Figure 3.8: Laser particle size analyser (Malvern Mastersizer).

Figure 3.9: Test sieves and mechanical sieve shaker.

3.4.1.2 Soil pH

Soil sample pH was determined by using aqueous soil suspensions method recommended by the international standard NF ISO 10390 (1994) (Pansu & Gautheyrou, 2006). Before soil pH analysis, the soil sample was dried at room temperature for three days and sieved to minus 2 mm. About 10 g of the soil sample was put in a test tube and filled with ultra-pure water with ratio of 1:5 (soil:water). The soil sample was placed on oscillating table and shaken for one hour. Then, the sample was left about two hours to let the residues to settle down before measurement of pH by using Fisher Scientific Accumet AB150 pH benchtop meters.

3.4.1.3 Organic matter (OM)

Organic matter (OM) content of soils was analysed using loss on ignition (LOI) method following the British Standard 1377 (BS 1377-3, 1990). The soil samples were prepared by drying the samples in oven at 105 °C for three days to remove the moisture. The dried soil samples were disaggregated and pulverized to pass through 2 mm nylon mesh. The initial mass of the soil sample (weight about 20 g) before the ignition process was determined and the soil samples placed in the crucible. The soil samples were heated up in a furnace at 440 °C for four hours. Then, the soil samples were cooled to room temperature before measuring the mass. The weight differences in soil samples of initial and after the ignition process were calculated. The percentages (%) of the weight differences were calculated which represent the percentage of the OM content in the soil. Triple procedures and measurements were done for each soil samples to get the representative results.

3.4.1.4 Cation exchange capacity (CEC)

Cation exchange capacity (CEC) of the soil samples were determined by using methylene blue spot test following NF P 94-068 method of Association Française de Normalisation (AFNOR) standard (Yukselen & Kaya, 2008). The soil samples were

dried in oven at 105 °C for 24 hours. The dried soil samples were disaggregated and homogenized to pass through 2-mm nylon mesh. Then, the soil samples were crushed and pulverized by using pestle and mortar, and sieved to 0.420 mm. The powdered soil samples were weighted to 7.5 g and mixed with 50 ml of ultra-pure water in a beaker. The mixture of soil samples and ultra-pure water were stirred by magnetic stirrer for one minute. A methylene blue solution was made by dissolving 5 g of methylene blue powder in 500 ml of ultra-pure water. The methylene blue solution was stirred by using magnetic stirrer for a minute.

About 5 ml of methylene blue solution was added to the soil sample solution and stirred again for a minute. After that, one drop of the mixture of methylene blue and sample solution was put on a filter paper to observe the feature of the absorbed drop spot. Addition more of the methylene blue solution to the soil sample solution was repeated (5 ml each time) until the light blue halo around dark blue spot appearance was represented by the drop spot. The appearance means that the test is positive which indicates the soil sample has fully absorbed methylene blue particles and has no longer absorb more excessive amount of the methylene blue. Amount of methylene blue solution which gives the positive result was recorded.

The CEC value for soil sample was calculated according to the Eq. (5) (Yukselen & Kaya, 2008):

$$C = \frac{100}{m_s} V_{cc} N_{mb} \qquad (5)$$

Where,

C = the cation exchange (meq /100 g soil)

m_s = weight of the sample (in grams)

V_{cc} = the volume of methylene blue added (ml)

N_{mb} = the normality of methylene blue substance (meq / ml)

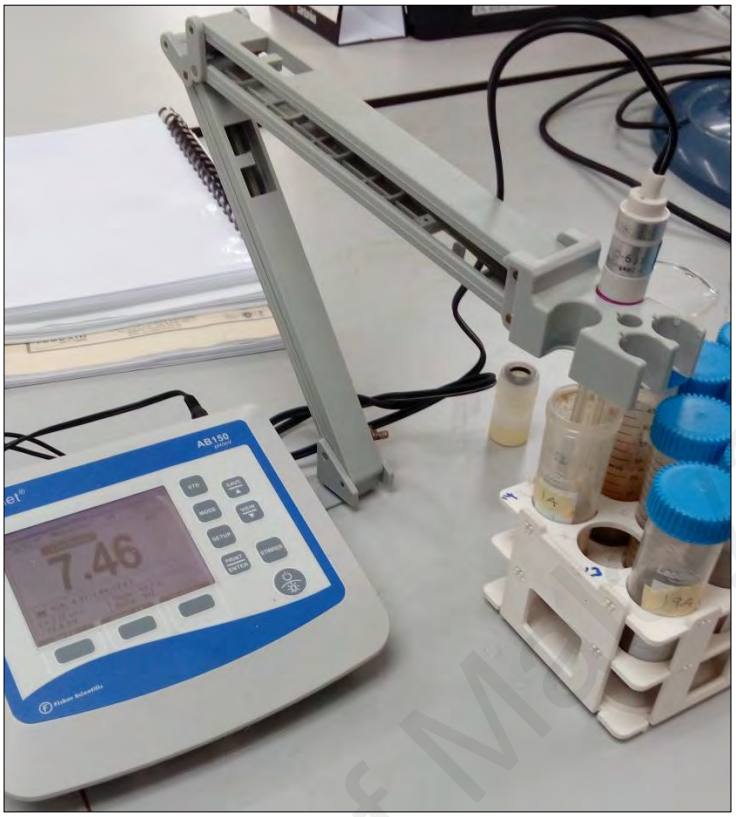

Figure 3.10: Measuring soil pH using Fisher Scientific Accumet AB150 pH benchtop meters.

Figure 3.11: Furnace used for loss on ignition (LOI) analysis.

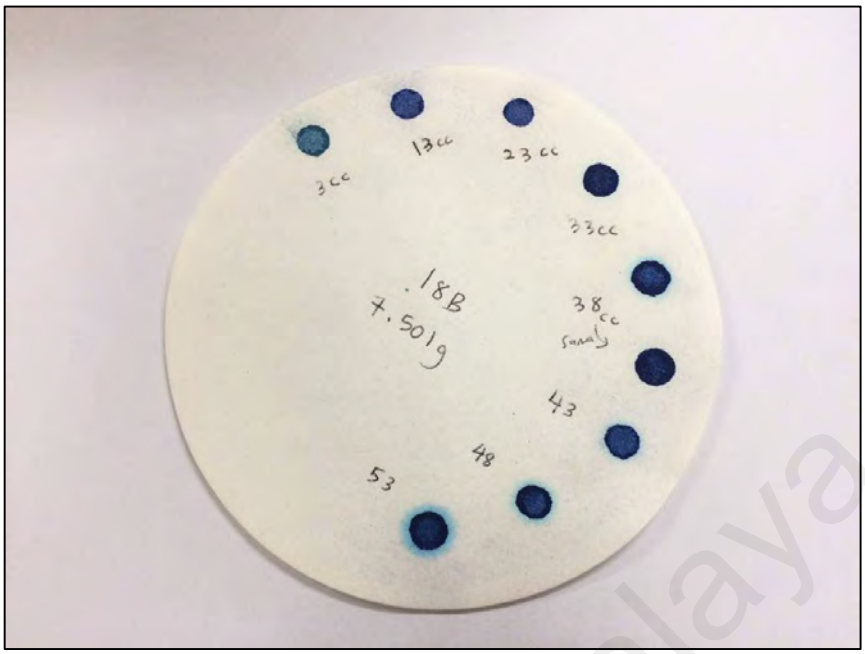

Figure 3.12: The spots of methylene blue and soil sample solution mixture on the filter paper.

3.4.2 Total concentration analysis

3.4.2.1 Soil sample total digestion procedure

The soil sample was digested before undergo total concentration analysis. Before digestion of soil sample, the soil was dried in oven at 40 °C for three days. Then, the soil was sieved to 2 mm and crushed using mortar until it becomes finer particles to pass through 0.063 mm nylon mesh. The powdered soil was weighed to about 0.02 g and placed in polytetrafluoroethylene (PTFE) weighing boat. The weighing boat with filled soil was put in a vessel. Then, the aqua regia mixture which combines nitric acid and hydrochloric acid in ratio of 1:3 was added in the vassel before the soil was digested in a microwave. The ratio of nitric acid and hydrochloric acid that used for digestion process in this analysis was proposed in 3051A method of United States of Environmental Protection Agency (USEPA) (Pansu & Gautheyrou, 2006). In this study, Perkin Elmer Titan Microwave Digestion System was used to digest the soil sample as shown in **Figure 3.12**. The digested soil solution was cooled to room temperature. After that, the digested soil solution was filtered to remove the residues and placed in a clean

test tube. 1 ml from the concentrated soil solution was poured into volumetric flask and diluted with 100 ml of ultra-pure water. The prepared soil solution was ready for total concentration analysis.

3.4.2.2 Heavy metals and REE analysis

Inductively coupled plasma mass spectrometry (ICP-MS) (Agilent Technologies 7500 Series) was used to measure the total concentration of selected heavy metals (As, Pb, Ni and Cd) and REE (La, Ce, Nd, Eu, Tb, Dy and Er) in the soil solution. All calibration standards were prepared from the Agilent multi element calibration standard 8500-6944 containing As, Pb, Ni, Cd, La, Ce, Nd, Tb, Dy, Er and Eu in 5 % HNO3. The stocks of the standard solution were prepared for the concentration of 10 ppb, 30 ppb, 50 ppb, 75 ppb and 100 ppb (10 mg/L = 10 ppm = 10000 ppb) which diluted by ultra-pure water for determining the concentration of elements in the digested soil samples.

Analytical precision estimated by duplicate analysis of three random samples was lower than 15.7 % for all analysed elements. The prepared blanks were always below instrumental detection limits. In order to ensure good reproducibility of ICP-MS and validate the method for determining the concentration of selected elements, Buffalo River Sediment Reference Material (SRM) 8704 was used troughout this work. SRM 8704 is one of environmental certified reference materials that can be used in calibration of ICP-MS (Turk et al., 2001). All of the information results of calibration and percentage recovery of standard reference material were represented in section **3.4.3**. Results of the total concentration of heavy metals and REE were recorded in mg/Kg unit.

3.4.3 Quality control and assurance

The data obtained from all of the laboratory analyses was guaranteed through application of the recommended standard sampling procedure, certified standard

methods and laboratory quality control and assurance methods. Reagent blank analysis, sample recovery and analysis of replicates were also applied in laboratory procedure. Ultra-pure filtered water stabilized at 18.2 µs/cm was used in the laboratory analyses.

Analyses of pH, OM, particle size distribution, CEC and soil digestion for total concentration analysis were performed in the laboratories of Department of Geology, University of Malaya. Total concentration analysis of heavy metals and REE by ICP-MS was performed in the laboratory of Department of Chemistry, University of Malaya. All reagents used for soil digestion procedure were of analytical reagent grade (Merck, Germany).

For precision assessment of physicochemical properties analysis of soil, calculated Relative Percent Difference (% RPD) between two results of duplicate samples were ranged from 0.4 % to 20.8 %. The % RPD for total concentration analysis of heavy metals and REE ranged from 0.3 % to 15.7 %. ICP-MS instrument for total concentration analysis was calibrated using standard solutions containing known concentration of the selected analyte elements from Agilent Technologies. For linear calibration plot, five standards namely 10, 30, 50, 75 and 100 mg/ml were prepared. In the calibration plot, the correlation coefficient was from 0.9962 to 0.9999 depending on the element. The calibration plot for each element (heavy metal and REE) was presented in a graph as shown in **Appendix D**. Limits of detection was below 0.1 which represents accuracy among the data.

Standard certified references, SRM 8704 Buffalo River Sediment from National Institute of Standards and Technology, NIST USA was analysed during the total concentration analysis using ICP-MS for quality assurance purposes. Four replicates samples with mass of 0.02 g each, were analysed in a similar manner as other soil samples. The percentage recoveries of the elements in the samples ranged from 91.18 % (Ni) to 121.52 % (Pb) for heavy metals and 78.56 % (Ce) to 79.54 % (Eu) for REE

(**Table 3.3**). Concentration of certified material fell within the acceptable limit range (75 to 125 %) (United States Environmental Protection Agency (ESEPA), 2010). Therefore, the method employed in this work is reliable.

Table 3.3: Recovery (%) results of ICP-MS using SRM 8704 Buffalo River Sediment standard samples.

Element (mg/Kg)	Pb	Ni	Cd	Ce	Eu
Obtained values	182.3 ± 8.57	39.1 ± 1.39	2.9 ± 0.37	52.24 ± 0.6	1.04 ± 0.9
SRM 8704	150 ± 17	42.9 ± 3.7	2.94 ± 0.29	66.5 ± 2.0	1.31 ± 0.038
% recovery	121.52	91.18	98.68	78.56	79.54

Figure 3.13: Perkin Elmer Titan Microwave Digestion System.

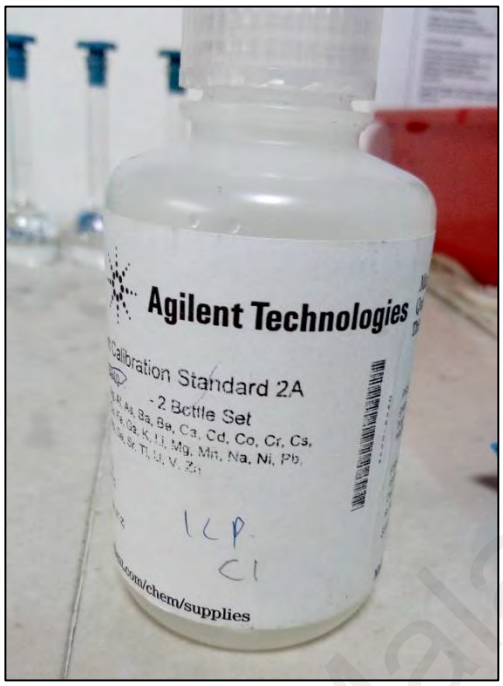

Figure 3.14: Agilent multi element calibration standard 8500-6944 containing As, Pb, Ni, Cd, La, Ce, Nd, Tb, Dy, Er and Eu in 5 % HNO3.

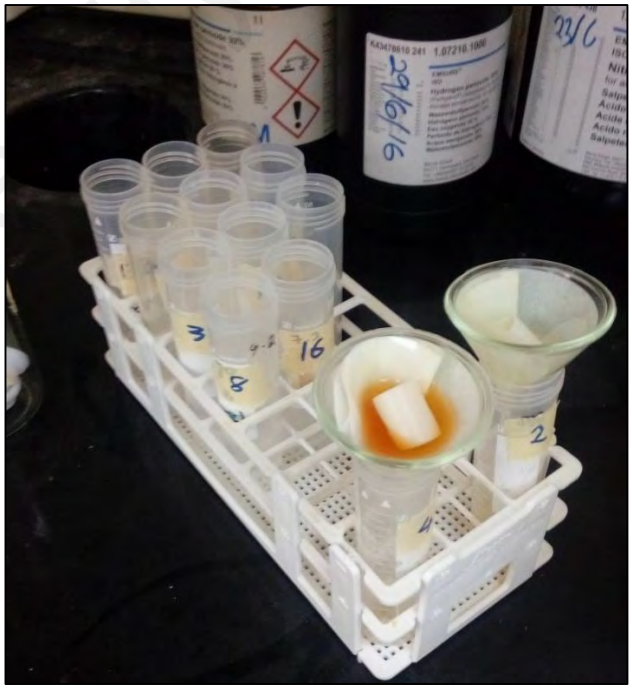

Figure 3.15: The digested soil solution was filtered into a test tube in soil sample digestion analysis. The procedure was done in fume cupboard.

Figure 3.16: Preparation of the stocks of standard solution to calibrate ICP-MS.

Figure 3.17: Inductively Coupled Plasma Mass Spectrometry (ICP-MS) machine (Agilent Technologies 7500 Series).

3.5 Spatial distribution analysis

Spatial distribution map of heavy metals and REE concentrations in top soils of Penang Island were generated using Surfer 11 software (Golden Software Inc., Colorado). Grid file was constructed to create a grid based map. Spaced XYZ data in the grid file were taken randomly and regularly. Grid node is located at a particular XY location which associated with Z value.

Different options for gridding methods can be selected in Surfer and each option has its own set of gridding options. Kriging interpolation technique which one of the gridding methods was applied in generating spatial distribution maps which provide the best linear unbiased estimates for spatial variables. This method also offers an automatic variogram modelling technique to express spatial variation and minimizes the error of predicted values which are estimated by spatial distribution (Webster & Oliver, 2001). Linear variogram model with slope of 0.096 were applied for all heavy metals and REE distribution data in Kriging gridding method. The spatial data in this study are the measured concentrations of selected heavy metals and REE in the top soils. The unknown concentration (linear regression estimator), $Z^*(u)$ is obtained by kriging and can be defined as (Eq 6) (Ramanitharan et al., 2005):

$$Z^*(u) - m(u) = \sum_{\alpha=1}^{N(h)} \lambda_\alpha [Z(u_\alpha) - m(u_\alpha)] \qquad (6)$$

Where, λ_α is weight assigned to the measured concentration $Z(u_\alpha)$, which is interpreted as a realization of the random variables, $Z(u_\alpha)$. The means, $m(u)$ and $m(u_\alpha)$ are the expected values of the random variables, $Z^*(u)$ and $Z(u_\alpha)$ and the mean $m(u)$ is used to represent the large scale variation or trend in the data (Ramanitharan et al., 2005).

The negative Z values for some heavy metals data were eliminated by clamping the grid values with formula max (A,0). Spatial distribution maps with defined range of concentrations (in mg/Kg) were constructed for heavy metals and REE. Distribution

patterns and high concentration area of heavy metals and REE in top soils of Penang Island was determined from the generated maps.

3.6 Contamination level assessment

Contamination level assessment of selected heavy metals and REE was evaluated in spatial distribution analysis. Three types of assessments were employed in this study including contamination factor (CF), geo-accumulation index (I_{geo}) and pollution load index (PLI). The assessments were computed using Microsoft Excel. Distributions of CF and I_{geo} of heavy metals and REE in top soils of Penang Island were mapped using Surfer 11 software (Golden Software Inc., Colorado) to identify the potentially polluted areas based on the contamination level results. The mapping techniques that used for CF and I_{geo} distribution values of heavy metals and REE were similar with the techniques applied for spatial distribution analysis.

3.6.1 Contamination factor (CF)

Contamination factor (CF) was calculated as proposed by Hakanson (1980) as shown in Eq. (7) below:

$$C_f = C_i/B_i \qquad (7)$$

Where,

C_f = Contamination factor (CF) value

C_i = The element concentration

B_i = Background value of the element

Result of CF value was described as following levels (Hakanson, 1980; Pekey et al., 2004):

$C_f < 1$ = No element enrichment

$1 \leq C_f < 3$ = Moderate contamination

$3 \leq C_f < 6$ = Considerable contamination

$C_f \geq 6$ = Very high contamination

3.6.2 Geo-accumulation index (I_{geo})

Equation of I_{geo} was proposed by Müller (1969) like following formula Eq. (8):

$$I_{geo} = \log_2(\frac{C_i}{1.5 \times B_i}) \quad (8)$$

Where,

I_{geo} = Geo-accumulation index (I_{geo}) value

C_i = The element concentration

B_i = Background value of the element

I_{geo} value was determined as following indicator (Müller, 1969):

$I_{geo} \leq 0$ = Unpolluted

$0 < I_{geo} \leq 1$ = Unpolluted to moderately polluted

$1 < I_{geo} \leq 2$ = Moderately polluted

$2 < I_{geo} \leq 3$ = Moderately to strongly polluted

$3 < I_{geo} \leq 4$ = Strongly polluted

$4 < I_{geo} \leq 5$ = Strongly to extremely polluted

$I_{geo} > 5$ = Extremely polluted

3.6.3 Pollution load index (PLI)

PLI was proposed by Liu et al. (2005) with the equation of Eq. (9):

$$PLI = \sqrt[n]{C_{f1} \times C_{f2} \times \dots\dots\dots \times C_{fn}} \quad (9)$$

Where,

PLI = Pollution load index (PLI) value

C_f = Contamination factor value

n = Number of sample

The PLI value of more than one is classified as polluted site whereas the PLI value of less than one is classified as unpolluted site (Harikumar et al., 2009).

3.6.4 Background value

Background value, B_i for heavy metals and REE concentration in soils were determined using statistical method proposed by Reimann et al. (2005) since the geochemical baseline data for the study area has not been established. Rule of [median ± 2 median absolute deviations (MAD)] was used to determine the background value of heavy metals and REE. According to Reimann et al. (2005), normal distribution data is desirable before any threshold estimation methods are applied. The concentration value of heavy metals and REE which not followed normal distribution was log-transformed before [median ± 2 MAD] was applied. Then, the result of the calculation was anti-logged to get the natural numbers (Reimann et al., 2005).

Heavy metals and REE background values, B_i are shown in **Table 3.4**. As the raw dataset of heavy metals and REE did not pass normality test, log transformation was applied to all dataset before substituting in [median ± 2 (MAD)] calculation. After calculation of [median ± 2 (MAD)], all results were antilog transformed to get the natural data.

Table 3.4: Background value of heavy metals and REE calculated from [median ± 2 median absolute deviation (MAD)] equation.

Heavy metals (mg/Kg)	Background value
As	691.8
Pb	182.0
Ni	29.5
Cd	2.5
REE (mg/Kg)	
La	134.9
Ce	331.1
Nd	131.8
Eu	1.95
Tb	2.95
Dy	13.80
Er	6.46

3.7 Statistical analysis

3.7.1 Principal component analysis (PCA)

Principal component analysis (PCA) was used to identify the relationship among heavy metals and also relationship among REE in spatial distribution analysis. In this analysis, high dimensionality of complex dataset of heavy metals and REE was reduced and transformed into orthogonal components (Slavkovic´ et al., 2004; Ağca, 2015). PCA is one of multivariate statistical analysis which requires the normal distribution of variables (Webster & Oliver, 2001). Therefore, the dataset of heavy metals and REE total concentrations was tested for their normality distributions before PCA. In this case, Shapiro-Wilk's test was used to test the normality of heavy metals and REE data due to the total of the samples were not more than 50 samples.

The data that showed non-normal distribution was transformed using logarithmic transformation (log transform) and/or Box-Cox transformation (Box-Cox transform) to get more normal and less skewness data (Webster & Oliver, 2001; Zhang & McGrath, 2004; Wu & Zhang, 2010). According to Zhang and McGrath (2004), many studies showed that environmental variables were always does not follow lognormal distribution. The data was retested again by Shapiro-Wilk's test after transformation to ensure the normality of data.

In this study, the raw data of heavy metals did not pass Shapiro-Wilk's normality test (S-W $p < 0.05$). In order to obtain normality requirement for multivariate statistical analysis of PCA, the raw dataset of all heavy metals were log transformed. However, after log transformed, all heavy metals raw data still did not pass Shapiro-Wilk's normality test (S-W $p < 0.05$). The heavy metals raw dataset was Box-Cox transformed to decrease the skewness of the data before analysed in PCA. All REE raw dataset also did not pass Shapiro-Wilk's normality test (S-W $p < 0.05$). Therefore, all REE raw dataset were log transformed in order to obtain normality requirement for PCA, a

multivariate statistical analysis. The log transformed of all REE raw dataset did passed Shapiro-Wilk's normality test (S-W $p > 0.05$).

Correlation test of dataset was done before selecting the type of rotation. Promax rotation method was applied to the data that showed positive correlation (> 0.32) whereas varimax rotation method was applied to the data that showed negative correlation (< 0.32). The components that extracted from PCA and also rotated space diagram that generated from the analysis were used to determine the relationship among heavy metals or REE. PCA was performed using IBM SPSS Statistics 21 software.

3.7.2 Pearson correlation analysis

Pearson correlation analysis was done to determine strength of relationship among heavy metals and REE, and also relationship between heavy metals and REE with soil physicochemical properties. The coefficient correlation, r in test represented the strength of relationship between two variables. The result of Pearson correlation was compared to the PCA result. This analysis was done using IBM SPSS Statistics 21 software.

3.8 Summary

The methodology adopted in this research was explained throughout this chapter. Equipments and apparatus used in the study have been given. Sampling locations map, landuse map and geology map of the study area have been defined. Sampling, preservation followed by laboratory analysis have been elaborated in detail. Concentration level analysis of selected heavy metals and REE in soils have been described. Different contamination level assessments have been quoted in the equations. Quality control and assurance maintained throughout the research has also been explained. Statistical data analysis using Pearson correlation analysis and PCA has also been explained.

CHAPTER 4: RESULTS AND DISCUSSION

4.1 Introduction

This chapter describes and presents all results and explanation on analysis of selected heavy metals and REE distributions in top soils of Penang Island. Tables, diagrams and maps with provided scales and legends are included for all data presentations. The results were also interpreted and compared with other studies.

4.2 Physicochemical properties of soil samples

Summarized statistical result of measured physicochemical properties of top soil samples is shown in **Table 4.1** and the overall results are represented in **Appendix B**. The results showed the range of pH of the soils was 3.84 to 8.30 with mean value of 6.53, organic matter content (OM %) ranged from 1.14 to 17.05 % with mean value of 3.67 %, cation exchange capacity (CEC) ranged from 1.24 to 19.93 meq/g with mean value of 4.10 meq/g.

For particle size distribution of 31 top soil samples, the mean values of 28 samples were between -1 and 0 which classified as very coarse grained whereas the mean values of three samples were between 5.0 and 6.0 which classified as medium silt. Standard deviation values of 28 samples were ranged from 0.35 to 0.50 which classified as well sorted whereas standard deviation values of three samples were ranged from 2.0 to 4.0 which classified as very poorly sorted. Kurtosis of all 31 samples were under 0.67 which classified as very platykurtic particle. The median for 28 samples were categorized as sand whereas another three samples were categorized as silt. The grain classifications of 31 top soil samples were plotted in USDA diagram as shown in **Figure 4.1**. Twenty-eight samples were classified as sand type and three samples were classified as silty clay loam type.

Table 4.1: Summarized statistical results of physicochemical properties of top soil samples.

Soil property	Mean	Minimum	Maximum	Median	Standard deviation
pH	6.53	3.84	8.30	6.74	1.26
OM (%)	3.67	1.14	17.05	3.01	3.02
CEC (meq/g)	4.10	1.24	19.93	3.32	4.29

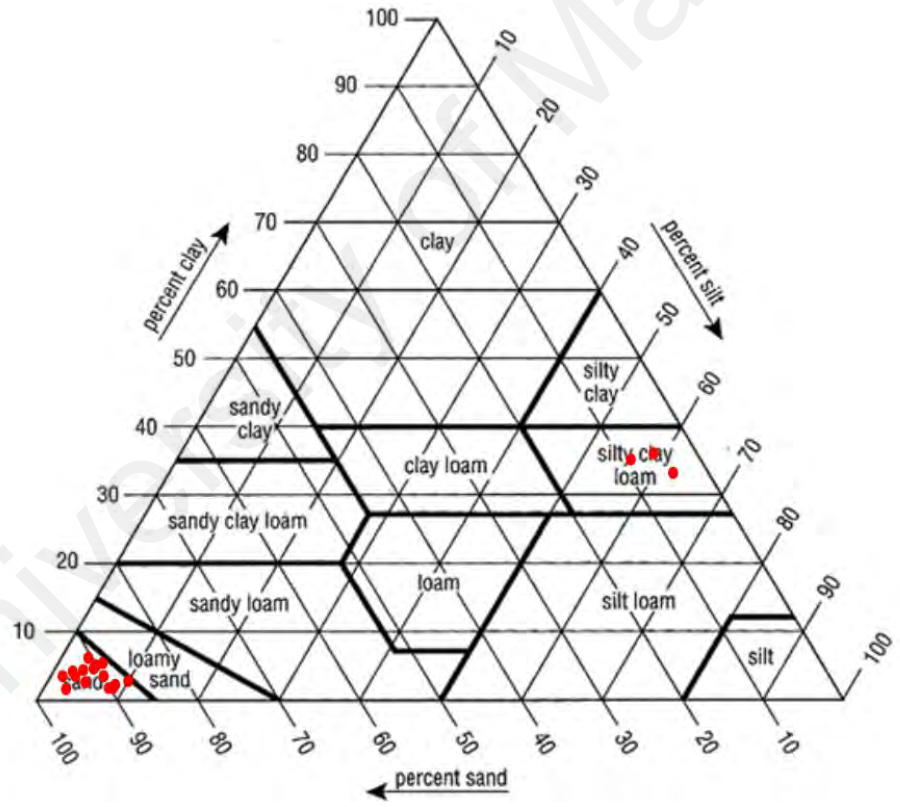

Figure 4.1: Classification of 31 top soil samples in triangular soil classification diagram of United States Department of Agriculture (USDA).

4.3 Concentration level

4.3.1 Concentration level of heavy metals

Summarized results of heavy metals concentration levels in top soils of Penang Island are shown in **Table 4.2**. The descending order of highest mean concentration level of heavy metals in top soils of Penang Island was Pb > As > Ni > Cd.

Concentration of As in top soils of Penang Island ranged from 67.9 to 2942.1 mg/Kg with mean value of 366.6 mg/Kg. In comparison with other urban top soils as shown in **Table 4.3**, minimum, maximum and mean concentration of As in top soils of Penang Island showed much higher than minimum, maximum and mean concentrations of Isfahan Province in Iran (Mehr et al., 2017), north east of Vaslui County in Romania (Ungureanu et al., 2016) and Rayong Province in Thailand (Simasuwannarong et al., 2012).

Concentration of Pb in top soils of Penang Island ranged from 42.1 to 7019.6 mg/Kg with mean value of 422.9 mg/Kg. In comparison with other urban top soils, concentration of Pb in top soils of Penang Island showed higher minimum, maximum and mean concentration values than top soils of Perlis in Malaysia (Mat Ripin et al., 2014), Yogyakarta in Indonesia (Budianta, 2012), Isfahan Province in Iran (Mehr et al., 2017), north east of Vaslui County in Romania (Ungureanu et al., 2016), Rayong Province in Thailand (Simasuwannarong et al., 2012) and Hangzhou city in China (Lu & Bai, 2010). However, among these compared urbans, Isfahan Province showed the nearest range and mean value of Pb concentration with range and mean value of Pb concentration in Penang Island (Mehr et al., 2017).

Concentration of Ni in top soils of Penang Island ranged from 6.5 to 1049.2 mg/Kg with mean value of 51.7 mg/Kg. In comparison with other urban top soils, concentration of Ni in top soils of Penang Island showed higher minimum and maximum values than

minimum and maximum concentrations of Ni in top soils of Perlis in Malaysia (Mat Ripin et al., 2014), Isfahan Province in Iran (Mehr et al., 2017) and north east of Vaslui County, Romania (Ungureanu et al., 2016). In top soils of northern Europe, concentration of Ni ranged up to 2690 mg/Kg which showed higher maximum value than maximum concentration of Ni in top soils of Penang Island (FOREGS, 2005). However, mean concentration of Ni in top soils of Penang Island showed lower than mean concentration of Ni in top soils of Isfahan Province (Mehr et al., 2017) but higher than mean concentration of Ni in top soils of north east of Vaslui County (Ungureanu et al., 2016). The value of mean concentration of Ni in top soils of Penang Island also showed not much variation with mean value of Ni concentration in top soils of both Isfahan Province (Mehr et al., 2017) and north east of Vaslui County (Ungureanu et al., 2016).

Concentration of Cd in top soils of Penang Island ranged from 0.2 to 16.7 mg/Kg with mean value of 1.6 mg/Kg. In comparison with other urban top soils, the range of Cd concentration in Penang Island showed nearest to the range of Cd concentration in Rayong Province, Thailand (Simasuwannarong et al., 2012) and northern Europe (FOREGS, 2005). The nearest mean of Cd concentration to the Penang Island was Hangzhou city, China which showed 1.20 mg/Kg (Lu & Bai, 2010). Among the compared urbans, Isfahan Province, Iran, showed higher maximum value of Cd concentration than Penang Island (Mehr et al., 2017). The lowest mean concentration of Cd among the compared urbans is represented by Perlis, Malaysia which the value is 0.06 mg/Kg (Mat Ripin et al., 2014).

Table 4.2: Summarized statistical results of concentration level of heavy metals in top soil samples of Penang Island (n = 31).

Heavy metal (mg/Kg)	Mean	Minimum	Maximum	Median	Standard deviation
As	366.6	67.9	2942.1	190.9	544.7
Pb	422.9	42.1	7019.6	100.0	1326.0
Ni	51.7	6.5	1049.2	13.6	186.1
Cd	1.6	0.2	16.7	0.6	3.0

Table 4.3: Comparison of range (R) and mean (M) concentrations of heavy metals in top soils of Penang Island with other urban areas.

Urban area	As (mg/Kg)	Pb (mg/Kg)	Ni (mg/Kg)	Cd (mg/Kg)	References
Perlis, Malaysia	-	R: 0.39 – 27.47 M: 2.58	R: 0.69 – 2.40 M: 1.57	R: 0 – 0.63 M: 0.06	Mat Ripin et al. (2014)
Yogyakarta, Indonesia	-	R: 16 – 95.20 M: 65.4	-	-	Budianta (2012)
Isfahan Province, Iran	R: 5.00-178.90 M: 16.17	R: 18.54-1929.86 M: 179.97	R: 26.40-125.60 M: 61.65	R: 0.25-74.72 M: 2.17	Mehr et al. (2017)
North east of Vaslui County, Romania	R: 6.70-16.30 M: 10.14	R: 16-84 M: 25.27	R: 24.00-73.00 M: 47.36	R: 0.02-0.80 M: 0.32	Ungureanu et al. (2016)
Rayong Province Thailand	R: 0.12-94.41 M: 26.23	R: 0.06-134.77 M: 19.97	-	R: 0.03-12.60 M: 3.56	Simasuwannarong et al. (2012)
Hangzhou city, China	-	R: 15.40-492.10 M: 88.20	-	R: 0.65-4.57 M: 1.20	Lu and Bai (2010)
Northern Europe	R: 0.32-282	R: 5.3-970	R: up to 2690	R: up to 14.1	FOREGS (2005)
This study, Penang Island	R: 67.9-2942.1 M: 366.6	R: 42.1-7019.6 M: 422.9	R: 6.5-1049.2 M: 51.7	R: 0.2-16.7 M: 1.6	This Study

Summarized results of heavy metals concentration levels in granite residual and Quaternary deposit top soils of Penang Island are shown in **Table 4.4** and **Table 4.5** respectively.

From the result of heavy metals concentration in granite residual soils and Quaternary deposit soils, the mean concentration of As in granite residual soils showed greater than the mean concentration of As in Quaternary deposit soils. According to FOREGS (2005), As is not preferentially enriched in felsic and mafic igneous rocks. In granitic rock, the concentration of As generally range from 1.5 to 1.9 mg/Kg (FOREGS, 2005). Concentration of As in granitic rock of Penang Island ranged from 0 to 3 mg/Kg (Cobbing et al., 1992; Ghani et al., 2013; Ng et al., 2015). Therefore, As is expected not derived from the granite parent rock. However, As in ionic form can easily replace other elements in primary rock-forming silicate minerals such as replacement of Fe^{3+} or Al^{3+} by As^{3+} (FOREGS, 2005). The granitic rock of Penang Island also contains apatite mineral which the substitution of P^{5+} by As^{5+} may elevated the concentration of As in this phosphate mineral (Cobbing et al., 1992; FOREGS, 2005).

The mean concentration of Pb in Quaternary deposit soils showed greater than the mean concentration of Pb in granite residual soils. The concentration Pb in granitic rock is generally low as 15 to 19 mg/Kg (FOREGS, 2005). Concentration of Pb in granitic rock of Penang Island ranged from 16.6 to 47 mg/Kg (Cobbing et al., 1992; Ghani et al., 2013; Ng et al., 2015). The species of Pb is mainly associated with clay minerals, Mn oxides, Fe and Al hydroxides and organic matter which are more abundant in Quaternary deposit than granite residual soil (FOREGS, 2005).

The mean concentration of Ni in Quaternary deposit soils showed greater than the mean concentration of Ni in granite residual soils. Ni concentration in granitic rock is generally low as 4.5 to 15 mg/Kg (FOREGS, 2005). Concentration of Ni in granitic rock of Penang Island ranged from 2 to 28.3 mg/Kg (Cobbing et al., 1992; Ghani et al.,

2013; Ng et al., 2015). Ni is commonly associated with Fe and Mn oxides especially in surface soil horizons and occur mainly in organically bound forms (FOREGS, 2005).

The mean concentration of Cd in granite residual soils showed not much variation (± 0.1) with the mean concentration of Cd in Quaternary deposit soils. Cd concentration in granitic rock is generally low typically 0.09 mg/Kg (FOREGS, 2005). In the surface environment, humic substance may bind Cd^{2+} strongly especially at high pH levels and Cd also can be absorbed by clay minerals and iron oxyhyroxide (FOREGS, 2005).

The descending order of highest maximum concentration of heavy metals in granitic rock of Penang Island was Pb > Ni > As where Cd concentration data not recorded (Cobbing et al., 1992; Ghani et al., 2013; Ng et al., 2015). The descending order is not similar to the descending order of highest average concentration of heavy metals in top soils of Penang Island (this study). In addition, the range concentration of heavy metals in the granitic rock of Penang Island were very low than the range concentration of heavy metals in top soils of Penang Island. It indicates that there will be anthropogenic source that contributes to the increase of heavy metals concentration in top soils of Penang Island.

Table 4.4: Summarized statistical results of concentration level of heavy metals in granite residual top soils of Penang Island (n = 12).

Heavy metal (mg/Kg)	Mean	Minimum	Maximum	Median
As	646.5	76.6	2942.1	288.9
Pb	351.1	66.8	2933.7	103.0
Ni	26.1	6.5	104.5	15.6
Cd	1.5	0.3	4.7	0.7

Table 4.5: Summarized statistical results of concentration level of heavy metals in Quaternary deposit top soils of Penang Island (n = 19).

Heavy metal (mg/Kg)	Mean	Minimum	Maximum	Median
As	189.8	67.9	522.6	135.4
Pb	468.3	42.1	7019.6	94.6
Ni	67.9	6.5	1049.2	12.6
Cd	1.6	0.2	16.7	0.6

Table 4.6: Comparison of mean (M) and range (R) concentrations of heavy metals in granite residual top soils of Penang Island with granite parent rock.

Sample	As (mg/Kg)	Pb (mg/Kg)	Ni (mg/Kg)	Cd (mg/Kg)	References
Granite rock	R: 1.5-1.9	R: 15-19	R: 4.5-15	M: 0.09	FOREGS (2005) (Europe)
Penang Island Granite (parent rock)	R: 0-3	R: 16.6-47	R: 2-28.3	-	Cobbing et al. (1992); Ghani et al. (2013); Ng et al. (2015)
This study, top soils of Penang Island	M: 646.5 R: 76.6-2942.1	M: 351.1 R: 66.8-2933.7	M: 26.1 R: 6.5-104.5	M: 1.5 R: 0.3-4.7	This Study

4.3.2 Concentration level of REE

Summarized REE concentration level results in top soils of Penang Island are shown in **Table 4.7**. Among REE, the descending order of highest mean concentration level in top soils of Penang Island was Ce > La > Nd > Dy > Er > Tb > Eu and which LREE showed higher average concentration level than HREE.

La concentration in top soils of Penang Island ranged from 34.0 to 218.9 mg/Kg with mean value of 82.1 mg/Kg. In comparison with other urban top soils as shown in **Table 4.8**, mean concentration of La in in top soils of Penang Island showed greater than mean concentration of La in top soils of Rodrigo de Gáspari public park (Figueiredo et al.,

2009), Buenos Aires public park (Figueiredo et al., 2009), Chico Mendes public park (Figueiredo et al., 2009), London (Yuan et al., 2017), Sweden and Europe (Sadeghi et al., 2013). However, among these urban areas, mean concentration of La in Rodrigo de Gáspari public park showed nearest to mean concentration of La in Penang Island which is 67.5 ± 11.9 mg/Kg (Figueiredo et al., 2009). Rodrigo de Gáspari public park, Buenos Aires public park, Chico Mendes public park showed minimum La concentration values near to the minimum La concentration value of Penang Island which were 48.0 mg/Kg, 23.3 mg/Kg and 21.3 mg/Kg respectively (Figueiredo et al., 2009). London (Yuan et al., 2017) and Europe (Sadeghi et al., 2013) showed the maximum La concentration values nearer to the maximum La concentration in Penang Island than other urbans which the values were 130.0 mg/Kg and 143.0 mg/Kg respectively.

Ce concentration in top soils of Penang Island ranged from 70.1 to 602.3 mg/Kg with mean value of 191.2 mg/Kg. In comparison with other urbans, mean and maximum values of Ce concentration in top soils of Penang Island showed greater than mean and maximum values of Ce concentration in top soils of Rodrigo de Gáspari public park (Figueiredo et al., 2009), Buenos Aires public park (Figueiredo et al., 2009), Chico Mendes public park (Figueiredo et al., 2009), London (Yuan et al., 2017), Sweden and Europe (Sadeghi et al., 2013). However, Rodrigo de Gáspari public park showed minimum and mean concentrations of Ce near to minimum and mean concentrations of Ce in Penang Island which the values were 85.0 mg/Kg and 144.8 ± 38.9 mg/Kg respectively (Figueiredo et al., 2009).

Nd concentration in top soils of Penang Island ranged from 28.8 to 201.9 mg/Kg with mean value of 72.9 mg/Kg. Mean concentration of Nd in top soils of Penang Island showed higher than mean concentration of Nd in top soils of Rodrigo de Gáspari public park (Figueiredo et al., 2009), Buenos Aires public park (Figueiredo et al., 2009), Chico Mendes public park (Figueiredo et al., 2009), London (Yuan et al., 2017), Sweden and

Europe (Sadeghi et al., 2013). Both London (Yuan et al., 2017) and Europe (Sadeghi et al., 2013) showed the maximum Nd concentration values nearer to the maximum Nd concentration in Penang Island than other urbans which the values were 122.8 mg/Kg and 132.0 mg/Kg respectively.

Eu concentration in top soils of Penang Island ranged from 0.14 to 5.86 mg/Kg with mean value of 1.16 mg/Kg. In comparison with other urbans, mean concentration of Eu in top soils of Penang Island showed higher than Buenos Aires public park (Figueiredo et al., 2009), Chico Mendes public park (Figueiredo et al., 2009), Sweden and Europe (Sadeghi et al., 2013). However, Rodrigo de Gáspari public park showed mean concentration of Eu higher than mean concentration of Eu in Penang Island which the value was 1.99 ± 0.46 mg/Kg (Figueiredo et al., 2009). Among all compared urban areas, Europe showed maximum Eu concentration near to maximum concentration of Eu in Penang Island which the value was 6.99 mg/Kg (Sadeghi et al., 2013).

Tb concentration in top soils of Penang Island ranged from 0.77 to 6.23 mg/Kg with mean value of 2.01 mg/Kg. In comparison with other urban areas, mean concentration of Tb in top soils of Penang Island showed greater than mean concentration of Tb in Rodrigo de Gáspari public park (Figueiredo et al., 2009), Buenos Aires public park (Figueiredo et al., 2009), Chico Mendes public park (Figueiredo et al., 2009), Sweden and Europe (Sadeghi et al., 2013). Maximum Tb concentration in Penang Island represented about near to the value of maximum Tb concentration in Europe which was 7.01 mg/Kg (Sadeghi et al., 2013).

Dy concentration in top soils of Penang Island ranged from 3.12 to 24.20 mg/Kg with mean value of 8.57 mg/Kg. Mean concentration of Dy in top soils of Penang Island showed greater than mean concentration of Dy in top soils of Sweden and Europe (Sadeghi et al., 2013). However, the maximum value of Dy concentration in Europe

showed higher than maximum Dy concentration in Penang Island which the value was 44.9 mg/Kg (Sadeghi et al., 2013).

Er concentration in top soils of Penang Island ranged from 0.99 to 12.63 mg/Kg with mean value of 4.16 mg/Kg. Mean concentration of Er in top soils of Penang Island showed higher than mean concentration of Er in top soils of Sweden and Europe (Sadeghi et al., 2013). However, the maximum Er concentration in Europe showed greater than maximum Er concentration in Penang Island which the value was 26.00 mg/Kg (Sadeghi et al., 2013).

Table 4.7: Summarized results of concentration level of REE in top soils of Penang Island (n=31).

	Mean	**Minimum**	**Maximum**	**Median**	**Standard deviation**
LREE (mg/Kg)					
La	82.1	34.0	218.9	78.0	38.4
Ce	191.2	70.1	602.3	172.7	103.5
Nd	72.9	28.8	201.9	69.0	36.1
HREE (mg/Kg)					
Eu	1.16	0.14	5.86	0.78	1.16
Tb	2.01	0.77	6.23	1.57	1.21
Dy	8.57	3.12	24.20	7.51	4.68
Er	4.16	0.99	12.63	3.57	2.48

Table 4.8: Comparison of mean (M) and range (R) concentrations of REE in top soils of Penang Island with other urban areas and the granite parent rock.

Urban area	La (mg/Kg)	Ce (mg/Kg)	Nd (mg/Kg)	Eu (mg/Kg)	Tb (mg/Kg)	Dy (mg/Kg)	Er (mg/Kg)	References
Top soils of Rodrigo de Gáspari public parks, São Paulo, Brazil	R: 48-85 M: 67.5 ± 11.9	R: 85-222 M: 144.8 ± 38.9	R: 34-68 M: 53.8 ± 12.0	R: 1.04-2.72 M: 1.99 ± 0.46	R: 0.61-1.01 M: 0.76 ± 0.12	-	-	Figueiredo et al. (2009)
Top soils of Buenos Aires public parks, São Paulo, Brazil	R: 23.3-28.5 M: 26.0 ± 2.7	R: 47.8-61.6 M: 56.1 ± 7.3	R: 16-19 M: 17.7 ± 1.5	R: 0.49-0.57 M: 0.52 ± 0.04	R: 0.38-0.61 M: 0.53 ± 0.13	-	-	Figueiredo et al. (2009)
Top soils of Chico Mendes public parks, São Paulo, Brazil	R: 21.3-39.8 M: 30.7 ± 6.2	R: 39-80 M: 62.7 ± 14.0	R: 12-23 M: 15.0 ± 4.4	R: 0.60-0.66 M: 0.46 ± 0.10	R: 0.39-0.52 M: 0.46 ± 0.05	-	-	Figueiredo et al. (2009)
London	R: 3.0-130.0 M: 25.2	R: 18.0-238.0 M: 50.9	R: 0.5-122.8 M: 22.3	-	-	-	-	Yuan et al. (2017)
Top soils of Sweden	R: 6.92-34.30 M:17.42	R: 13.80-83.00 M: 37.67	R: 6.71-31.80 M: 15.14	R: 0.24-1.29 M: 0.65	R: 0.22-1.08 M: 0.49	R: 1.48-6.18 M: 2.95	R: 0.95-3.96 M: 1.88	Sadeghi et al. (2013)
Top soils of Europe	R: 1.10-143 M: 25.9	R: 2.45-267 M: 52.2	R: 1.14-132 M: 22.4	R: 0.05-6.99 M: 0.85	R: 0.03-7.01 M: 0.64	R: 0.18-44.9 M: 3.58	R: 0.12-26.00 M: 2.10	Sadeghi et al. (2013)
Penang Island Granite	R: 21-63	R: 31-127	R: 17-47	R: 0.61-1.15	R: 0.72-1.27	R: 4.09-7.67	R: 2.52-4.57	Cobbing et al. (1992); Ghani et al. (2013); Ng et al. (2015)
This study, Penang Island	M: 82.1 R: 34.0-218.9	M: 191.2 R: 70.1-602.3	M: 72.9 R: 28.8-201.9	M: 1.16 R: 0.14-5.86	M: 2.01 R: 0.77-6.23	M: 8.57 R: 3.12-24.20	M: 4.16 R: 0.99-12.63	This study

Summarized REE concentration level results in granite residual and Quaternary deposit top soils of Penang Island are shown in **Table 4.9** and **Table 4.10** respectively. The mean concentration of all REE in granite residual soils showed greater than the mean concentration of all REE in Quaternary deposit soils. The descending order of highest maximum range of REE in granitic rock, the parent rock of Penang Island was Ce > La > Nd > Dy > Er > Tb > Eu (Cobbing et al., 1992; Ghani et al., 2013; Ng et al., 2015) which is similar to the descending order of highest mean concentration of REE in top soils of Penang Island (this study). Concentration of LREE is always greater than concentration of HREE in granite residual soils (Kabata-Pendias & Mukherjee, 2007; Yusoff et al., 2013). According to Kabata-Pendias and Mukherjee (2007), LREE tend to concentrate more in weathered materials than HREE. LREE are also more mobile than HREE (Kabata-Pendias & Mukherjee, 2007). In Brazil, a study of REE concentration in soil of granite showed mean concentration of LREE was greater than mean concentration of HREE (Silva et al., 2017). Therefore, the concentrations of REE in top soils of Penang Island were suggested to be derived mainly from the granite, parent rock of the area.

Table 4.9: Summarized statistical results of concentration level of REE in granite residual top soils of Penang Island (n=12).

	Mean	**Minimum**	**Maximum**	**Median**
LREE (mg/Kg)				
La	99.4	48.1	218.9	88.9
Ce	241.8	111.0	602.3	197.0
Nd	87.0	38.6	201.9	77.0
HREE (mg/Kg)				
Eu	1.83	0.32	5.86	1.34
Tb	2.79	0.82	6.23	2.30
Dy	10.58	3.12	24.20	8.70
Er	5.38	0.99	12.63	4.24

Table 4.10: Summarized statistical results of concentration level of REE in Quaternary deposit top soils of Penang Island (n=19).

	Mean	Minimum	Maximum	Median
LREE (mg/Kg)				
La	71.1	34.0	128.8	74.9
Ce	159.2	70.1	285.8	162.6
Nd	64.0	28.8	111.8	65.9
HREE (mg/Kg)				
Eu	0.74	0.14	1.66	0.75
Tb	1.52	0.77	2.71	1.45
Dy	7.30	3.62	13.88	7.09
Er	3.39	1.54	6.18	3.32

4.4 Spatial distribution

4.4.1 Spatial distribution of heavy metals

Spatial distribution map of As is shown in **Figure 4.2**. The map displayed high As concentration in centre part of Penang Island but more to the north east part of Penang Island. This high concentration of As was located in Bandar Air Itam. Bandar Air Itam characterized residential, business and industrial areas which surrounded by agriculture area and some quarries. Contamination of As in soil always reported being associated with agriculture activities which can be derived from pesticides, fertilizer, sludge and manure (Kabata-Pendias & Mukherjee, 2007). In Rayong Province, Thailand, spatial pattern of As was mainly distributed in eastern part of study area which occupied by agriculture area and in the south western part of study area which occupied by chemical and petrochemical industries, the industrial estate, and the ports (Simasuwannarong et al., 2012). In Isfahan Province, Iran, spatial distribution of As showed high concentration in Kelishad and Abrisham cities which were suspected to be correlated with mineralogy and Pb-Zn mining area (Mehr et al., 2017).

Based on spatial distribution map of Pb as shown in **Figure 4.3**, the distribution of Pb displayed two high concentration areas which located in the north east of Penang Island and in the north of Penang Island. George Town was the high Pb concentration place in the north east of Penang Island whereas Batu Ferringhi was the high Pb concentration in the north of Penang Island. However, between these two locations, concentration of Pb in George Town showed greater than the concentration of Pb in Batu Ferringhi.

The expected source of high Pb concentration in George Town and Batu Ferringhi were traffic emission. George Town is a developed city since the end of 18th century and was the first British port town in South East Asia (Hassan, 2009; Shamsuddin et al., 2012). Batu Ferringhi beach is the most popular tourism place in Penang Island and attracts many international, domestic and local tourists which may lead to traffic congestion (Mohd Noor et al., 2015). Common high Pb concentration areas were always reported along high traffic roads and in vicinity of mining and industrial activities (Kabata-Pendias & Mukherjee, 2007). In northeast of Vaslui County, Romania, distribution of Pb showed high concentration in the vicinity areas inhabited by humans and near a major road carrying large amount of traffic (Ungureanu et al., 2016). Spatial distribution of Pb in Yibin City, Sichuan Province, China showed high concentration in the vicinity of industrial buildings and near road junctions and, major roads carrying many traffic (Guo et al., 2012).

Spatial distribution map of Ni is shown in **Figure 4.4**. The map displayed one major concentric pattern of high Ni in the east of Penang Island. The highest Ni concentration in this concentric pattern was located in Jelutong. Jelutong consists of residential and industrial areas based on the land use map of Penang Island. In Gaborone, Bostwana, Ni concentration was found high concentrated in urban area compared to rural area. The expected cause of high Ni concentration in the urban area was residential waste

especially liquid waste (Zhai et al., 2003). In American cities, Ni content in municipal sludge ranged between 29 and 800 mg/Kg (Kabata-Pendias & Mukherjee, 2007). Ni pollution can also be associated with emissions from metal processing operations and from increasing combustion of coal and oil (Kabata-Pendias & Pendias, 1984; Alloway, 2013). In Turkey, high Ni concentration in soils was reported around the Tunçbilek Thermal Power Plant which the concentration ranged from 16.6 to 2385.0 mg/Kg (Özkul, 2016).

Spatial distribution map of Cd is shown in **Figure 4.5**. Based on the map, distribution of Cd displayed a main wide and elongated concentric pattern of high Cd concentration in north east of Penang Island. Highest concentration of Cd in this concentric pattern was located in George Town. George Town characterized as residential and business areas which the development had started since the end of 18th century (Hassan, 2009; Shamsuddin et al., 2012). In Kerman city, Iran, high concentration of Cd was found in top soils near gas stations (Hamzeh et al., 2011). The high concentration of Cd in George Town was also similar to high concentration area of Pb. Associated Cd-Pb concentrations were always related to traffic emissions (Wong et al., 2006; Hamzeh et al., 2011; Ağca, 2015). In southeast China, similar high concentration of Cd and Pb was found in the middle part of the area which near to the intersection of two highways (Huang et al., 2018).

4.4.2 Spatial distribution of REE

Spatial distribution maps of LREE (La, Ce and Nd) in top soils of Penang Island are shown in **Figure 4.6**, **Figure 4.7** and **Figure 4.8**. Based on the maps, all LREE spatial distributions displayed two high concentration areas which is in the north east of Penang Island and in the north west portion of Penang Island. The high concentration of LREE in the north east of Penang Island was located in George Town whereas the high concentration of LREE in the north west of Penang Island was located in Teluk Bahang.

However, concentration of LREE in George Town showed greater than concentration of LREE in Teluk Bahang.

Spatial distribution maps of HREE (Eu, Tb, Dy and Er) in top soils of Penang Island are shown in **Figure 4.9**, **Figure 4.10**, **Figure 4.11** and **Figure 4.12**. Spatial distribution map of Eu and Tb displayed similar high concentration area in Bandar Air Itam in the centre of Penang Island. Bandar Air Itam also showed high concentration of As which was surrounded by residential area, business area, agriculture area and some quarries. Another area of slightly high concentration of Eu and Tb was George Town. Spatial distribution of Dy and Er showed similar high concentration areas which in Balik Pulau in southwest of Penang Island and in George Town. Balik Pulau is dominated by agriculture area.

Different distribution patterns of LREE and HREE in entire Penang Island except in George Town were expected to be influenced by weathering of parent material. All LREE concentrated in Teluk Bahang whereas most HREE concentrated in Balik Pulau and Bandar Air Itam. These distribution patterns of REE may result from different degree of erosion in these areas. Teluk Bahang and some of Batu Feringghi areas were highly vegetated area whereas Balik Pulau and Bandar Air Itam were surrounded by agriculture area. There were some quarries in area of Bandar Air Itam. Balik Pulau was situated at foothills of highly terrain of granites. These high terrains of granites comprise Batu Maung Granite, Sungai Ara Granite and Tanjung Bunga Granite. Most part on the top of these high terrain areas were occupied by agriculture activities. Based on soil erosion map of 2005 of Penang Island, these high terrains were marked as a very high erosion area (Pradhan et al., 2012). Concentrations of most HREE in soil were suggested to be originated from weathering products of granites. The exposure of deeper soil profiles above granite bedrocks which contain higher HREE concentrations

(Yusoff et al., 2013) indicated that the soils were undergone highly erosional impacts from agriculture activities and tropical climate of Malaysia.

In Sweden, spatial distribution of REE also displayed different distribution patterns between LREE (La, Ce, Nd and Sm) and HREE (Tb, Dy, Ho, Er, Tm, Yb and Lu) which was predicted to be influenced by weathering of parent materials. The result of distribution showed that LREE have strong enrichment over HREE in soils overlying the Archean rocks in northern Sweden, Archean and Palaeoproterozoic basement rocks in Jämtland and Västerbotten, and younger granites in Bohuslan. In contrast, the HREE show strong enrichment in soils overlying high-grade metamorphic rocks of the Sveconorwegian Orogen in southern Sweden (Sadeghi et al., 2013). In Brazil, spatial distribution of LREE (La, Ce, Pr, Nd and Sm) showed different pattern from spatial distribution of HREE (Eu, Gd, Tb, Dy, Ho, Er, Tm, Yb and Lu) which they were expected to be influenced by leaching and erosion of parent materials (Paye et al., 2016).

However, similar high concentration of most LREE and HREE in George Town were expected to be related to historical place of this area. These high concentrations of LREE and HREE were suspected to be originated from coals that found in this area which cover the area up to 1800 m^2 at Fort Cornwallis historical building near to Royal Malaysian Navy. Coal contains naturally high REE concentrations (Pazand, 2015; Folgueras et al., 2017). Fort Cornwallis was built by Francis Light, captain of British armies as defensive fortress in 1786. The coal that found in this area was expected to be derived from use of coal as fuel by British Navy. The transition from burning coal to burning oil in the Royal Navy's fuel supplies was applied during 1898 to 1939 (Brown, 2003). In Dhanbad, India, high concentrations of REE (La, Ce, Pr, Nd, Sm, Eu, Gd, Tb, Dy, Ho, Er, Tm, Yb, Lu, Sc and Y) were found in top soils around Jharia coalfield (Masto et al., 2011).

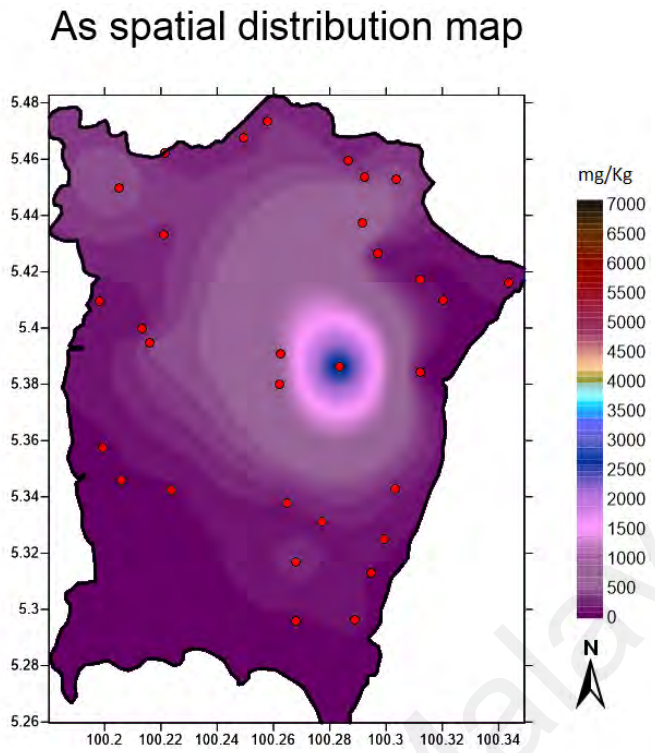

Figure 4.2: Spatial distribution map of As in top soils of Penang Island.

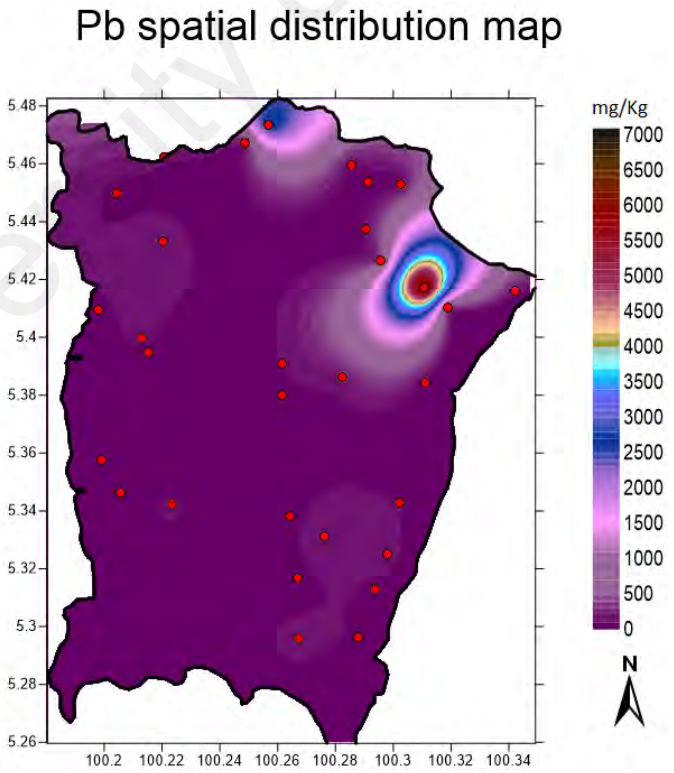

Figure 4.3: Spatial distribution map of Pb in top soils of Penang Island.

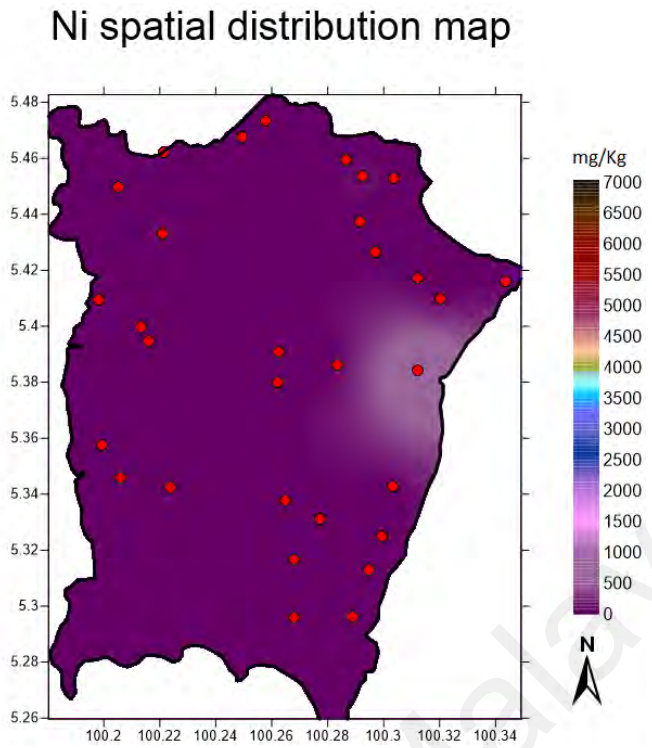

Figure 4.4: Spatial distribution map of Ni in top soils of Penang Island.

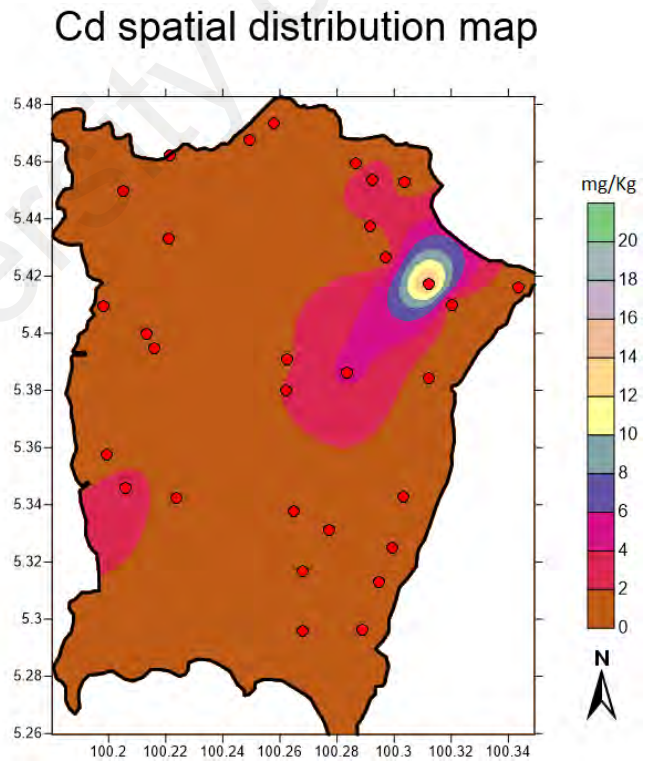

Figure 4.5: Spatial distribution map of Cd in top soils of Penang Island.

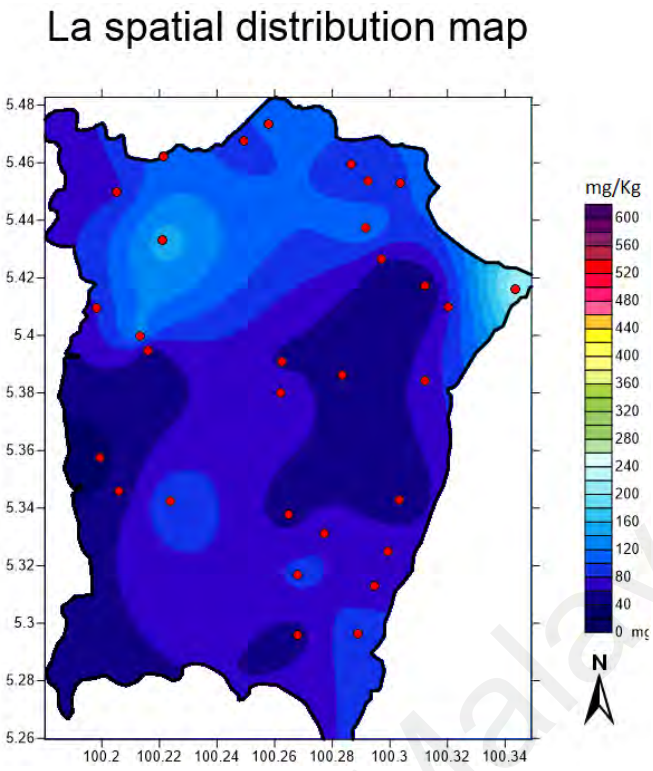

Figure 4.6: Spatial distribution map of La in top soils of Penang Island.

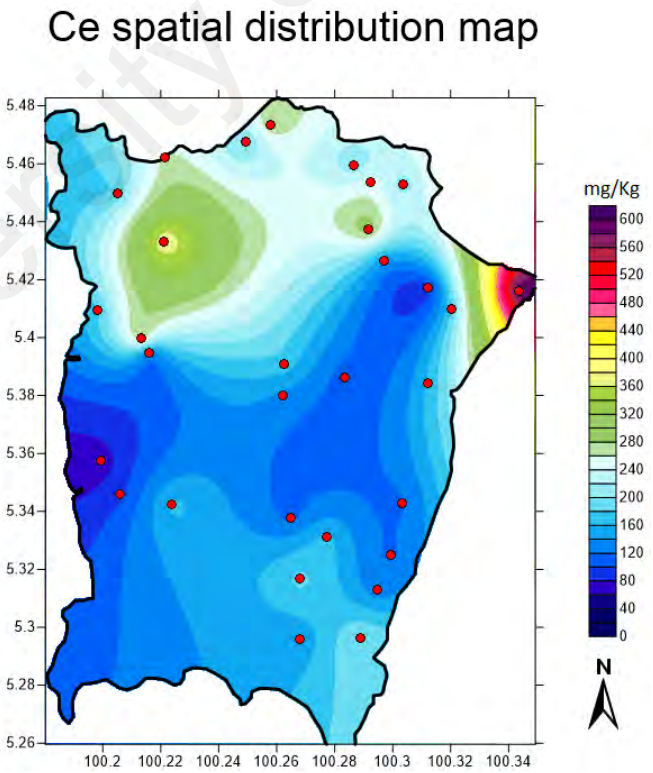

Figure 4.7: Spatial distribution map of Ce in top soils of Penang Island.

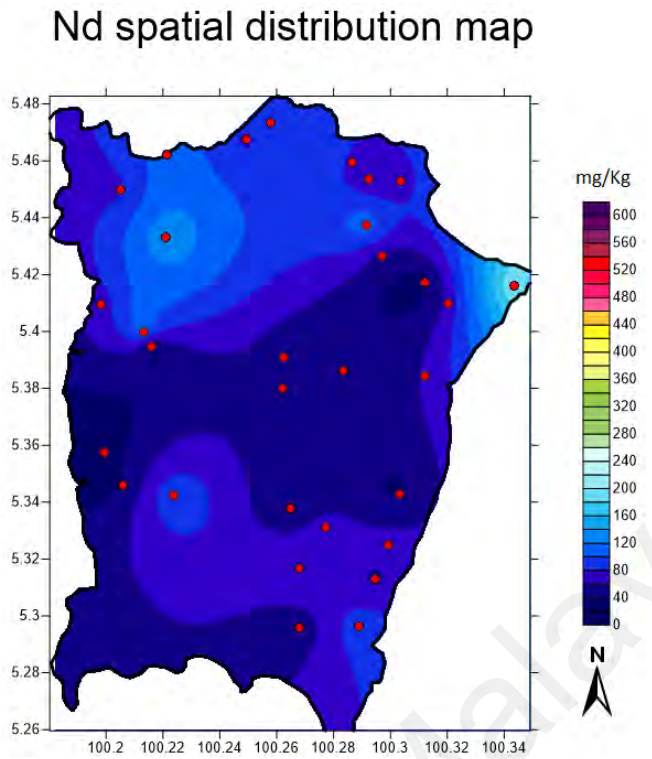

Figure 4.8: Spatial distribution map of Nd in top soils of Penang Island.

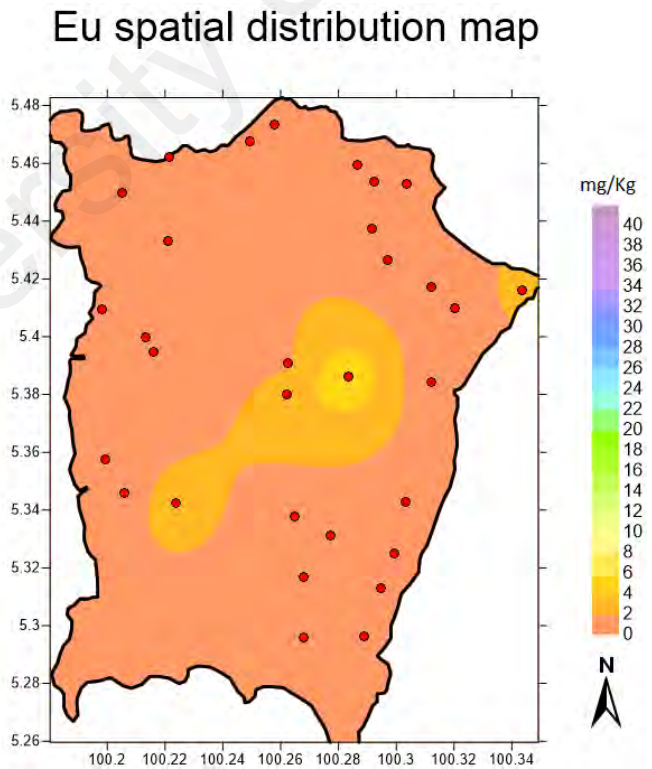

Figure 4.9: Spatial distribution map of Eu in top soils of Penang Island.

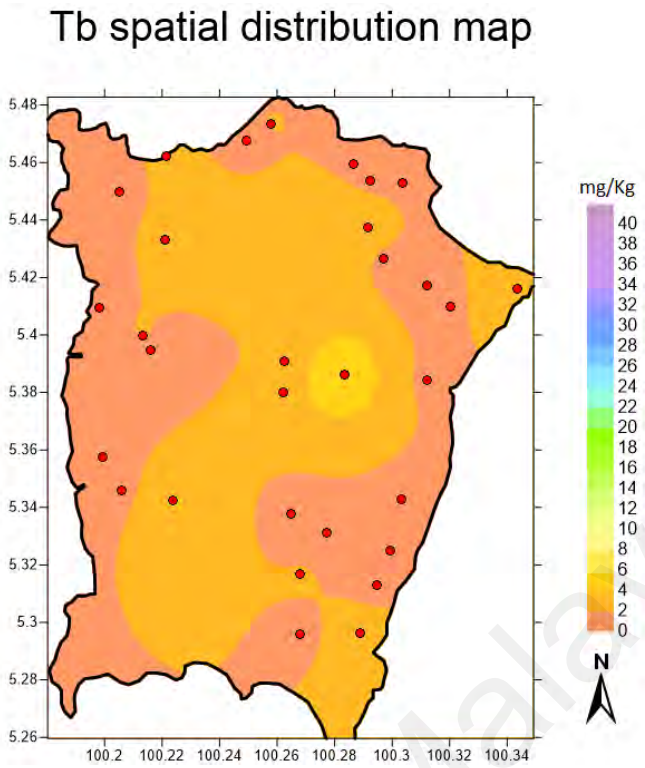

Figure 4.10: Spatial distribution map of Tb in top soils of Penang Island.

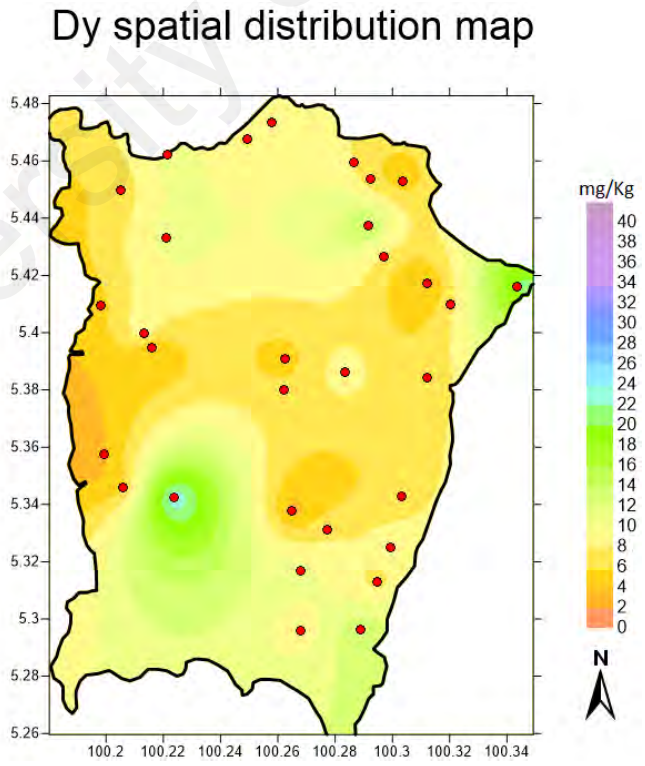

Figure 4.11: Spatial distribution map of Dy in top soils of Penang Island.

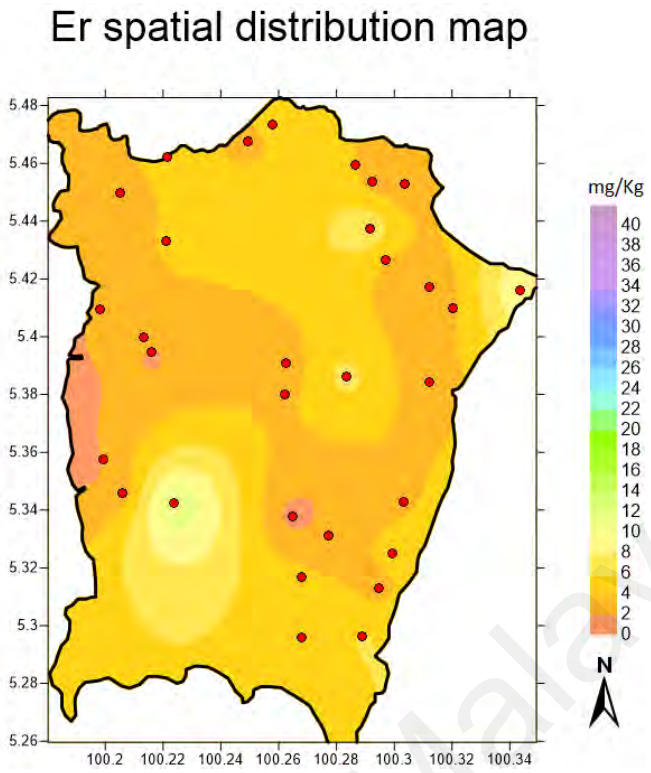

Figure 4.12: Spatial distribution map of Er in top soils of Penang Island.

4.5 Contamination level assessment

4.5.1 Contamination factor (CF) assessment

Summarized results of CF assessment of heavy metals in top soils of Penang Island are shown in **Table 4.11**. Results of the CF assessment showed that CF value of As ranged from 0.10 to 4.25 which classified as 'no element enrichment' to 'considerable contamination' levels, CF value of Pb ranged from 0.23 to 38.58 which classified as 'no element enrichment' to 'very high contamination' levels, CF value of Ni ranged from 0.22 to 35.56 which classified as 'no element enrichment' to 'very high contamination' levels and CF value of Cd ranged from 0.06 to 6.80 which classified as' no element enrichment' to 'very high contamination' levels. The descending order of highest CF mean value among heavy metals was Pb > Ni > Cd > As.

CF distribution maps of As, Pb, Ni and Cd in top soils of Penang Island are shown in **Figure 4.13**, **Figure 4.14**, **Figure 4.15** and **Figure 4.16**. CF distribution map of As displayed a main concentric pattern of high CF value with level over 'no element

enrichment' (CF ≥ 1) in centre of Penang Island. The highest CF value of As within this concentric pattern was located in Bandar Air Itam which the level reached 'considerable contamination' level.

CF distribution maps of Pb showed two major concentric patterns of high CF value with the level over 'no element enrichment' (CF ≥ 1) in the north of Penang Island and the north east of Penang Island. The highest CF value in the concentric pattern of north of Penang Island was Batu Ferringhi whereas the highest CF value in the concentric pattern of north east of Penang Island was George Town. Both of highest CF value areas of Pb reached 'very high contamination' levels.

In CF distribution map of Ni, there were three areas of high CF value with the level over 'no element enrichment' (CF ≥ 1). The highest CF value was located in the east of Penang Island and showed a large concentric pattern. Within this large concentric pattern, the highest CF value of Ni was located in Jelutong which the CF value reached 'very high contamination' level. Another two areas of high CF value of Ni were located in Teluk Bahang, north west of Penang Island and Tanjung Bunga, north of Penang Island. Both areas showed 'moderate contamination' levels.

CF distribution maps of Cd showed one major concentric pattern of CF level over 'no element enrichment' level (CF ≥ 1) in the north east of Penang Island. The highest CF value of Cd in this concentric pattern was located in George Town which similar to the highest CF value area of Pb. The highest CF value of Cd in George Town was categorized as 'very high contamination' level. Another small area that showed slightly high CF value of Cd was located in Balik Pulau, south west of Penang Island which showed 'moderate contamination' level.

Results of CF assessment of REE in top soils of Penang Island are shown in **Table 4.13**. For LREE, CF value of La ranged from 0.25 to 1.62 which classified as 'no

element enrichment' to 'moderate contamination' levels, CF value of Ce ranged from 0.21 to 1.82 which classified as 'no element enrichment' to 'moderate contamination' levels and CF value of Nd ranged from 0.22 to 1.53 which classified as 'no element enrichment' to 'moderate contamination' levels. For HREE, CF value of Eu ranged from 0.07 to 3.00 which categorized as 'no element enrichment' to 'moderate contamination' levels, CF value of Tb ranged from 0.26 to 2.11 which categorized as 'no element enrichment' to 'moderate contamination' levels, CF value of Dy ranged from 0.23 to 1.75 which categorized as 'no element enrichment' to 'moderate contamination' levels and CF value of Er ranged from 0.15 to 1.96 which categorized as 'no element enrichment' to 'moderate contamination' levels. The descending order of highest average CF value of REE was Tb> Er > Dy > La > Eu > Ce > Nd.

CF distribution maps of LREE (La, Ce and Nd) are shown in **Figure 4.17**, **Figure 4.18** and **Figure 4.19**. All CF distribution maps of LREE showed two small areas of CF values over 'no element enrichment' level (CF ≥ 1) in Teluk Bahang, north east of Penang Island and in George Town, north west of Penang Island. Both areas of high CF value of LREE were classified as 'moderate contamination' levels.

CF distribution maps of HREE (Eu, Tb, Dy and Er) are shown in **Figure 4.20**, **Figure 4.21**, **Figure 4.22** and **Figure 4.23**. CF distribution map of Eu showed two areas of CF value over 'no element enrichment' level (CF ≥ 1) which in the centre of Penang Island and in George Town, north east of Penang Island. The high CF value in the centre of Penang Island showed combination areas of Bandar Air Itam and Balik Pulau. However, both high CF value areas were classified as similar level of 'moderate contamination'.

CF distribution maps of Tb showed four areas of high CF values with over 'no element enrichment' level (CF ≥ 1) in the north, north east, centre and south west of Penang Island. These high CF value areas were represented by Tanjung Bunga in north

of Penang Island, George Town in north east of Penang Island, Bandar Air Itam in centre of Penang Island and Balik Pulau in south west of Penang Island. However, all of these high CF values areas of Tb were classified as 'moderate contamination' level.

CF spatial distribution map of Dy and Er displayed similar three areas of high CF values over the 'no element enrichment' level (CF ≥ 1) in north, north east and south west of Penang Island. These high CF value areas were represented by Tanjung Bunga in north of Penang Island, George Town in north east of Penang Island and Balik Pulau in south west of Penang Island. All of these high CF values of Dy and Er areas were classified as 'moderate contamination' levels.

Table 4.11: Contamination factor (CF) assessment results of heavy metals in top soils of Penang Island.

Heavy metal	Mean	Minimum	Maximum	Contamination Level
As	0.53	0.10	4.25	No element enrichment to considerable contamination
Pb	2.32	0.23	38.58	No element enrichment to very high contamination
Ni	1.75	0.22	35.56	No element enrichment to very high contamination
Cd	0.64	0.06	6.80	No element enrichment to very high contamination

Table 4.12: Areas of high heavy metals contamination factor (CF) values (CF ≥ 1) in top soils of Penang Island.

Heavy metal	High CF value area	Level of CF
As	Bandar Air Itam	Considerable contamination
Pb	George Town	Very high contamination
	Batu Ferringhi	Very high contamination
Ni	Jelutong	Very high contamination
	Teluk Bahang	Moderate contamination
	Tanjung Bunga	Moderate contamination
Cd	George Town	Very high contamination
	Balik Pulau	Moderate contamination

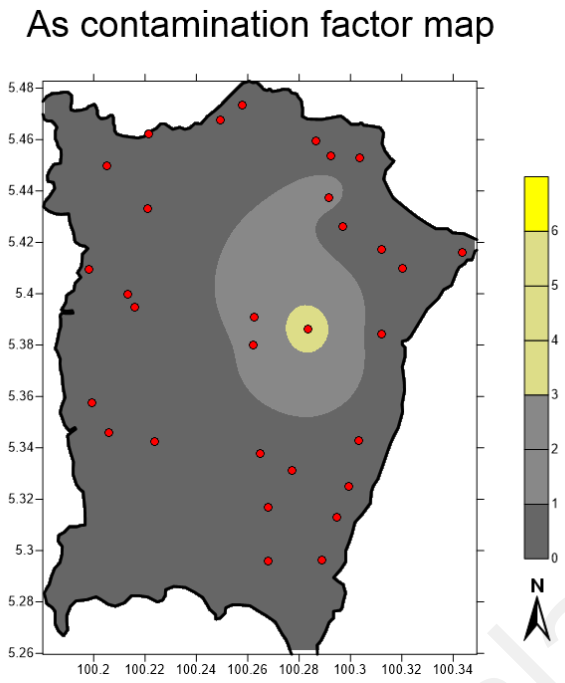

Figure 4.13: Contamination factor (CF) distribution map of As in top soils of Penang Island.

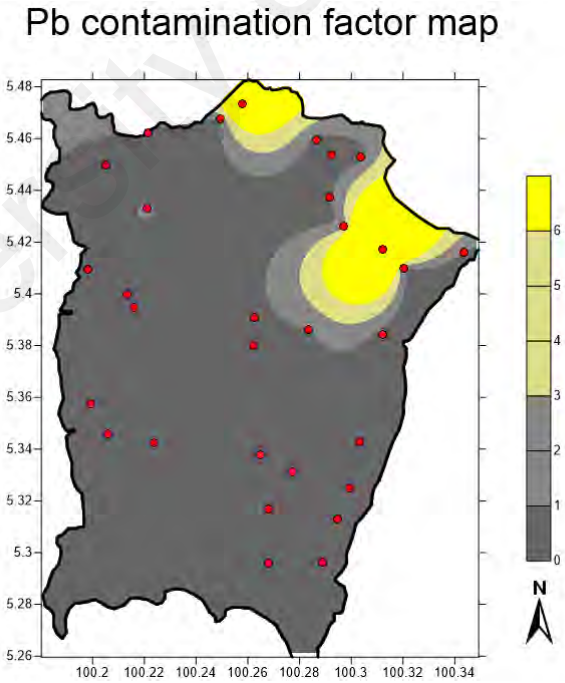

Figure 4.14: Contamination factor (CF) distribution map of Pb in top soils of Penang Island.

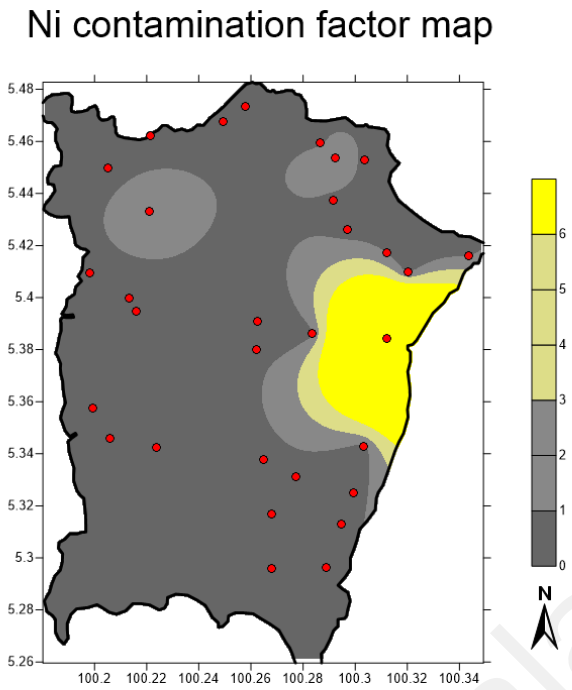

Figure 4.15: Contamination factor (CF) distribution map of Ni in top soils of Penang Island.

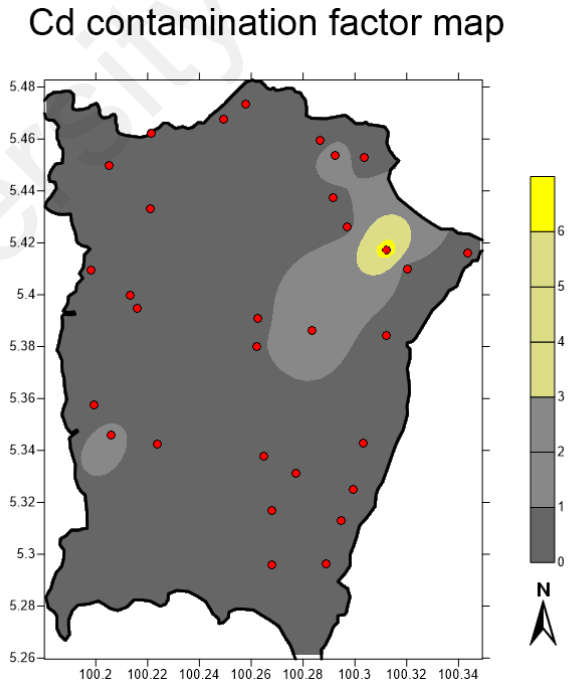

Figure 4.16: Contamination factor (CF) distribution map of Cd in top soils of Penang Island.

Table 4.13: Contamination factor (CF) assessment results of REE in top soils of Penang Island.

	Mean	**Minimum**	**Maximum**	**Contamination Level**
LREE				
La	0.61	0.25	1.62	No element enrichment to moderate contamination
Ce	0.58	0.21	1.82	No element enrichment to moderate contamination
Nd	0.55	0.22	1.53	No element enrichment to moderate contamination
HREE				
Eu	0.60	0.07	3.00	No element enrichment to moderate contamination
Tb	0.68	0.26	2.11	No element enrichment to moderate contamination
Dy	0.62	0.23	1.75	No element enrichment to moderate contamination
Er	0.64	0.15	1.96	No element enrichment to moderate contamination

Table 4.14: Areas of high REE contamination factor (CF) values (CF ≥ 1) in top soils of Penang Island.

REE	**High CF value area**	**Level of CF**
All LREE	Teluk Bahang	Moderate contamination
	George Town	Moderate contamination
Eu	Bandar Air Itam	Moderate contamination
	Balik Pulau	Moderate contamination
Tb	Tanjung Bunga	Moderate contamination
	George Town	Moderate contamination
	Bandar Air Itam	Moderate contamination
	Balik Pulau	Moderate contamination
Dy and Er	Tanjung Bunga	Moderate contamination
	George Town	Moderate contamination
	Balik Pulau	Moderate contamination

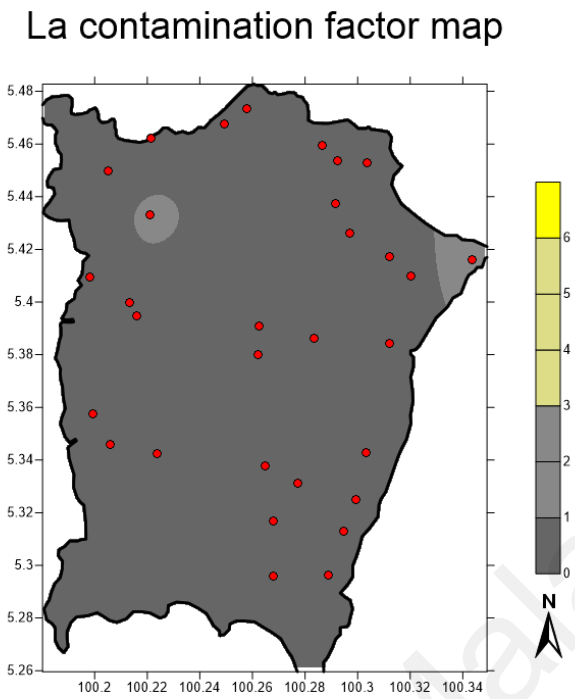

Figure 4.17: Contamination factor (CF) distribution map of La in top soils of Penang Island.

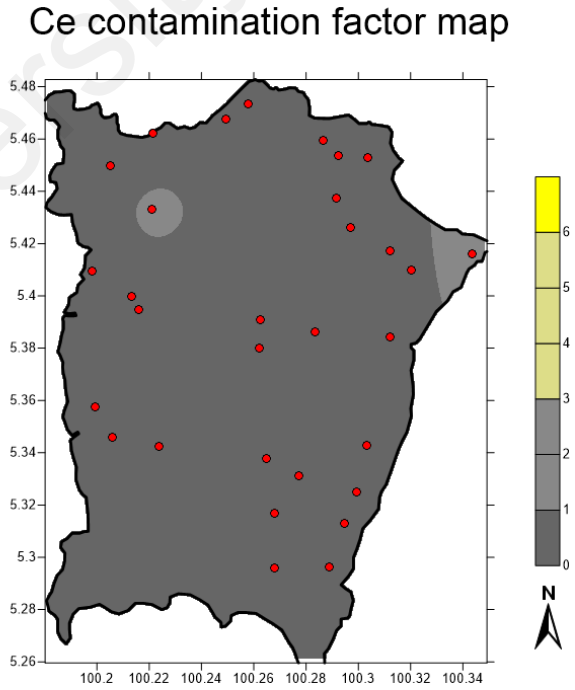

Figure 4.18: Contamination factor (CF) distribution map of Ce in top soils of Penang Island.

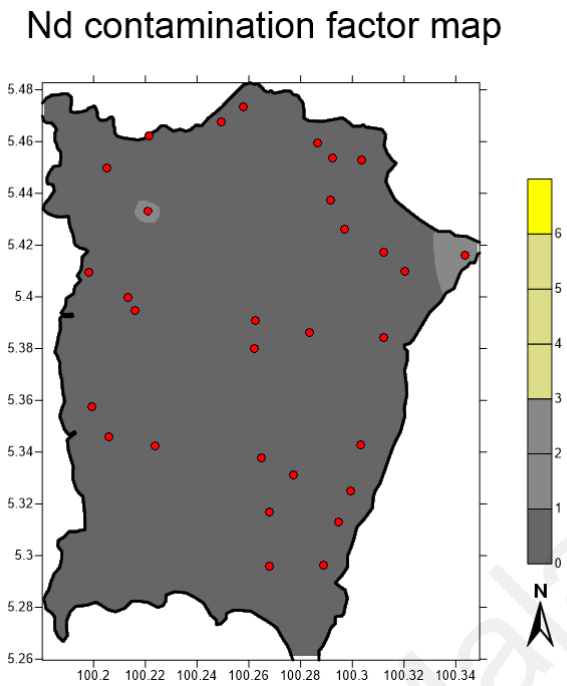

Figure 4.19: Contamination factor (CF) distribution map of Nd in top soils of Penang Island.

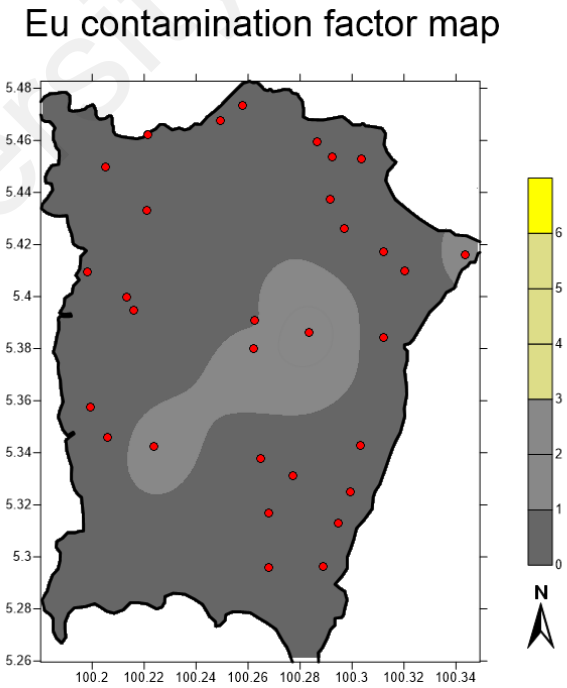

Figure 4.20: Contamination factor (CF) distribution map of Eu in top soils of Penang Island.

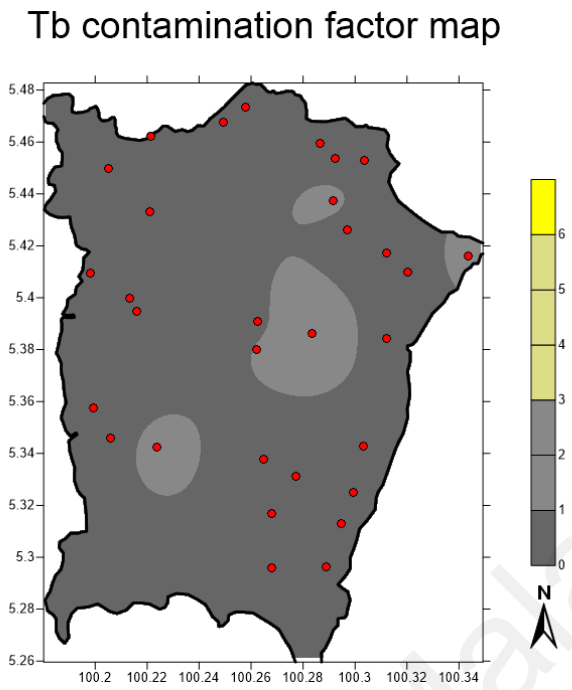

Figure 4.21: Contamination factor (CF) distribution map of Tb in top soils of Penang Island.

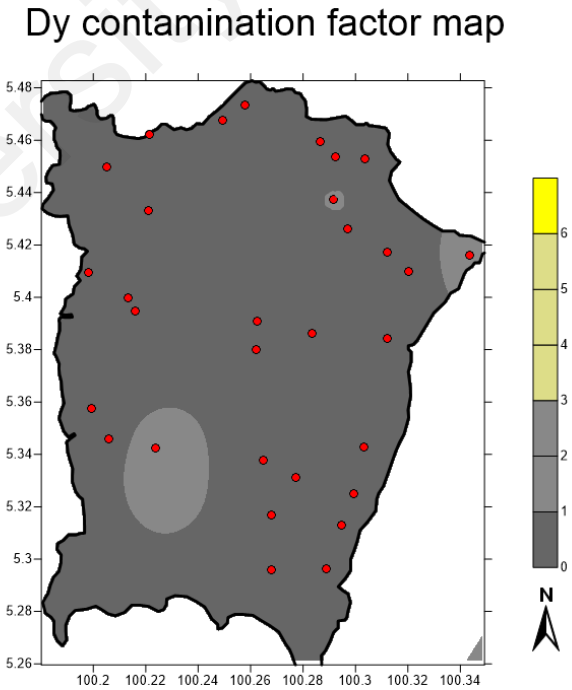

Figure 4.22: Contamination factor (CF) distribution map of Dy in top soils of Penang Island.

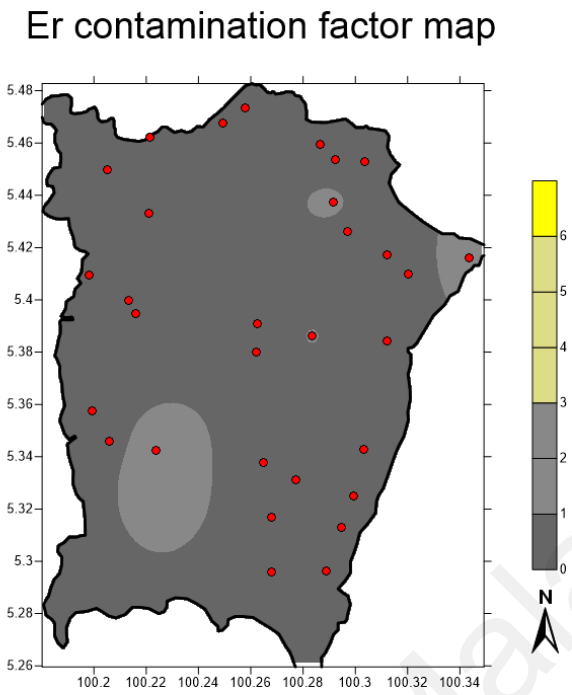

Figure 4.23: Contamination factor (CF) distribution map of Er in top soils of Penang Island.

4.5.2 Geo-accumulation index (I_{geo}) assessment

Results of I_{geo} assessment of heavy metals in top soils of Penang Island are shown in **Table 4.15**. The results represented that I_{geo} value of As ranged from -3.93 (unpolluted level) to 1.50 (moderately polluted level), I_{geo} value of Pb ranged from -2.70 (unpolluted level) to 4.68 (strongly to extremely polluted level), I_{geo} value of Ni ranged from -2.77 (unpolluted level) to 4.57 (strongly to extremely polluted level) and I_{geo} value of Cd ranged from -4.55 (unpolluted level) to 2.18 (moderately to strongly polluted level). The descending order of highest I_{geo} average value among heavy metals was Pb > Ni > Cd > As.

I_{geo} distribution maps of As, Pb, Ni and Cd in top soils of Penang Island are shown in **Figure 4.24**, **Figure 4.25**, **Figure 4.26** and **Figure 4.27**. Based on I_{geo} distribution map of As, the distribution represented a concentric pattern of I_{geo} values over 'unpolluted' level ($I_{geo} > 0$) in the centre of Penang Island. In this concentric pattern, the highest I_{geo}

value of As was located in Bandar Air Itam which was categorized as 'moderately polluted' level.

In I_{geo} distribution map of Pb, the distribution showed two concentric patterns of I_{geo} values over 'unpolluted' level ($I_{geo} > 0$) which located in the north of Penang Island and in the north east of Penang Island. The concentric pattern in the north of Penang Island showed the highest I_{geo} value of Pb in Batu Ferringhi whereas the concentric pattern in the north east of Penang Island showed highest I_{geo} value of Pb in George Town. Both highest I_{geo} values of Pb areas were classified as 'strongly to extremely polluted' levels.

I_{geo} distribution map of Ni displayed a concentric pattern of I_{geo} value over 'unpolluted' level ($I_{geo} > 0$) in the east of Penang Island. In this concentric pattern, the highest I_{geo} value of Ni was located in Jelutong which the I_{geo} value was classified as 'strongly to extremely polluted' level. Another two slightly high I_{geo} value of Ni ($I_{geo} > 0$) were located in Teluk Bahang in north west of Penang Island and Tanjung Bunga in north of Penang Island. Both areas showed I_{geo} value of 'unpolluted to moderately polluted' levels.

I_{geo} distribution map of Cd displayed a small concentric pattern of I_{geo} level over 'unpolluted' level ($I_{geo} > 0$) in north east of Penang Island. The highest I_{geo} value of Cd in this concentric pattern was located in George Town which categorized as 'moderately to strongly polluted' level. Another small area that showed slightly high I_{geo} value of Cd ($I_{geo} > 0$) was Bandar Air Itam which located in centre of Penang Island. The I_{geo} value of this area was classified as 'unpolluted to moderately polluted' level.

Results of I_{geo} assessment of REE in top soils of Penang Island are shown in **Table 4.17**. For LREE, the results showed that I_{geo} value of La ranged from -2.57 (unpolluted level) to 0.11 (unpolluted to moderately polluted level), I_{geo} value of Ce ranged from -2.82 (unpolluted level) to 0.28 (unpolluted to moderately polluted level) and I_{geo} value

of Nd ranged from -2.78 (unpolluted level) to 0.03 (unpolluted to moderately polluted level).

I_{geo} assessment results of HREE showed that I_{geo} value of Eu ranged from -4.34 (unpolluted level) to 1.00 (unpolluted to moderately polluted level), I_{geo} value of Tb ranged from -2.52 (unpolluted level) to 0.49 (unpolluted to moderately polluted level), I_{geo} value of Dy ranged from -2.73 (unpolluted level) to 0.23 (unpolluted to moderately polluted level) and I_{geo} value of Er ranged from -3.30 (unpolluted level) to 0.38 (unpolluted to moderately polluted level). The descending order of average highest I_{geo} value of REE was Tb > Er > La > Dy > Ce > Nd > Eu but all of the average values of REE were classified as unpolluted level.

I_{geo} distribution maps of LREE (La, Ce and Nd) are shown in **Figure 4.28**, **Figure 4.29** and **Figure 4.30**. I_{geo} distribution maps of all LREE displayed similar small area of high I_{geo} values over 'unpolluted' level ($I_{geo} > 0$) in George Town, north east of Penang Island. This area of high I_{geo} value of LREE was classified as 'unpolluted to moderately polluted' level.

I_{geo} distribution maps of HREE (Eu, Tb, Dy and Er) are shown in **Figure 4.31**, **Figure 4.32**, **Figure 4.33** and **Figure 4.34**. I_{geo} spatial distribution maps of Eu and Tb displayed similar small area of high I_{geo} values over 'unpolluted' level ($I_{geo} > 0$) in Bandar Air Itam, centre of Penang Island. This area of high I_{geo} values of Eu and Tb was classified as 'unpolluted to moderately polluted' level.

I_{geo} spatial distribution maps of Dy showed a small area of I_{geo} value over 'unpolluted' level ($I_{geo} > 0$) in Balik Pulau, south west of Penang Island. This area of high I_{geo} value of Dy was classified as 'unpolluted to moderately polluted' level.

I_{geo} spatial distribution maps of Er showed two small areas of I_{geo} values over 'unpolluted' level ($I_{geo} > 0$) in Balik Pulau, south west of Penang Island and George

Town, north east of Penang Island. Both areas of high I_{geo} values of Er were classified as 'unpolluted to moderately polluted' levels. The high I_{geo} values of Er in Balik Pulau is similar to the area of high I_{geo} values of Dy.

Table 4.15: Geo-accumulation index (I_{geo}) assessment results of heavy metals in top soils of Penang Island.

Heavy metal	Mean	Minimum / contamination level	Maximum / contamination level
As	-2.24	-3.93 / Unpolluted	1.50 / Moderately polluted
Pb	-1.09	-2.70 / Unpolluted	4.68 / Strongly to extremely polluted
Ni	-1.40	-2.77 / Unpolluted	4.57 / Strongly to extremely polluted
Cd	-2.23	-4.55 / Unpolluted	2.18 / Moderately to strongly polluted

Table 4.16: Areas of high heavy metals geo-accumulation index (I_{geo}) values ($I_{geo} > 0$) in top soils of Penang Island.

Heavy metal	High I_{geo} value area	Level of I_{geo}
As	Bandar Air Itam	Moderately polluted
Pb	Batu Ferringhi	Strongly to extremely polluted
	George Town	Strongly to extremely polluted
Ni	Jelutong	Strongly to extremely polluted
	Teluk Bahang	Unpolluted to moderately polluted
	Tanjung Bunga	Unpolluted to moderately polluted
Cd	George Town	Moderately to strongly polluted
	Bandar Air Itam	Unpolluted to moderately polluted

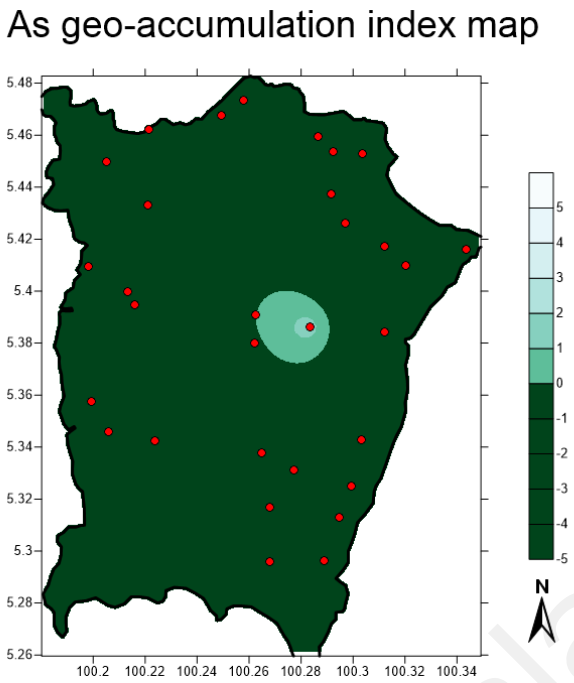

Figure 4.24: Geo-accumulation index (I_{geo}) distribution map of As in top soils of Penang Island.

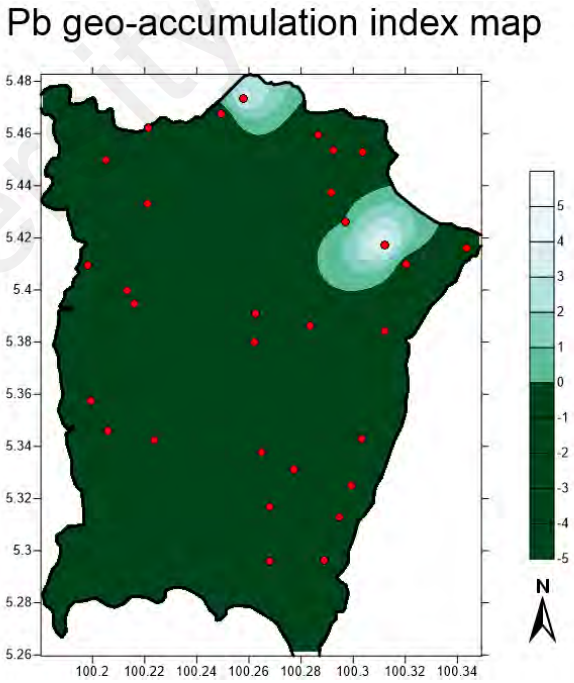

Figure 4.25: Geo-accumulation index (I_{geo}) distribution map of Pb in top soils of Penang Island.

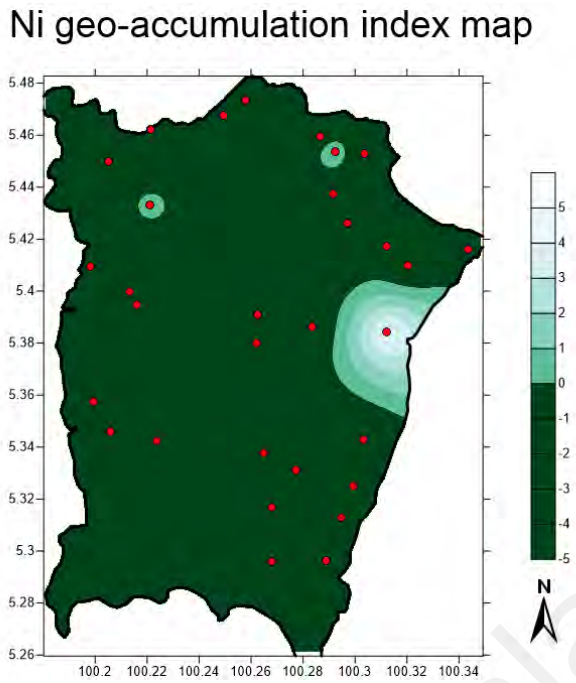

Figure 4.26: Geo-accumulation index (I_{geo}) distribution map of Ni in top soils of Penang Island.

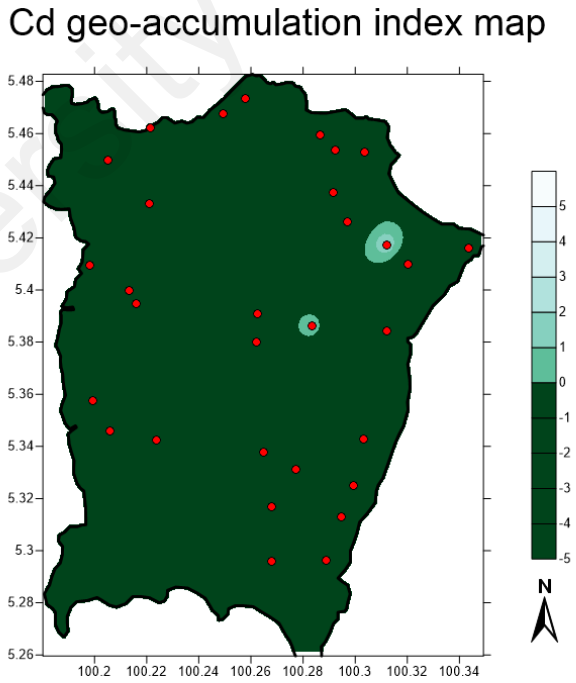

Figure 4.27: Geo-accumulation index (I_{geo}) distribution map of Cd in top soils of Penang Island.

Table 4.17: Geo-accumulation index (I_{geo}) assessment results of REE in top soils of Penang Island.

	Mean	**Minimum / contamination level**	**Maximum / contamination level**
LREE			
La	-1.43	-2.57 / Unpolluted	0.11 / Unpolluted to moderately polluted
Ce	-1.53	-2.82 / Unpolluted	0.28 / Unpolluted to moderately polluted
Nd	-1.59	-2.78 / Unpolluted	0.03 / Unpolluted to moderately polluted
HREE			
Eu	-1.80	-4.34 / Unpolluted	1.00 / Unpolluted to moderately polluted
Tb	-1.33	-2.52 / Unpolluted	0.49 / Unpolluted to moderately polluted
Dy	-1.44	-2.73 / Unpolluted	0.23 / Unpolluted to moderately polluted
Er	-1.42	-3.30 / Unpolluted	0.38 / Unpolluted to moderately polluted

Table 4.18: Areas of high REE geo-accumulation index (I_{geo}) values ($I_{geo} > 0$) in top soils of Penang Island.

REE	**High I_{geo} value area**	**Level of I_{geo}**
All LREE	George Town	Unpolluted to moderately polluted
Eu and Tb	Bandar Air Itam	Unpolluted to moderately polluted
Dy	Balik Pulau	Unpolluted to moderately polluted
Er	Balik Pulau	Unpolluted to moderately polluted
	George Town	Unpolluted to moderately polluted

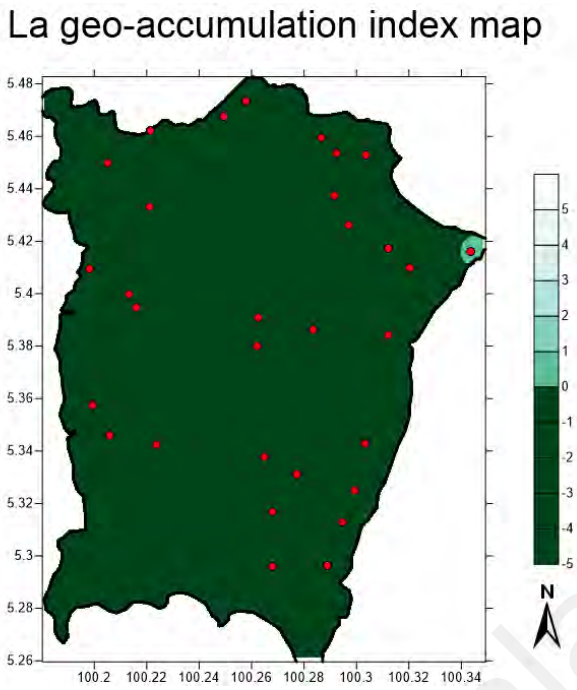

Figure 4.28: Geo-accumulation index (I_{geo}) distribution map of La in top soils of Penang Island.

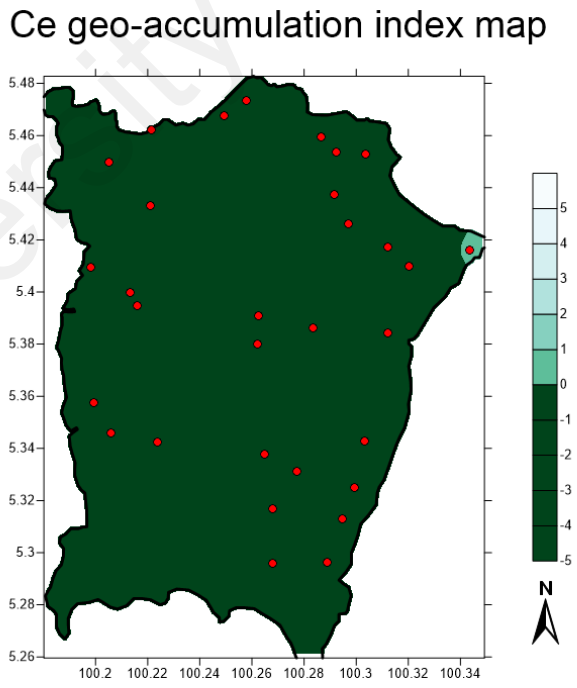

Figure 4.29: Geo-accumulation index (I_{geo}) distribution map of Ce in top soils of Penang Island.

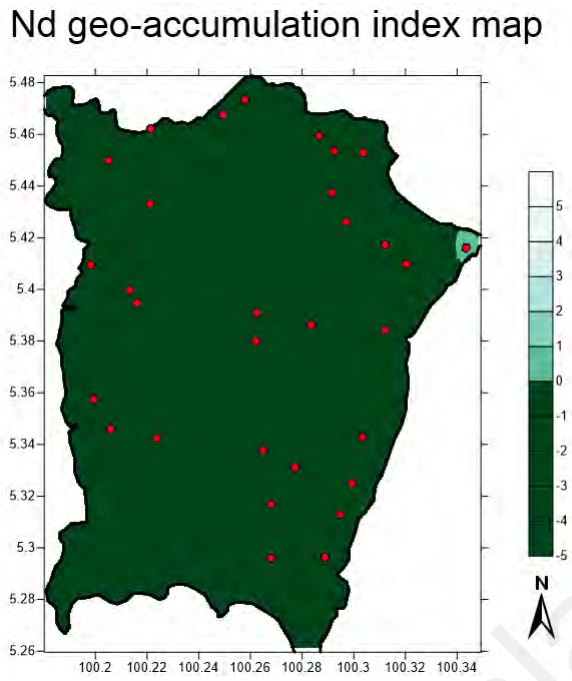

Figure 4.30: Geo-accumulation index (I_{geo}) distribution map of Nd in top soils of Penang Island.

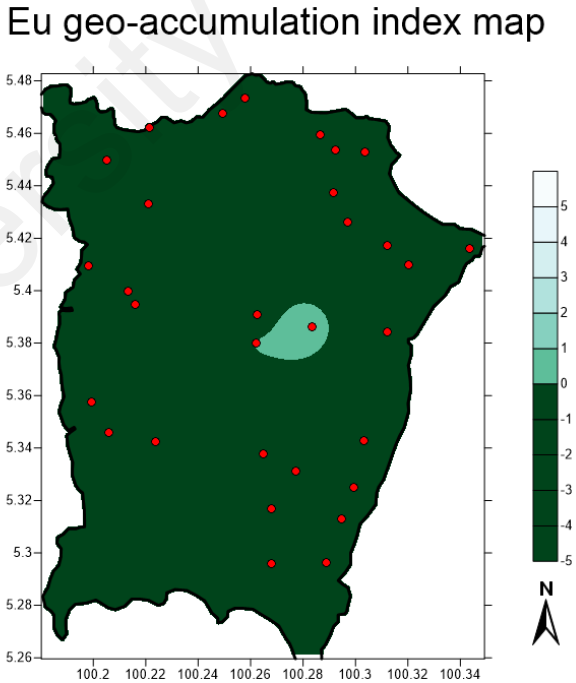

Figure 4.31: Geo-accumulation index (I_{geo}) distribution map of Eu in top soils of Penang Island.

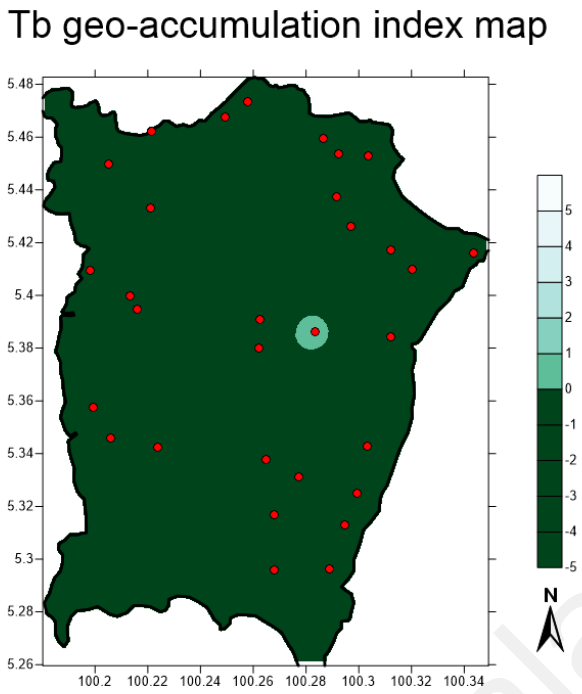

Figure 4.32: Geo-accumulation index (I_{geo}) distribution map of Tb in top soils of Penang Island.

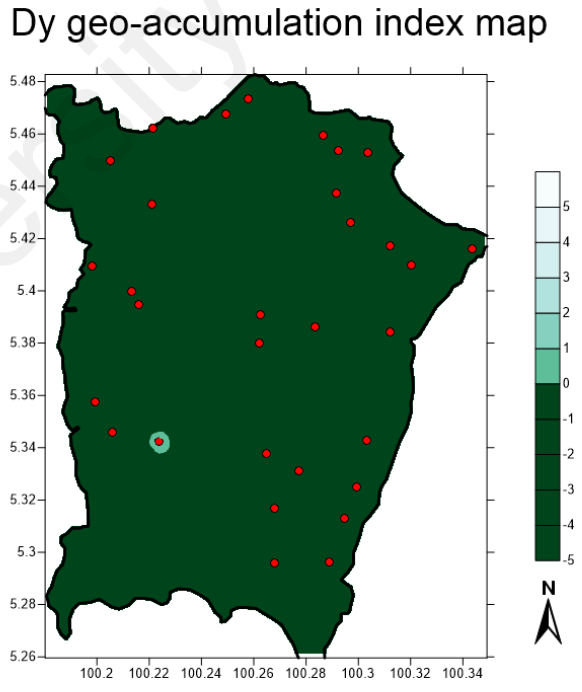

Figure 4.33: Geo-accumulation index (I_{geo}) distribution map of Dy in top soils of Penang Island.

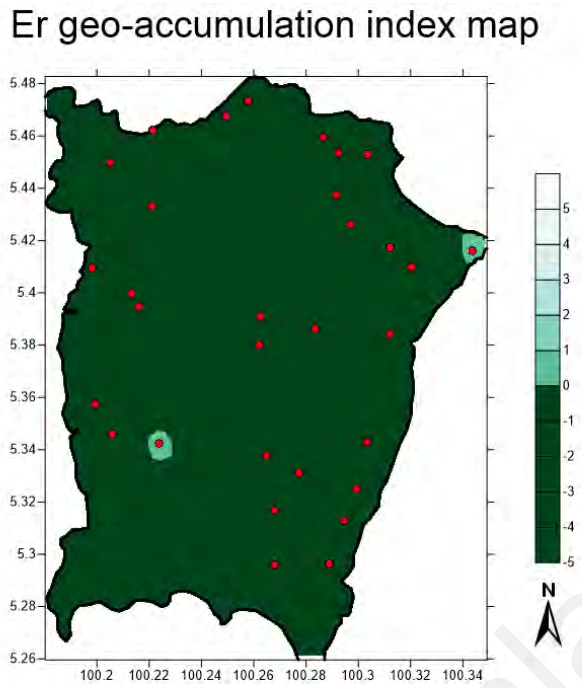

Figure 4.34: Geo-accumulation index (I_{geo}) distribution map of Er in top soils of Penang Island.

4.5.3 Pollution load index (PLI) assessment

PLI assessment result of heavy metals contamination level in top soils of Penang Island is shown in **Table 4.19**. All heavy metals showed PLI values less than one which classified the overall top soils of Penang Island as unpolluted levels. The descending order of highest PLI value of heavy metals was Pb > Ni > Cd > As.

Result of PLI assessment of REE in top soils of Penang Island is shown in **Table 4.20**. All REE represented PLI values less than one which their contamination levels in the top soils of Penang Island were categorized as unpolluted levels. The descending order of highest PLI value of REE was Tb > La and Er > Dy > Ce > Nd > Eu.

Table 4.19: Pollution load index (PLI) results of heavy metals contamination level in top soils of Penang Island.

Heavy metal	PLI value	Contamination Level
As	0.32	Unpolluted
Pb	0.70	Unpolluted
Ni	0.57	Unpolluted
Cd	0.32	Unpolluted

Table 4.20: Pollution load index (PLI) assessment results of REE contamination level in top soils of Penang Island.

	PLI value	Contamination Level
LREE		
La	0.56	Unpolluted
Ce	0.52	Unpolluted
Nd	0.50	Unpolluted
HREE		
Eu	0.43	Unpolluted
Tb	0.60	Unpolluted
Dy	0.55	Unpolluted
Er	0.56	Unpolluted

4.5.4 Comparison and improvement for contamination level assessment

Based on the contamination level assessment, both CF and I_{geo} assessments determined some areas of high index values. Summarized results of CF and I_{geo} contamination level assessments are shown in **Table 4.21**. Based on the result, there are some different between the areas of high CF values ($CF \geq 1$) and areas of high I_{geo} values ($I_{geo} > 0$) for heavy metals and REE. For example, Balik Pulau was classified under high CF value of Cd but not classified under high I_{geo} values of Cd.

The different results between CF and I_{geo} are depending on different proposed equations. CF assessment represented ratio of element concentration to the element background value (Hakanson, 1980). However, I_{geo} assessment represented the highness of the element concentration load in the soil with respect to the background value (Müller, 1969). The proposed terminology for the result values is also different for CF and I_{geo} assessments. The range of value for contamination classification of CF result is wider than the range of value for contamination classification of I_{geo} result. Thus, these differences of CF and I_{geo} assessments yield different result of contamination level.

Table 4.21: Summarized results of contamination factor (CF) and geo-accumulation index (I_{geo}) assessments of heavy metals and REE in top soils of Penang Island.

	Area	**Level of CF (CF ≥ 1)**	**Level of I_{geo} (I_{geo} > 0)**
Heavy metal			
As	Bandar Air Itam	Considerable contamination	Moderately polluted
Pb	Batu Ferringhi	Very high contamination	Strongly to extremely polluted
	George Town	Very high contamination	Strongly to extremely polluted
Ni	Jelutong	Very high contamination	Strongly to extremely polluted
	Teluk Bahang	Moderate contamination	Unpolluted to moderately polluted
	Tanjung Bunga	Moderate contamination	Unpolluted to moderately polluted
Cd	George Town	Very high contamination	Moderately to strongly polluted
	Balik Pulau	Moderate contamination	-
	Bandar Air Itam	-	Unpolluted to moderately polluted
REE			
LREE	Teluk Bahang	Moderate contamination	-
	George Town	Moderate contamination	Unpolluted to moderately polluted
Eu	Bandar Air Itam	Moderate contamination	Unpolluted to moderately polluted
	Balik Pulau	Moderate contamination	-
Tb	Tanjung Bunga	Moderate contamination	-
	George Town	Moderate contamination	-
	Bandar Air Itam	Moderate contamination	Unpolluted to moderately polluted
	Balik Pulau	Moderate contamination	-
Dy	Tanjung Bunga	Moderate contamination	-
	George Town	Moderate contamination	-
	Balik Pulau	Moderate contamination	Unpolluted to moderately polluted
Er	Tanjung Bunga	Moderate contamination	-
	George Town	Moderate contamination	Unpolluted to moderately polluted
	Balik Pulau	Moderate contamination	Unpolluted to moderately polluted

Due to the different results of the contamination levels and the areas of high CF and I_{geo} values for heavy metals and REE obtained, one suggested technique was proposed to standardize the result for both CF and I_{geo} assessments. The suggested technique named as contamination index (CI) assessment which calculated as following equation:

$$CI = C_f + I_{geo} \qquad (1)$$

Where,

CI = Contamination Index (CI)

C_f = Contamination Factor (CF) value

I_{geo} = Geo-accumulation Index (I_{geo}) value

The classification diagram of the result of CI is shown in **Figure 4.35** and summarized as following terminology:

CI > 1 = Low contamination

1 ≥ CI > 10 = Moderate contamination

10 ≥ CI > 20 = High contamination

20 ≥ CI = Very high contamination

Results of CI assessment of heavy metals in top soils of Penang Island are shown in **Table 4.22** and **Table 4.23**. The results showed CI value of As ranged from -3.84 to 5.76 which classified as 'low contamination' to 'moderate contamination' levels, CI value of Pb ranged from -2.46 to 43.26 which classified as 'low contamination' to 'very high contamination' levels, CI value of Ni ranged from -2.55 to 40.12 which classified as 'low contamination' to 'very high contamination' levels and CI value of Cd ranged from -4.84 to 8.98 which classified as 'low contamination' to 'moderate contamination' levels. The descending order of highest average CI value of heavy metals was Pb > Ni > Cd > As.

The CI distribution maps of As, Pb, Ni and Cd are shown in **Figure 4.36**, **Figure 4.37**, **Figure 4.38** and **Figure 4.39**. Based on the CI distribution map of As, one area of high CI value over 'low contamination' level (CI ≥ 1) was located in Bandar Air Itam in the centre of Penang Island. The CI value of As in this area was classified as 'moderate contamination' level.

There were two concentric patterns of high CI value over 'low contamination' level (CI ≥ 1) in the CI distribution map of Pb. These two concentric patterns were located in north and north east of Penang Island. The highest level of CI in north Penang Island concentric pattern was located in Batu Ferringhi which was classified as 'high contamination' level. The highest level of CI in north east Penang Island concentric pattern was located in George Town which was classified as 'very high contamination' level.

In CI distribution map of Ni, one concentric pattern and two small areas showed high CI value over 'low contamination' level (CI ≥ 1). The concentric pattern was located in east of Penang Island which the highest level of CI was located in Jelutong. This highest level of CI in Jelutong was classified as 'very high contamination' level. Another two small areas of high CI value were located in Teluk Bahang, north west of Penang Island and Tanjung Bunga, north of Penang Island. Both areas of high CI values were classified as 'moderate contamination' levels.

The CI distribution map of Cd displayed a large and two small areas of high CI value over 'low contamination' level (CI ≥ 1). The large area of high CI value was located in north east of Penang Island which showed elongated pattern and comprised areas of George Town and Bandar Air Itam. The two small areas of high CI values were located in Tanjung Bunga, north of Penang Island and Balik Pulau, south west of Penang Island.

Results of CI assessment of REE in top soils of Penang Island are shown in **Table 4.24** and **Table 4.25**. The results showed CI value of La ranged from -2.32 to 1.74 which classified as 'low contamination' to 'moderate contamination' levels, CI value of Ce ranged from -2.61 to 2.10 which classified as 'low contamination' to 'moderate contamination' levels, CI value of Nd ranged from -2.56 to 1.56 which classified as 'low contamination' to 'moderate contamination' levels, CI value of Eu ranged from -4.27 to 4.01 which classified as 'low contamination' to 'moderate contamination' levels, CI value of Tb ranged from -2.26 to 2.60 which classified as 'low contamination' to 'moderate contamination' levels, CI value of Dy ranged from -2.50 to 1.98 which classified as 'low contamination' to 'moderate contamination' levels and CI value of Er ranged from -3.15 to 2.34 which classified as 'low contamination' to 'moderate contamination' levels. The descending order of highest average CI value of REE was Tb > Er > La and Dy > Ce > Nd > Eu.

The CI distribution maps of LREE (La, Ce and Nd) are shown in **Figure 4.40**, **Figure 4.41** and **Figure 4.42**. Based on the CI distribution maps, all LREE showed a small area of high CI value over 'low contamination' level (CI ≥ 1) which located in George Town, north east of Penang Island. This area of high CI values of LREE was classified as 'moderate contamination' levels.

The CI distribution maps of HREE (Eu, Tb, Dy, and Er) are shown in **Figure 4.43**, **Figure 4.44**, **Figure 4.45** and **Figure 4.46**. Both CI distribution maps of Eu and Tb displayed similar three areas of high CI value over 'low contamination' level (CI ≥ 1) which located in Bandar Air Itam in centre of Penang Island, George Town in north east of Penang Island and Balik Pulau in south west of Penang Island. The area of high CI values of Eu and Tb in Bandar Air Itam showed larger than areas of high CI values of Eu and Tb in George Town and Balik Pulau.

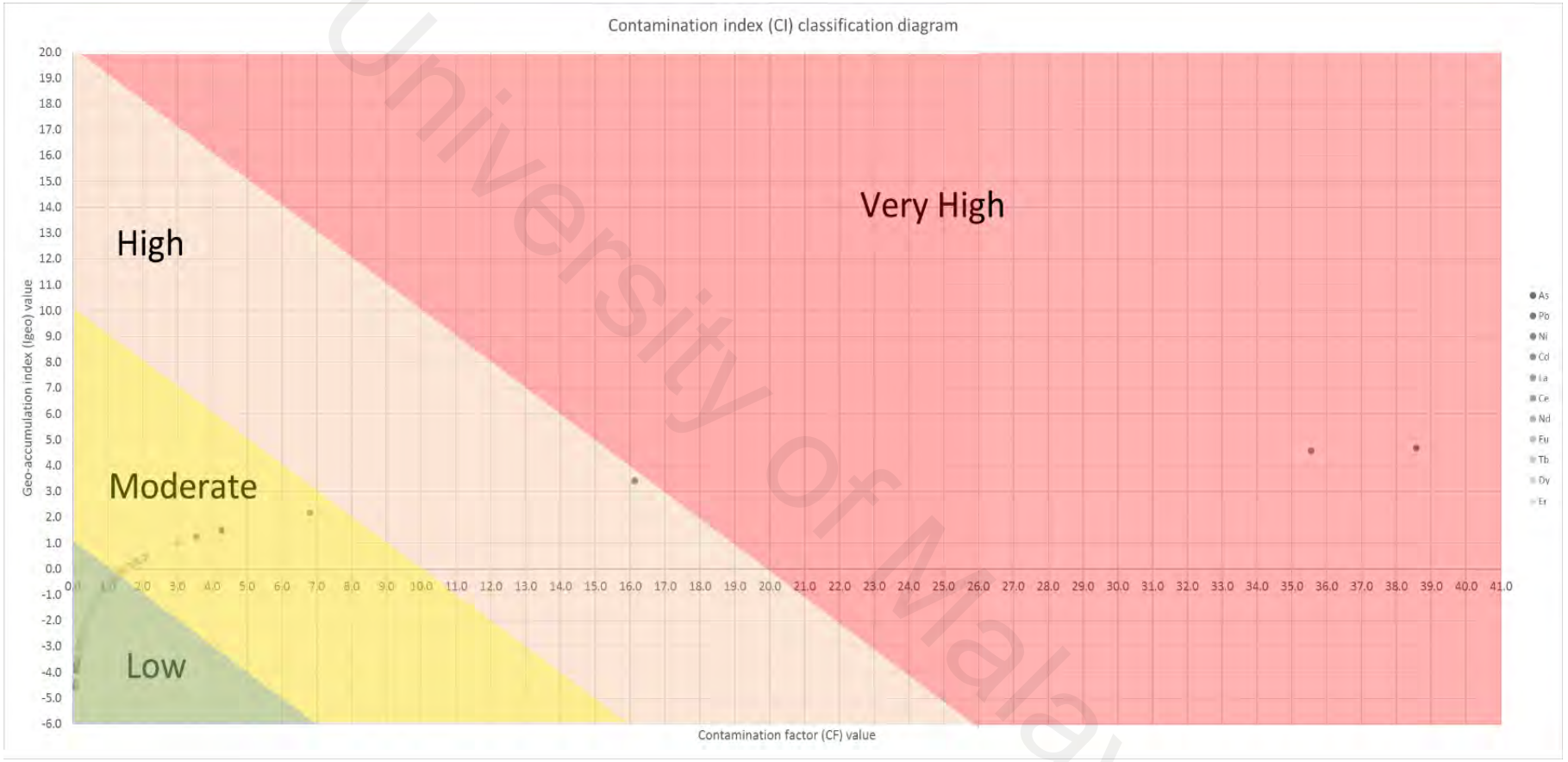

Figure 4.35: Contamination index (CI) classification diagram.

All of these three areas of high CI values of Eu and Tb were classified as 'moderate contamination' levels. Both CI distribution maps of Dy and Er showed similar two areas of high CI value over 'low contamination' level (CI ≥ 1) which located in George Town in north east of Penang Island and Balik Pulau in south west of Penang Island. Both areas of high CI values of Dy and Er were classified as 'moderate contamination' levels.

Table 4.22: Contamination index (CI) assessment results of heavy metals in top soils of Penang Island.

Heavy metal	Mean	Minimum	Maximum	Contamination level
As	-1.71	-3.84	5.76	Low contamination to moderate contamination
Pb	1.23	-2.46	43.26	Low contamination to very high contamination
Ni	0.35	-2.55	40.12	Low contamination to very high contamination
Cd	-1.58	-4.48	8.98	Low contamination to moderate contamination

Table 4.23: Areas of high heavy metals contamination index (CI) values (CI ≥ 1) in top soils of Penang Island.

Heavy metal	High CI value area	Level of CI
As	Bandar Air Itam	Moderate contamination
Pb	Batu Ferringhi	High contamination
	George Town	Very high contamination
Ni	Jelutong	Very high contamination
	Teluk Bahang	Moderate contamination
	Tanjung Bunga	Moderate contamination
Cd	George Town	Moderate contamination
	Bandar Air Itam	Moderate contamination
	Tanjung Bunga	Moderate contamination
	Balik Pulau	Moderate contamination

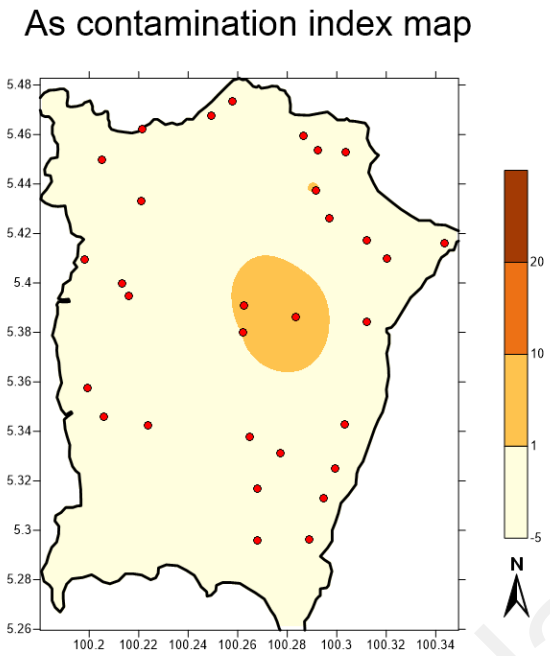

Figure 4.36: Contamination index (CI) distribution map of As in top soils of Penang Island.

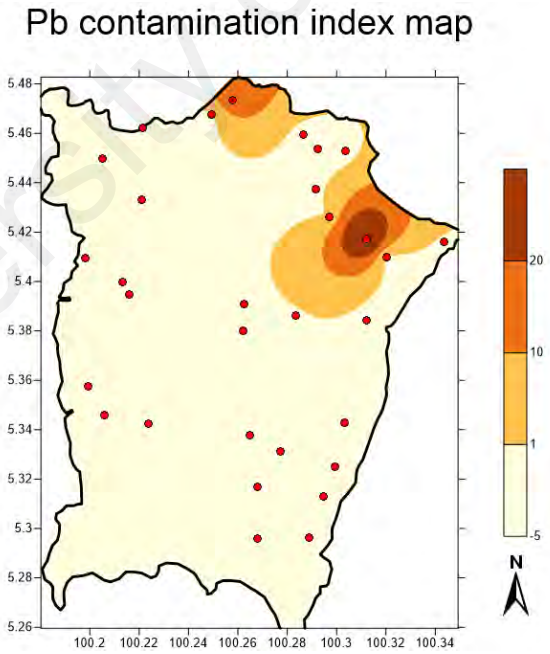

Figure 4.37: Contamination index (CI) distribution map of Pb in top soils of Penang Island.

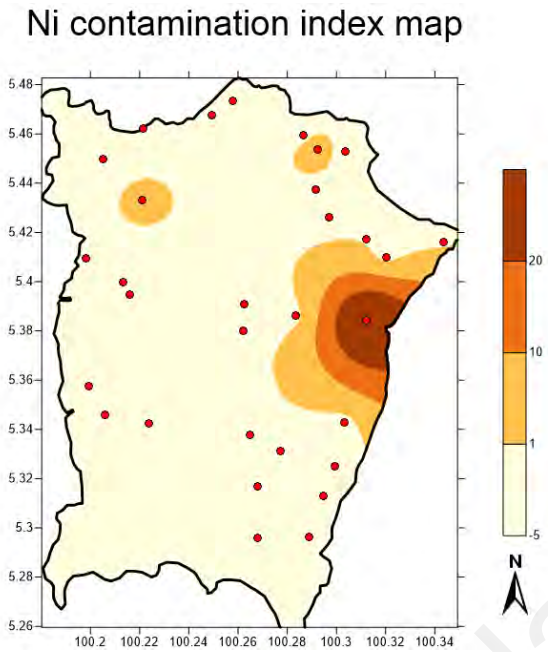

Figure 4.38: Contamination index (CI) distribution map of Ni in top soils of Penang Island.

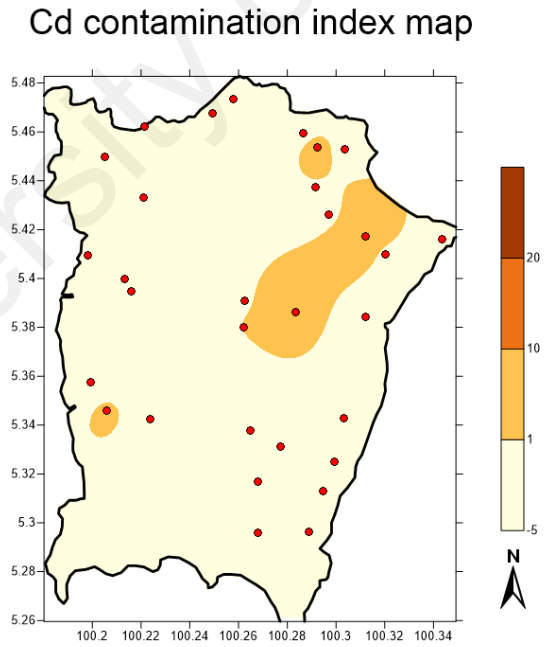

Figure 4.39: Contamination index (CI) distribution map of Cd in top soils of Penang Island.

Table 4.24: Contamination index (CI) assessment results of REE in top soils of Penang Island.

	Mean	Minimum	Maximum	Contamination Level
LREE				
La	-0.82	-2.32	1.74	Low contamination to moderate contamination
Ce	-0.95	-2.61	2.10	Low contamination to moderate contamination
Nd	-1.03	-2.56	1.56	Low contamination to moderate contamination
HREE				
Eu	-1.21	-4.27	4.01	Low contamination to moderate contamination
Tb	-0.65	-2.26	2.60	Low contamination to moderate contamination
Dy	-0.82	-2.50	1.98	Low contamination to moderate contamination
Er	-0.78	-3.15	2.34	Low contamination to moderate contamination

Table 4.25: Areas of high REE contamination index (CI) values (CI ≥ 1) in top soils of Penang Island.

REE	High CF value area	Level of CF
All LREE	George Town	Moderate contamination
Eu and Tb	Bandar Air Itam	Moderate contamination
	George Town	Moderate contamination
	Balik Pulau	Moderate contamination
Dy and Er	George Town	Moderate contamination
	Balik Pulau	Moderate contamination

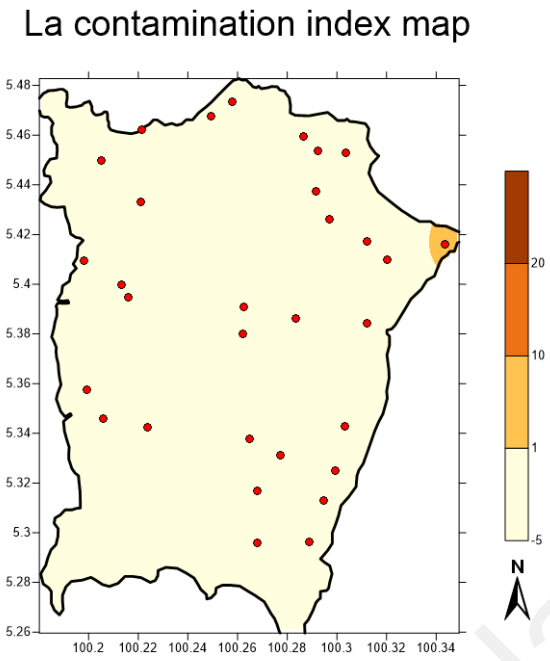

Figure 4.40: Contamination index (CI) distribution map of La in top soils of Penang Island.

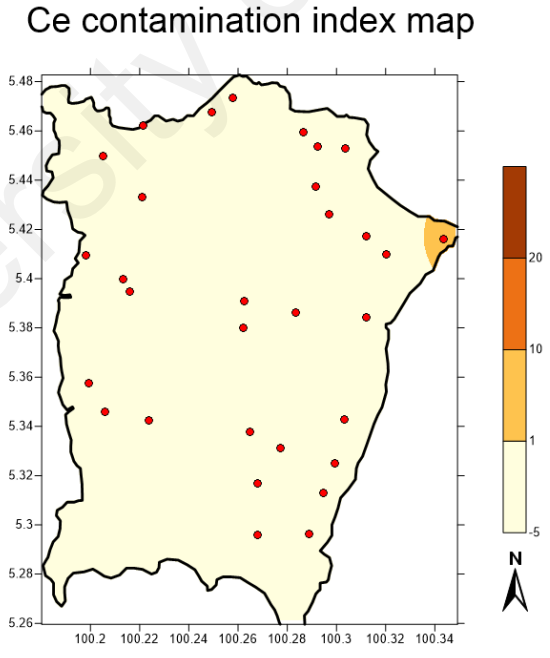

Figure 4.41: Contamination index (CI) distribution map of Ce in top soils of Penang Island.

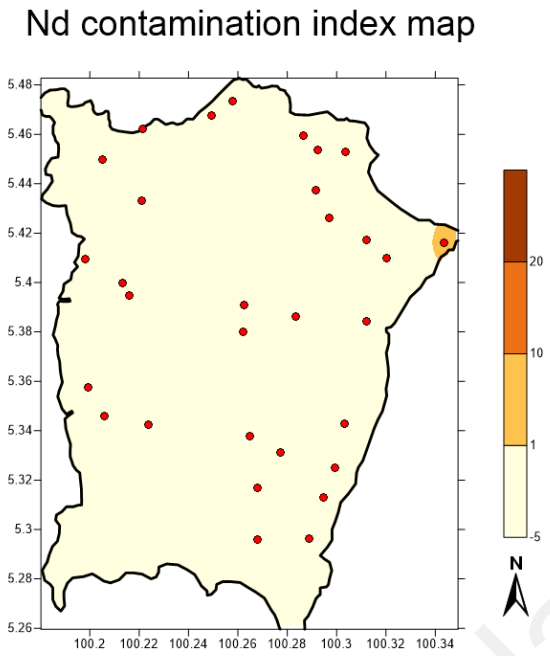

Figure 4.42: Contamination index (CI) distribution map of Nd in top soils of Penang Island.

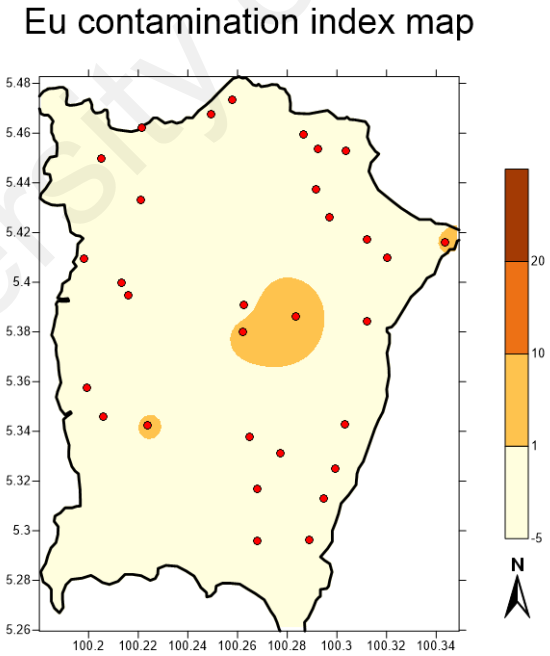

Figure 4.43: Contamination index (CI) distribution map of Eu in top soils of Penang Island.

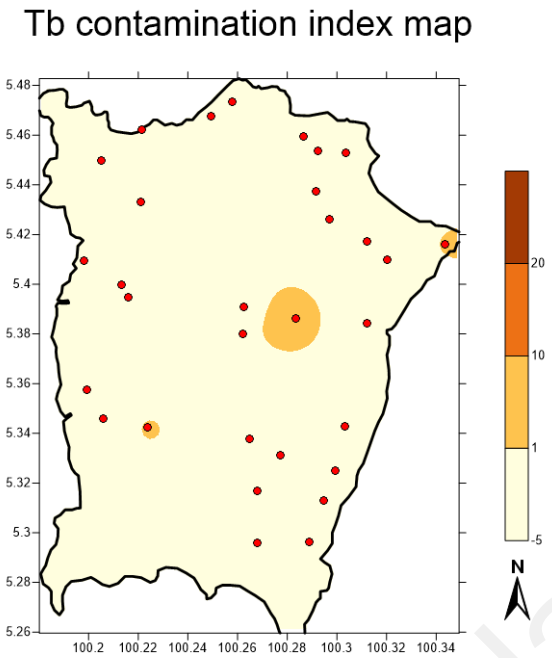

Figure 4.44: Contamination index (CI) distribution map of Tb in top soils of Penang Island.

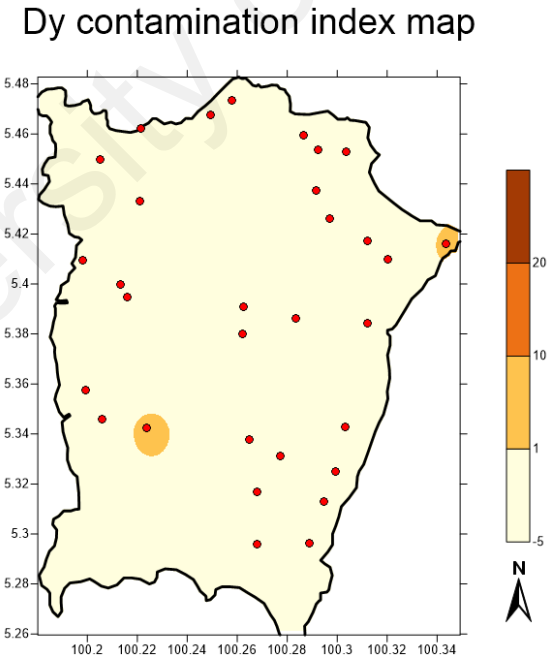

Figure 4.45: Contamination index (CI) distribution map of Dy in top soils of Penang Island.

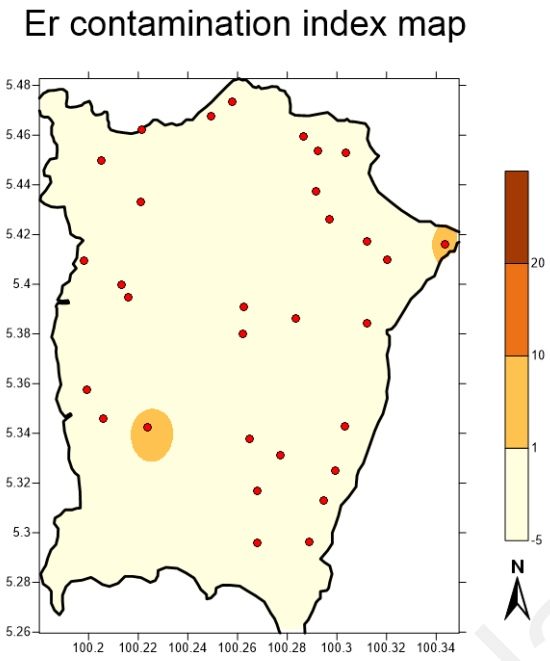

Figure 4.46: Contamination index (CI) distribution map of Er in top soils of Penang Island.

4.6 Statistical analysis

4.6.1 Statistical analysis of heavy metals and soil physicochemical properties

PCA results of heavy metals are shown in **Table 4.26** and **Table 4.27**. Result of initial eigenvalues in **Table 4.26** showed that two factors were extracted from available dataset. These two factors explain 67.353 % of the total variance. Rotated component matrix for heavy metal dataset in **Table 4.27** showed As, Cd and Pb were associated with the first component (F1) with values of -0.691, 0.869 and 0.595 respectively. F1 was responsible for 40.135 % of the total variance. Second component (F2) which responsible for 27.218 % of the total variance was represented by Ni with value of 0.941. In rotated space of PCA, components of heavy metals were plotted in diagram as shown in **Figure 4.47**. The nearest distance among heavy metals was represented by Cd and Pb components. Therefore, Cd and Pb showed correlation in PCA of heavy metals.

Result of Pearson correlation analysis of heavy metals concentration and soil physicochemical properties in top soils of Penang Island is shown in **Table 4.28**.

Among heavy metals, only Pb and Cd showed correlation between each other with positive correlation (0.839).

Both PCA and Pearson correlation analysis showed relationship between Pb and Cd. Association of Pb and Cd in soils is always related to traffic emissions (Wong et al., 2006; Hamzeh et al., 2011; Simasuwannarong et al., 2012; Ağca, 2015). In Rayong Province, Thailand, result of Pearson correlation analysis among heavy metals also showed correlation between Pb and Cd with positive correlation (0.9251) (Simasuwannarong et al., 2012). In Zhangzhou city, Fujian, China, Pb and Cd also showed positive correlation (0.957) in Pearson correlation analysis and classified under similar component in PCA (Cui et al., 2011).

Correlation between heavy metals and soil physicochemical properties was only represented by Cd concentration and OM with positive correlation (0.357). The correlation coefficient value of Cd and OM is not too high. Cd has a strong affinity to OM and can be bonded by humic substance to a greater extent than the major inorganic ligands especially at high pH levels (FOREGS, 2005).

4.6.2 Statistical analysis of REE and soil physicochemical properties

Summarized results of PCA of REE are shown in **Table 4.29** and **Table 4.30**. Based on result in **Table 4.29**, two factors were extracted from available dataset which explains 91.699 % of the total variance. Rotated component matrix of REE in **Table 4.30** displayed that La, Ce and Nd (LREE) were associated with F1 with values of 0.98, 0.94 and 0.99 respectively whereas Eu, Tb, Dy and Er (HREE) were associated with F2 with values of 0.84, 0.93, 0.84 and 0.91 respectively. F1 was subjected to cover up to 70.220 % of the total total variance whereas F2 was subjected to cover up to 21.479 % of the total variance. The rotated space diagram in **Figure 4.48** showed the nearest distance of REE was represented by La-Ce-Nd and Tb-Er-Dy. However, Eu showed isolated from other REE but nearer to Tb-Er-Dy than La-Ce-Nd.

Pearson correlation results of REE concentration levels and soil physicochemical properties in top soils of Penang Island are shown in **Table 4.31**. Based on the results, all LREE showed positive correlations between each other. The correlations among LREE were represented by La and Ce (0.952), La and Nd (0.989) and, Ce and Nd (0.940). All HREE showed positive correlations between each other which represented by Eu and Tb (0.886), Eu and Dy (0.441), Eu and Er (0.598), Tb and Dy (0.704), Tb and Er (0.806) and, Dy and Er (0.969). Between LREE and HREE, all LREE showed positive correlations with all HREE except Eu. The correlations were represented by La and Tb (0.455), La and Dy (0.706), La and Er (0.597), Ce and Tb (0.378), Ce and Dy (0.592), Ce and Er (0.495), Nd and Tb (0.461), Nd and Dy (0.753) and, Nd and Er (0.640).

Both PCA and Pearson correlation analysis showed correlation of REE by separation between LREE and HREE. Similar correlations were also showed by a study of REE distribution in top soil of Sweden where the relationships among REE were represented by separation groups of LREE and HREE (Sadeghi et al., 2013). The separation between groups of LREE and HREE was expected to be related with the different weathering scale of granitic soil. In granite residual soils, concentration of LREE is always greater than concentration of HREE (Kabata-Pendias & Mukherjee, 2007; Yusoff et al., 2013).

Between all REE and soil physicochemical properties, only Nd showed correlation with OM but with negative correlation (-0.359). The correlation coefficient between Nd and OM was -0.359 which is not too strong. In study of REE contamination in soils around Tshamilemba Canal in Katanga, Democratic Republic of the Congo, the correlation analysis showed that Nd was negatively correlated with OM (-0.3) (Atibu et al., 2016). Nd is one of LREE group member. Organic REE complexes tend to have greater stability with HREE than LREE (Aide & Aide, 2012).

4.6.3 Statistical analysis among heavy metals and REE

Results of Pearson correlation analysis between heavy metals and REE concentration levels in top soils of Penang Island are shown in **Table 4.32**. Based on the results, only As from heavy metals group showed correlation with Eu and Tb from REE group. The correlations represented by As and Eu with positive correlation (0.755) and, As and Tb with positive correlation (0.755).

In ionic form, As easily replaces other elements in primary rock-forming silicate minerals like replacement of Fe^{3+} or Al^{3+} by As^{3+} (FOREGS, 2005). The apatite composition in granitic rock of Penang Island may increase the concentration of As in this phosphate mineral by substitution of P^{5+} by As^{5+} (Cobbing et al., 1992; FOREGS, 2005). Both Eu and Tb are group of HREE which are more associated to refractory minerals like zircon which may contains in granite parent rock (Ramos et al., 2016). Therefore, relationships between As with Eu and Tb were expected to be related to the mineralogy of the parent rock and soils of the area.

Table 4.26: Total variance explained of principle component analysis (PCA) of heavy metals.

Total Variance Explained									
	Initial Eigenvalues			Extraction Sums of Squared Loadings			Rotation Sums of Squared Loadings		
Component	Total	% of Variance	Cumulative %	Total	% of Variance	Cumulative %	Total	% of Variance	Cumulative %
1	1.605	40.135	40.135	1.605	40.135	40.135	1.591	39.777	39.777
2	1.089	27.218	67.353	1.089	27.218	67.353	1.103	27.576	67.353
3	.958	23.944	91.297						
4	.348	8.703	100.000						

Table 4.27: Extracted components from Varimax with Kaiser normalization rotation method in principle component analysis (PCA) of heavy metals.

	Component Matrix		Rotated Component Matrix	
Element	F1	F2	F1	F2
Ni	0.222	0.917	0.067	**0.941**
As	-0.682	0.113	**-0.691**	-0.002
Cd	0.903	0.131	**0.869**	0.279
Pb	0.525	-0.466	**0.595**	-0.373

Table 4.28: Results of Pearson correlation analysis of heavy metals and soil physicochemical properties.

	Clay (%)	Silt (%)	Sand (%)	pH	CEC	OM (%)	As (mg/Kg)	Pb (mg/Kg)	Cd (mg/Kg)	Ni (mg/Kg)
Clay (%)	1									
Silt (%)	0.986**	1								
Sand (%)	-0.994**	-0.998**	1							
pH	-0.094	-0.135	0.121	1						
CEC	0.974**	0.948**	-0.960**	0.041	1					
OM (%)	0.684**	0.734**	-0.719**	-0.056	0.673**	1				
As (mg/Kg)	-0.167	-0.176	0.174	-0.066	-0.118	-0.066	1			
Pb (mg/Kg)	-0.078	-0.044	0.056	0.128	-0.056	0.187	-0.086	1		
Cd (mg/Kg)	0.004	0.051	-0.035	0.120	0.004	0.357*	0.157	0.839**	1	
Ni (mg/Kg)	-0.058	-0.059	0.059	-0.321	-0.130	-0.051	-0.099	-0.044	-0.043	1

** Correlation is significant at the 0.01 level (2-tailed).
*Correlation is significant at the 0.05 level (2-tailed).

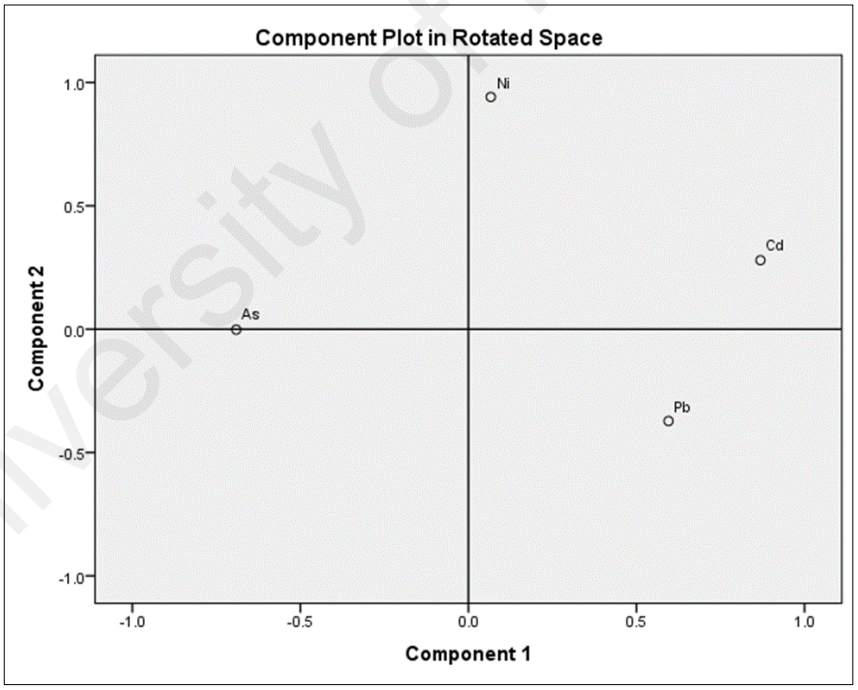

Figure 4.47: Component of heavy metals in rotated space diagram in principle component analysis (PCA).

Table 4.29: Total variance explained of principle component analysis (PCA) of REE.

Total Variance Explained							
	Initial Eigenvalues			Extraction Sums of Squared Loadings			Rotation Sums of Squared Loadings
Component	Total	% of Variance	Cumulative %	Total	% of Variance	Cumulative %	Total
1	4.915	70.220	70.220	4.915	70.220	70.220	4.396
2	1.504	21.479	91.699	1.504	21.479	91.699	3.714
3	.357	5.099	96.798				
4	.123	1.753	98.551				
5	.081	1.154	99.706				
6	.016	.226	99.932				
7	.005	.068	100.000				

Table 4.30: Extracted components from Promax with Kaiser normalization rotation method in principle component analysis (PCA) of REE.

Structure Matrix		
	Component	
	1	2
Ce	**0.94**	0.36
Eu	0.11	**0.84**
Tb	0.65	**0.93**
Dy	0.81	**0.84**
Er	0.69	**0.91**
La	**0.98**	0.48
Nd	**0.99**	0.49

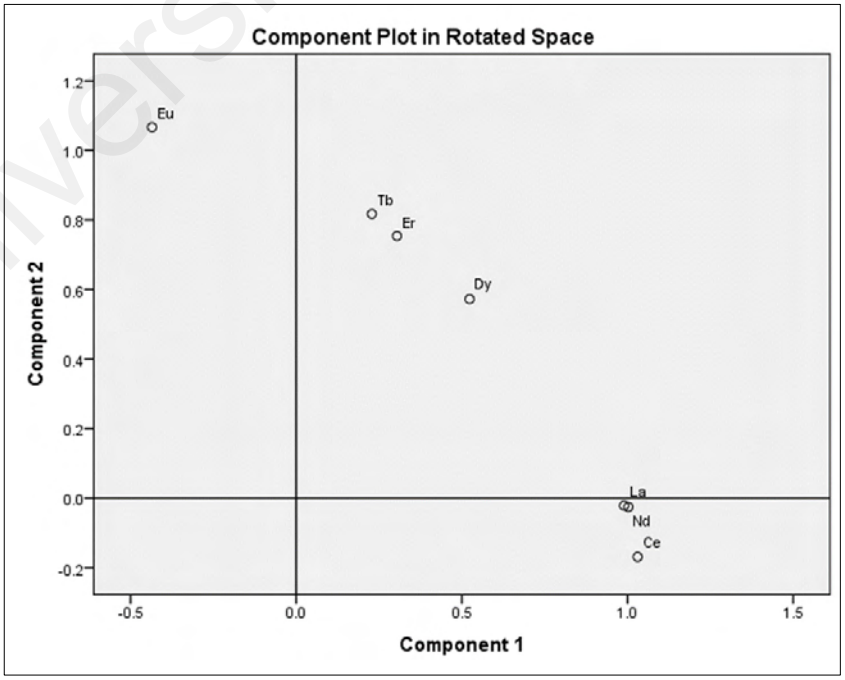

Figure 4.48: Component of REE in rotated space diagram in principle component analysis (PCA).

Table 4.31: Results of Pearson correlation analysis of REE and soil physicochemical properties.

	Clay (%)	Silt (%)	Sand (%)	pH	CEC	OM (%)	La (mg/ Kg)	Ce (mg/ Kg)	Nd (mg/ Kg)	Eu (mg/ Kg)	Tb (mg/ Kg)	Dy (mg/ Kg)	Er (mg/ Kg)
Clay (%)	1												
Silt (%)	0.986**	1											
Sand (%)	-0.994**	-0.998**	1										
pH	-0.094	-0.135	0.121	1									
CEC	0.974**	0.948**	-0.960**	0.041	1								
OM (%)	0.684**	0.734**	-0.719**	-0.056	0.673**	1							
La (mg/ Kg)	-0.273	-0.268	0.271	-0.068	-0.316	-0.339	1						
Ce (mg/ Kg)	-0.264	-0.262	0.264	-0.107	-0.301	-0.344	0.952**	1					
Nd (mg/ Kg)	-0.268	-0.262	0.265	-0.048	-0.314	-0.359*	0.989**	0.940**	1				
Eu (mg/ Kg)	-0.052	-0.063	0.060	0.060	-0.015	0.024	0.136	0.081	0.120	1			
Tb (mg/ Kg)	-0.273	-0.279	0.278	0.025	-0.266	-0.234	0.455*	0.378*	0.461**	0.886**	1		
Dy (mg/ Kg)	-0.281	-0.282	0.283	0.083	-0.309	-0.349	0.706**	0.592**	0.753**	0.441*	0.704**	1	
Er (mg/ Kg)	-0.258	-0.265	0.263	0.113	-0.267	-0.303	0.597**	0.495**	0.640**	0.598**	0.806**	0.969**	1

** Correlation is significant at the 0.01 level (2-tailed).
* Correlation is significant at the 0.05 level (2-tailed).

Table 4.32: Results of Pearson correlation analysis of heavy metals and REE.

	Ni (mg/Kg)	As (mg/Kg)	Cd (mg/Kg)	Pb (mg/Kg)	La (mg/Kg)	Ce (mg/Kg)	Nd (mg/Kg)	Eu (mg/Kg)	Tb (mg/Kg)	Dy (mg/Kg)	Er (mg/Kg)
Ni (mg/Kg)	1										
As (mg/Kg)	-0.099	1									
Cd (mg/Kg)	-0.043	0.157	1								
Pb (mg/Kg)	-0.044	-0.086	0.839**	1							
La (mg/Kg)	-0.051	-0.094	-0.279	-0.134	1						
Ce (mg/Kg)	-0.023	-0.061	-0.216	-0.102	0.952**	1					
Nd (mg/Kg)	-0.038	-0.120	-0.286	-0.137	0.989**	0.940**	1				
Eu (mg/Kg)	-0.134	0.755**	0.084	-0.103	0.136	0.081	0.120	1			
Tb (mg/Kg)	-0.116	0.686**	-0.046	-0.159	0.455*	0.378*	0.461**	0.886**	1		
Dy (mg/Kg)	-0.103	0.003	-0.235	-0.146	0.706**	0.592**	0.753**	0.441*	0.704**	1	
Er (mg/Kg)	-0.125	0.181	-0.159	-0.133	0.597**	0.495**	0.640**	0.598**	0.806**	0.969**	1
** Correlation is significant at the 0.01 level (2-tailed). * Correlation is significant at the 0.05 level (2-tailed).											

4.7 Summary

The results showed that the mean concentration level of selected heavy metals and REE in top soils of Penang Island was in order of Pb > As > Ce > La > Nd > Ni > Dy > Er > Tb > Cd > Eu. George Town, Batu Ferringhi, Jelutong and Bandar Air Itam represented high concentration areas of heavy metals. Teluk Bahang, Bandar Air Itam, George Town and Balik Pulau displayed high concentration areas of REE. The high concentration of heavy metals in top soils of Penang Island was expected to be derived from anthropogenic source whereas the high concentration of REE in top soils of Penang Island was expected to be influenced by weathering of parent material (granite) and anthropogenic source. Based on the contamination level assessments, both CF and I_{geo} assessments showed different results of level classification and areas of high contamination level. In proposed assessment that combine both CF and I_{geo} assessments, CI assessment represented the areas that showed high level contamination of heavy metals were Bandar Air Itam, Batu Ferringhi, George Town, Jelutong, Teluk Bahang, Tanjung Bunga and Balik Pulau whereas areas of high level contamination of REE were George Town, Bandar Air Itam and Balik Pulau. PLI assessment showed the contamination levels of heavy metals and REE were classified as 'unpolluted' level. The statistical analysis represented that among heavy metals; the relationship was showed by Pb and Cd which was expected to be related to traffic emissions. Among REE, the relationship was dividing REE into LREE and HREE which was predicted to be influenced by weathering of parent material. Between heavy metals and REE, the relationships were represented by As with Eu and Tb which were expected to be influenced by mineralogy of the soils and rock of the area. Among heavy metals and REE, only Cd and Nd showed correlation with soil physicochemical properties which both correlated with OM. Positive correlation of Cd and negative correlation of Nd with OM were expected to be related to the natural chemical behaviour of them.

CHAPTER 5: CONCLUSION

5.1 Introduction

This chapter summarizes all the findings from the study of distribution of selected heavy metals and REE in top soils of Penang Island.

5.2 Concentration level of heavy metals

The concentration level of heavy metals in top soils of Penang Island showed concentration of As ranged from 67.9 to 2942.1 mg/Kg with mean value of 366.6 mg/Kg, concentration of Pb ranged from 42.1 to 7019.6 mg/Kg and mean value of 422.9 mg/Kg, concentration of Ni ranged from 6.5 to 1049.2 mg/Kg with mean value of 51.7 mg/Kg and concentration of Cd ranged from 0.2 to 16.7 mg/Kg with mean value of 1.6 mg/Kg. The descending order of highest mean concentration level of heavy metals was Pb > As > Ni > Cd.

In comparison between granite residual soil and Quaternary deposit soil samples, As mean concentration in granite residual soils was higher than As mean concentration in Quaternary deposit soils. Pb and Ni mean concentrations in Quaternary deposit soils were higher than Pb and Ni mean concentrations in granite residual soils. Cd mean concentration in Quaternary deposit soils was higher than Cd mean concentration in granite residual soil.

5.3 Concentration level of REE

The concentration level of REE in top soils of Penang Island represented that concentration of La ranged from 34.0 to 218.9 mg/Kg with mean value of 82.1 mg/Kg, concentration of Ce ranged from 70.1 to 602.3 mg/Kg with mean value of 191.2 mg/Kg, concentration of Nd ranged from 28.8 to 201.9 mg/Kg with mean value of 72.9 mg/Kg, concentration of Eu ranged from 0.14 to 5.86 mg/Kg with mean value of 1.16 mg/Kg, concentration of Tb ranged from 0.77 to 6.23 with mean value of 2.01 mg/Kg,

concentration of Dy ranged from 3.12 to 24.20 mg/Kg with mean value of 8.57 mg/Kg and concentration of Er ranged from 0.99 to 12.63 mg/Kg with mean value of 4.16 mg/Kg. The descending order of highest average concentration level of REE was Ce > La > Nd > Dy > Er > Tb > Eu.

In comparison between granite residual soil and Quaternary deposit soil samples, all REE showed mean concentrations in granite residual soils were higher than mean concentrations in Quaternary deposit soils.

5.4 Spatial distribution of heavy metals

There were four high concentration areas of heavy metals have been determined from spatial distribution analysis:

i. High concentration of As in Bandar Air Itam.
ii. High concentration of Pb and Cd in George Town.
iii. High concentration of Pb in Batu Ferringhi.
iv. High concentration of Ni in Jelutong.

All high concentrations of heavy metals in top soils of Penang Island were expected to be derived from anthropogenic source.

5.5 Spatial distribution of REE

Based on spatial distribution analysis of REE, high concentration areas of REE have been determined:

i. High concentration of La, Ce and Nd (LREE) in Teluk Bahang.
ii. High concentration of Tb and Eu in Bandar Air Itam.
iii. High concentration of Dy and Er in Balik Pulau.
iv. High concentration of most REE in George Town.

High concentration of REE in top soils of Penang Island except George Town was expected to be derived from parent material. However, high concentration of most REE

in George Town was predicted to be originated from anthropogenic source which was related to historical place of the area.

5.6 Contamination level assessment

5.6.1 Contamination factor (CF) assessment

CF assessment of heavy metals and REE concentrations in top soils of Penang Island showed:

i. As concentration ranged from 'no element enrichment' to 'considerable contamination' levels.
ii. Pb, Ni and Cd concentrations were ranged from 'no element enrichment' to 'very high contamination' levels.
iii. All REE concentrations were ranged from 'no element enrichment' to 'moderate contamination' levels.

The areas that showed high CF values with the level over 'no element enrichment' ($CF \geq 1$) were:

i. Bandar Air Itam represented 'considerable contamination' level of As and 'moderate contamination' level of Eu and Tb.
ii. George Town represented 'very high contamination' level of Pb and Cd and, 'moderate contamination' of LREE, Tb, Dy and Er.
iii. Batu Ferringhi showed 'very high contamination' level of Pb.
iv. Jelutong showed 'very high contamination' level of Ni.
v. Teluk Bahang represented 'moderate contamination' level of Ni and LREE.
vi. Tanjung Bunga represented 'moderate contamination' level of Ni, Tb, Dy and Er.
vii. Balik Pulau represented 'moderate contamination' level of Cd and HREE.

5.6.2 Geo-accumulation index (I_{geo}) assessment

I_{geo} assessment of heavy metals and REE concentrations in top soils of Penang Island had determined:

i. As concentration ranged from 'unpolluted' to 'moderately polluted' levels.
ii. Pb and Ni concentrations were ranged from 'unpolluted' to 'strongly to extremely polluted' levels.
iii. Cd concentration ranged from 'unpolluted' to 'moderately to strongly polluted' levels.
iv. All REE concentrations were ranged from 'unpolluted' to 'unpolluted to moderately polluted' levels.

The areas that showed high I_{geo} values with over 'unpolluted' level ($I_{geo} > 0$) were:

i. Bandar Air Itam represented 'moderately polluted' level of As and 'unpolluted to moderately polluted' level of Cd, Eu and Tb.
ii. Batu Ferringhi showed 'strongly to extremely polluted' level of Pb.
iii. George Town represented 'strongly to extremely polluted' level of Pb, 'moderately to strongly polluted' level of Cd, 'unpolluted to moderately polluted' level of LREE and Er.
iv. Jelutong showed 'strongly to extremely polluted' level of Ni.
v. Teluk Bahang and Tanjung Bunga represented 'unpolluted to moderately polluted' level of Ni.
vi. Balik Pulau showed 'unpolluted to moderately polluted' level of Dy and Er.

5.6.3 Contamination index (CI) assessment

In the proposed assessment which combined CF and I_{geo} assessments, contamination index (CI) assessment was represented:

i. As and Cd concentrations were ranged from ‘low contamination’ to ‘moderate contamination’ levels.
ii. Pb and Ni concentrations were ranged from ‘low contamination’ to ‘very high contamination’ levels.
iii. All REE concentrations were ranged from ‘low contamination’ to ‘moderate contamination’ levels.

The areas that showed high CI values with the level over ‘no element enrichment’ (CI ≥ 1) were:

i. Bandar Air Itam represented ‘moderate contamination’ level of As, Cd, Eu and Tb.
ii. Batu Ferringhi showed ‘high contamination’ level of Pb.
iii. George Town represented ‘very high contamination’ level of Pb and ‘moderate contamination’ level of Cd and all REE.
iv. Jelutong represented ‘very high contamination’ level of Ni.
v. Teluk Bahang showed ‘moderate contamination’ level of Ni.
vi. Tanjung Bunga showed ‘moderate contamination’ level of Ni and Cd.
vii. Balik Pulau represented ‘moderate contamination’ level of Cd and HREE.

5.7 Statistical analysis

Both PCA and Pearson correlation analysis of heavy metals displayed relationship between Pb and Cd. Only Cd showed correlation with OM in relationship between heavy metals and soil physicochemical properties with positive correlation in Pearson correlation analysis. Both PCA and Pearson correlation analysis of REE showed relationship that separated LREE and HREE. The relationship between REE and soil physicochemical properties was only represented by Nd and OM with negative

correlation in Pearson correlation analysis. Between heavy metals and REE the relationships were represented by As with Eu and Tb with positive correlations.

5.8 Recommendation for future study

The anthropogenic sources of high concentration of heavy metals in top soils of Penang Island need to be investigated to identify the real factor that contributes to the heavy metals in the soils. The suspected sources of contamination of heavy metals such as traffic and industrial emissions dust and residential waste sludge need to be collected and analysed. The research on the impact of historical material, coal in George Town on the REE contamination in soils surrounded the area is also recommended for future study. Soil samples should be collected in other similar historical areas which can be compared with this study REE concentration results. Other than that, the geochemical baseline for entire top soils of Malaysia also have to be determined to assess and evaluate the concentration level of chemical elements in order to prevent the contamination of hazardous elements in the soils.

REFERENCES

Abrahams, P. W. (2002). Soils: their implications to human health. *Science of the Total Environment, 291,* 1-32.

Ağca, N. (2015). Spatial distribution of heavy metal content in soils around an industrial area in Southern Turkey. *Arabian Journal of Geosciences, 8*, 1111-1123.

Aguilar, J., Dorronsoro, C., Fernández, E., Fernández, J., García, I., Martín, F., Sierra, M., & Simón, M. (2007). Arsenic contamination in soils affected by a pyrite-mine spill (Aznalcóllar, SW Spain). *Water, Air, & Soil Pollution, 180*, 271-281.

Ahmad, F., Yahaya, A. S., & Farooqi, M. A. (2006). Characterization and geotechnical properties of Penang residual soil with emphasis on landslides. *American Journal of Environmental Sciences, 2*(4), 121-128.

Aide, M. T., & Aide, C. (2012). Rare earth elements: their importance in understanding soil genesis. *International Scholarly Research Network, 2012*, 1-11.

Alloway, B. J. (2013). *Heavy metals in soils* (3rd ed.). Dordrecht: Springer.

Argyraki, A., & Kelepertzis, E. (2014). Urban soil geochemistry in Athens, Greece: the importance oflocal geology in controlling the distribution of potentially harmfultrace elements. *Science of the Total Environment, 482-483,* 366-377.

Arham, Z., Asmin, L. O., Rosmini, & Nurdin, M. (2017). Heavy metal content of cocoa plantation soil in East Kolaka, Indonesia. *Oriental Journal of Chemistry, 3*(33), 1164-1170.

Arifin, Z., Puspitasari, R., & Miyazaki, N. (2012). Heavy metal contamination in Indonesian coastal marine ecosystems: a historical perspective. *Coastal Marine Science, 35*(1), 227-233.

Ashworth, D. J., & Alloway, B. J. (2008). Influence of dissolved organic matter on the solubility of heavy metals in sewage-sludge-amended soils. *Communications in Soil Science and Plant Analysis, 39*, 538-550.

Atibu, E. K., Devarajan, N., Lafitte, A., Giuliani, G., Salumu, J. A., Muteb, R. C., Mulaji, C. K., Otamonga, J. P., Elongo, V., Mpiana, P. T., & Poté, J. (2016). Assessment of trace metal and rare earth elements contamination in rivers around abandoned and active mine areas. The case of Lubumbashi River and Tshamilemba Canal, Catanga, Democratic Republic of the Congo. *Chemie der Erde, 76*, 353-362.

Aubert, D., Stille, P., & Probst, A. (2001). REE fractionation during granite weathering and removal by waters and suspended loads: Sr and Nd isotopic evidence. *Geochimica et Cosmochimica Acta, 65*(3), 387-406.

Barbieri, M. (2016). The importance of enrichment factor (EF) and geo-accumulation index (I_{geo}) to evaluate the soil contamination. *Journal of Geology and Geophysics, 5*(1), 1-4.

Bempah, C. K., Ewusi, A., Yeboah, S. O., Asabere, S. B., Mensah, F., Baoteng, J., & Voigt, H. J. (2013). Distribution of arsenic and heavy metals from mine tailing dams at Obuasi Municipality of Ghana. *American Journal of Engineering Research, 2*(5), 61-70.

Benhaddya, M. L., & Hadjel, M. (2013). Spatial distribution and contamination assessment of heavy metals in surface soils of Hassi Messaoud, Algeria. *Environmental Earth Sciences, 71*, 1473-1486.

Benson, N. U., Enyong, P. A., & Fred-Ahmadu, O. H. (2016). Trace metal contamination characteristics and health risk assessment *commelina africana* L. and psammitic sandflats in the Niger Delta, Nigeria. *Applied and Environmental Soil Science, 16,* 1-14.

Berkowitz, B., Dror, I., & Yaron, B. (2008). *Contaminant geochemistry: interactions and transport in the subsurface environment.* Berlin: Springer Verlag.

Birke, M., & Rauch, U. (2000). Urban geochemistry: Investigations in the Berlin Metropolitan Area. *Environmental Geochemistry and Health, 22*(3), 233-248.

Brioschi, L., Steinmann, M., Lucot, E., Pierret, M. C., Stille, P., Prunier, J., & Badot, P. M. (2013). Transfer of rare earth elements (REE) from natural soil to plant systems: implications for the environmental availability of anthropogenic REE. *Plant Soil, 366*, 143-163.

Brown, W. M. (2003). *The royal navy's fuel supplies, 1898-1939; the transition from coal to oil* (PhD thesis). Retrieved on 13 August 2017, from https://kclpure.kcl. ac.uk/portal/en/ theses/the-royal-navys-fuel-supplies-18981939--the-transition-from-coal-to-oil

Bruins, M. R., Kapil, S., & Oehme, F. W. (2000). Microbial resistance to metals in the environment. *Ecotoxicology and Environmental Safety, 45*, 198–207.

BS 1377-1. (1990). *Methods of test for soils for civil engineering purposes: part 1: general requirements and sample preparation*. London: British Standard Institution.

BS 1377-2. (1990). *Methods of test for soils for civil engineering purposes: part 2: classification tests*. London: British Standard Institution.

BS 1377-3. (1990). *Methods of test for soils for civil engineering purposes: part 3: chemical and electro-chemical tests*. London: British Standard Institution.

Budianta, W. (2012). Lead contamination in soil of Yogyakarta City, Indonesia. *Journal of Southeast Asian Applied Geology, 4*(2), 90-98.

Buttafuoco, G., Guagliardi, I., Tarvainen, T. & Jarva, J. (2017). A multivariate approach to study the geochemistry of urban topsoil in the city of Tampere, Finland. *Journal of Geochemical Exploration, 181*, 191-204.

Buttafuoco, G., Tarvainen, T., Jarva, J. & Guagliardi, I. (2016). Spatial variability trigger values of arsenic in the surface urban soils of the cities of Tampere and Lahti, Finland. *Environmental Earth Sciences, 75*(896), 1-13.

Carr, R., Zhang, C., Moles, N., & Harder, M. (2008). Identification and mapping of heavy metal pollution in soils of a sports ground in Galway City, Ireland, using a portable XRF analyser and GIS. *Environmental Geochemistry and Health, 30*, 45-52.

Chen, H., Teng, Y., Lu, S., Wang, Y., & Wang, J. (2015). Contamination features and health risk of soil heavy metals in China. *Science of the Total Environment, 512-513*, 143-153.

Cheng, H., Hao, F., Ouyang, W., Liu, S., Chunye, L., & Wenjing, Y. (2012). Vertical distribution of rare earth elements in a wetland soil core from the Sanjiang Plain in China. *Journal of Rare Earths, 30*(7), 731-738.

Chinoim, N., & Sinbuathong, N. (2010, August). Heavy metal contamination of soils from organic paddy fields in Thailand. In *Soil Solutions for a Changing World*. Symposium conducted at the meeting of the 19th World Congress of Soil Science of Brisbane, Australia.

Cidu, R., Biddau, R., & Vittori Antisari, L. (2013). Investigation on REE transported by airborne dust and deposited on vegetation. *Procedia Earth and Planetary Science, 7*, 69-72.

Cobbing, E. J., Pitfield, P. E. J., Darbyshire, D. P. F., & Mallick, D. I. J. (1992). *The Granites of the South-East Asian Tin Belt.* London: British Geological Survey, Overseas Memoir.

Cui, Z. A., Qiao, S. Y., Bao, Z. Y., & Wu, N. Y. (2011). Contamination and distribution of heavy metals in urban and suburban soils in Zhangzhou City, Fujian, China. *Environmental Earth Sciences, 64,* 1607-1615.

Dantu, S. (2014). Spatial distribution and geochemical baselines of major/trace elements in soils of Medak district, Andhra Pradesh, India. *Environmental Earth Sciences, 72*(4), 955-981.

Department of Statistics Malaysia. (2013). *Penang basic information 2013*. Retrieved on 25 June 2016, from https://www.penang.gov.my/images/pdf/statistik %20sosioekonomi/1.%20 DEMOGRAFI%20&%20EKONOMI.pdf

Diatta. J. B. (2006). The impact of additional Pb input on the dynamics of Pb-enriched agricultural soils. *Polish Journal of Environmental Studies, 15*(2), 219-227.

Dung, T. T. T., Cappuyns, V., Swennen, R., & Phung, K. Y. (2013). From geochemical background determination to pollution assessment of heavy metals in sediments and soils. *Reviews in Environmental Science and Bio/Technology, 12*, 335-353.

Egashira, K., Fujii, K., Yamasaki, S., & Virakornphanich, P. (1997). Rare earth element and clay minerals of paddy soils from the central region of the Mekong River, Laos. *Geoderma, 3-4*(78), 237-249.

Facchinelli, A., Saechi, E., & Mallen, L. (2001). Multivariate statistical and GIS-based approach to identify heavy metal sources in soils. *Environmental Pollution, 114*, 313–324.

Figueiredo, A. M. G., Camargo, S. P., & Sígolo, J. B. (2009). Determination of REE in urban park soils from São Paulo city for fingerprint of traffic emission contamination. *Associação Brasileira de Energia Nuclear, 978,* 1-7.

Fiket, Z., Medunic, G., & Kniewald, G. (2016). Rare earth elements distribution in soil nearby thermal power plant. *Environmental Earth Sciences, 75*(598), 1-9.

Folgueras M. B., Alonso, M., & Fernández, F. J. (2017). Coal and sewage sludge ashes as sources of rare earth elements. *Fuel, 192,* 128-139.

Forum of Europian Geological Surveys (FOREGS). (2005). *Geochemical atlas of Europe*. Retrieved on 13 July 2017, from http://weppi.gtk.fi/publ/ foregsatlas/maps_table.php

Ghani, A. A., Searle, M., Robb, L., & Chung, S. L. (2013). Transitional I S type characteristic in the main range granite, Peninsular Malaysia. *Journal of Asian Earth Sciences, 76,* 225-240.

Ghazali, S. (2013). Sense of place and the politics of "insider-ness" in villages undergoing transition: the case of city *kampung* on Penang Island. In T. Bunnell, D. Parthasarathy & C. Thompson (Eds.), *Cleavage, connection and conflict in rural, urban and contemporary Asia* (pp. 117-142). Dordrecht: Springer.

Goh, B. P. L., & Chou, L. M. (1997). Heavy metal levels in marine sediments of Singapore. *Environmental Monitoring and Assessment, 44*(1), 67-80.

Gulan, L., Milenkovic, B., Zeremski, T., Milic, G., & Vuckovic, B. (2017). Persistent organic pollutants, heavy metals and radioactivity in the urban soil of Pristina City, Kosovo and Metohija. *Chemosphere, 171*, 415-426.

Guo, G., Wu, F., Xie, F., & Zhang, R. (2012). Spatial distribution and pollution assessment of heavy metals in urban soils from southwest China. *Journal of Environmental Sciences, 24*(3), 410-418.

Hakanson, L. (1980). An ecological risk index for aquatic pollution control: a sedimentological approach. *Water Research, 14*, 975–1001.

Hamzeh, M. A., Aftabi, A., & Mirzaee, M. (2011). Assessing geochemical influence of traffic and other vehicle-related activities on heavy metal contamination in urban soils of Kerman city, using a GIS-based approach. *Environmental Geochemistry and Health, 33*, 577-594.

Hao, L., Tian, M., Zhao, X., Zhao, Y., Lu, J., & Bai, R. (2016). Spatial distribution and sources of trace elements in surface soils, Changchun, China: insights from stochastic models and geostatistical analyses. *Geoderma, 273*, 54-63.

Harikumar, P. S., Nasir, U. P., & Mujeebu Rahma, M. P. (2009). Distribution of heavy metals in the core sediments of a tropical wetland system. *International Journal of Environmental Science and Technology, 6,* 225-232.

Hassan, A. S. (2009). The British colonial 'divide and rule' concept: its influence to transport access in inner city of George Town, Penang. *Transportation, 36*, 309-324.

Hassan, K. (1990). A summary of quaternary geology investigations in Seberang Perai, Pulau Pinang and Kuala Kurau. *Geological Society of Malaysia, 26*, 47-53.

Huang, Y., Chen, Q., Deng, M., Japenga, J., Li, T., Yang, X., & He, Z. (2018). Heavy metal pollution and health risk assessment of agricultural soils in a typical peri-urban area in southeast China. *Journal of Environmental Management, 207,* 159-168.

Humsa, T. Z., & Srivastava, R. K. (2015). Impact of rare earth mining and processing on soil and water environment at Chavara Kollam, Kerala: a case study. *Procedia Earth and Planetary Science, 11*, 566-581.

Imperato, M., Adamo, P., Naimo, D., Arienzo, M., Stanzione, D., & Violante, P. (2003). Spatial distribution of heavy metals in urban soils of Naples city (Italy). *Environmental Pollution, 124,* 247-256.

Kabata-Pendias, A., & Mukherjee, A. B. (2007). *Trace elements from soil to human*. Berlin: Springer Verlag.

Kabata-Pendias, A., & Pendias, H. (1984). *Trace elements in soils and plants*. United States: CRC Press.

Kamaruzzaman, B. Y., Hasrizal, B. S., & Jamil, B. T. (2004). Kadar pengenapan dan kepekatan beberapa logam berat pada permukaan sedimen di hutan paya bakau Bebar, Pahang. *Pertanika Journal of Science & Technology, 12*(1), 81-92.

Kamaruzzaman, B. Y., Husain M. L., Shazili N. A. M., Sulong, I., & Rashid, K.A. (2002). Study on the distribution of some heavy metals and pollution status of a tropical microtidal river: the Chukai-Kemaman River, Terengganu, Malaysia. *Dimensions of Pollution, 1*, 115-130.

Kamaruzzaman, B. Y., Miskan, M., Fikriah, F., Rahman, M. M., Ong, M. C., & Hasrizal, S. (2017). Rare earth elements behaviour at West Coast of Peninsular Malaysia rocky shore ecosystem using *Saccostrea Cucullata* as bioindicator. *Asian Journal of Chemistry, 10*(29), 2211-2215.

Kamaruzzaman, B. Y., Nurulnadia M. Y., Noor Azhar M. S., Ong M. C., Shahbudin S., Ahmed Jalal K. C., & Joseph B. (2011). Heavy metal concentration in the surface sediment of Tanjung Lumpur Mangrove Forest, Kuantan, Malaysia. *Sains Malaysiana, 40*(2), 89-92.

Karimi, A., Haghnia, G. H., Ayoubi, S., & Safari, T. (2017). Impacts of geology and land use on magnetic susceptibility and selected heavy metals in surface soils of Mashhad plain, northeastern Iran. *Journal of Applied Geophysics, 138,* 127-134.

Kyung, T. R., Kwon, H. K., & Jung, S. P. (2013). Toxicological evaluations of rare earths and their impacts to workers: A literature review. *Safety and Health at Work, 4*, 12-26.

Li, B. P., Jin, M., Xian, L. W., & Hong, H. (2016). Heavy metals in soils from a typical county in Shanxi Province, China: levels, sources and spatial distribution. *Chemosphere, 148,* 248-254.

Li, F., Fan, Z., Xiao, P., Oh, K., Ma, X., & Hou, W. (2009). Contamination, chemical speciation and vertical distribution of heavy metals in soils of an old and large industrial zone in Northeast China. *Environmental Geology, 57,* 1815-1823.

Liang, J., Feng, C., Zeng, G., Gao, X., Zhong, M., Li, X., Li, X., He, X., & Fang, Y. (2017). Spatial distribution and source identification of heavy metals in surface soils in a typical coal mine city, Lianyuan, China. *Environmental Pollution, 225,* 681-690.

Lim, J. Y., Matsumoto, Y., Chee, S. Y., Hong, C. W., Inoue, T., Usami A., Iwatsuki, E., & Yagi, A. (2017, August). Characteristics of water quality of rivers related to land-use in Penang Island, Malaysia. In H. Abdul Aziz (Chair), *Sustainable technology and practice for infrastructure and community resilience.* Paper presented at the proceedings of The International Conference of Global Network for Innovative Technology and Awam International Conference in Civil Engineering of Penang, Malaysia.

Liu, W. H., Zhao, J. Z., & Ouyang, Z. Y. (2005). Impacts of sewage irrigation on heavy metal distribution and contamination in Beijing, China. *Environmental International, 31*, 805–812.

Lu, S. G., & Bai, S. Q. (2010). Contamination and potential mobility assessment of heavy metals in urban soils of Hangzhou, China: relationship with different land uses. *Environmental Earth Sciences, 60*, 1481-1490.

Lucian, C. (2017). Characterization of particle size distribution in expansive soils using logarithmic density distribution. *International Journal of Engineering Trends and Technology, 4*(3)*,* 161-169.

Manta, D. S., Angelone, M., Bellanca, A., Neri, R., & Sprovieri, M. (2002). Heavy metals in urban soils: a case study from the city of Palermo (Sicily), Italy. *The Science of the Total Environment, 300*, 229-243.

Masood Khan, A., Yusoff, I., Abu Bakar, N. K., Abu Bakar, A. F., & Alias, Y. (2017). Erratum to: assessing anthropogenic levels, speciation, and potential mobility of rare earth elements (REEs) in ex-tin mining area. *Environmental Science and Pollution Research, 23*(24), 25039-25055.

Masto, R. E., Ram, L. C., Verma, S. K., Selvi, V. A., George, J., Tripathi, R. C., Srivastava, N. K., Mohanty, D., Jha, S. K., Sinha, A. K., & Sinha, A. (2011). Rare earth elements in soils of Jharia coalfield. *World Academy of Science, Engineering and Technology, 52,* 720-725.

Mat Ripin, S. N., Hasan, S., Kamal, M. L., & Mohd Hashim, N. S. (2014). Analysis and pollution assessment of heavy metal in soil, Perlis. *The Malaysian Journal of Analytical Sciences, 8*(1)*,* 155-161.

Maulana, A., Yonezu, K., & Watanabe, K. (2014). Geochemistry of rare earth elements (REE) in the weathered crusts from the granitic rocks in Sulawesi Island, Indonesia. *Journal of Earth Science, 3*(25), 460-472.

Mehr, M. R., Keshavarzi, B., Moore, F., Sharifi, R., Lahijanzadeh, A., & Kermani, M. (2017). Distribution, source identification and health risk assessment of soil heavy metals in urban areas of Isfahan Province, Iran. *Journal of African Earth Sciences, 132*, 16-26.

Meuser, H. (2010). *Contaminated urban soils.* Dordrecht: Springer.

Mirsal, I. A. (2008). *Soil pollution* (2nd ed.). Berlin: Springer Verlag.

Mohd Noor, H., Mohd Zainol, R., Ling, N. G., Mapjabil, J., Ismail, R., Ab Rahman, B., & Kumalah, M. J. (2015). Faktor budaya dan bukan budaya dalam mempengaruhi lawatan ulangan: kajian kes pelancong asing Pulau Pinang. *Malaysian Journal of Society and Space, 12*, 52-63.

Mohd Saad, F. N., Nik Abdul Rahman, N. N., Abdul Kadir, M. O., & Mohd Omar, F. (2000). Identification of pollution sources within the Sungai Pinang river basin. *Project Report Penang: Universiti Sains Malaysia, 1,* 478-485.

Müller, G. (1969). Index of geo-accumulation in sediments of the Rhine River. *GeoJournal, 2*, 108–118.

Mustafa, S., Marzuki, M., Ramli, R. S., Mapjabil, J., Zainal Abidin, M. K., & Yusoh, M. P. (2015). Pengurusan bandar warisan UNESCO dan penglibatan komuniti tempatan: kes kajian di George Town, Pulau Pinang. *Malaysian Journal of Society and Space, 12*, 87-99.

Nannoni, F., & Protano, G. (2016). Chemical and biological methods to evaluate the availability of heavy metals in soils of the Siena urban area (Italy). *Science of the Total Environment, 568*, 1-10.

Nezhad, M. T. K., Tali, M. G., Mahmoudi, M. H., & Pazira, E. (2011). Assessment of As and Cd contamination in topsoils of Northern Gorveh (Western Iran): role of parent material, land use and soil properties. *Environmental Earth Sciences, 64,* 1203-1213.

Ng, S. W. P., Chung, S. L., Robb, L. J., Searle, M. P., Ghani, A. A., Whitehouse, M. J., Oliver, G. J. H., Sone, M., Gardiner, N. J., & Roselee, M. H. (2015). Petrogenesis of Malaysian Granitoids in the Southeast Asian tin belt: Part 1. Geochemical and Sr-Nd isotopic characteristics. *Geological Society of America Bulletin, 127*(9-10), 1209-1237.

Noor Azhar, M. S., Kamaruzzaman B. Y., Rosnan Y., & Nor Antonina A. (2003). Speciation of Cu, Pb and Zn in sediments of Ibai Estuary, Kuala Terengganu, Malaysia. *Dimensions of Pollution, 2,* 43-52.

Ong, M. C., Fok, F. M., Sultan, K., & Joseph, B. (2016). Distribution of heavy metals and rare earth elements in the surface sediments of Penang river estuary, Malaysia. *Open Journal of Marine Science, 6*, 79-92.

Ong, M. C., Joseph, B., Shazili, N. A. M., Ghazali, A., & Mohamad, M. N. (2015). Heavy metals concentration in surficial sediments of Bidong Island, South China Sea off the East Coast of Peninsular Malaysia. *Asian Journal of Earth Sciences, 8,* 74-82.

Ong, M. C, Kamaruzzaman, B. Y., & Joseph, B. (2009). Geochemical studies of Setiu Lagoon, Terengganu, Malaysia. *Malaysian Journal of Science, 28*(2), 217–222.

Özkul, C. (2016). Heavy metal contamination in soils around the Tunçbilek Thermal Power Plant (Kütahya, Turkey). *Environmental Monitoring and Assessment, 188*(284), 1-12.

Pan, Y., & Li, H. (2015). Trace elements in scalp hair from potentially exposed individuals in the vicinity of the Bayan Obo mine in Baotou, China. *Environmental Toxicology and Pharmacology, 40*(3), 678-685.

Pansu, M., & Gautheyrou, J. (2006). *Handbook of soil analysis*. New York: Springer Heidelberg.

Paye, H. D. S., Mello, J. W. V. D., Mascarenhas, G. R. L. D. M., & Gasparon, M. (2016). Distribution and fractionation of the rare earth elements in Brazilian soils. *Journal of Geochemical Exploration, 161,* 27-41.

Pazand, K. (2015). Geochemical properties of rare earth elements (REE) in coals of Abyek coalfield, North Iran. *Arabian Journal of Geosciences, 8,* 4855-4862.

Pekey, H., Karakaş, D., Ayberk, S., Tolun, L., & Bakoğlu, M. (2004). Ecological risk assessment using trace elements from surface sediments of Izmit Bay (Northeastern Marmara Sea) Turkey. *Marine Pollution Bulletin, 48*, 946–953.

Polprasert, C. (1982). Heavy metal pollution in the Chao Phraya River estuary, Thailand. *Water Research, 6*(16), 775-784.

Pradhan, B., Chaudhari, A., Adinarayana, J., & Buchroithner (2012). Soil erosion assessment and its correlation with landslide events using remote sensing data and GIS: a case study at Penang Island, Malaysia. *Environmental Monitoring and Assessment, 184*, 715-727.

Qishlaqi, A., Moore, F., & Forghani, G. (2009). Characterization of metal pollution in soils under two landuse patterns in the Angouran region, NW Iran: a study based on multivariate data analysis. *Journal of Hazardous Materials, 172*, 372-384.

Ramanitharan, K., Steinberg, L., & Piringer, G. (2005). Geostatistical Modeling and Mapping of Sediment Contaminant Concentrations. In E. J. Calabrese, P. T. Kostecki & J. Dragun (Eds.), *Contaminated Soils, Sediments and Water* (pp. 565-583). Boston: Springer.

Ramos, S. J., Dinali, G. S., Oliveira, C., Martins, G. C., Moreira, C. G., Siqueira, J. O., & Guilherme, L. R. G. (2016). Rare earth elements in the soil environment. *Current Pollution Reports, 2*, 28-50.

Reimann, C., Filzmoser, C., & Garrett, R. G. (2005). Background and threshold: critical comparison of methods of determination. *Science of the Total Environment, 346*, 1-16.

Ren, L., Cohen, D. R., Rutherford, N. F., Zissimos, A. M., & Morisseau, E. G. (2015). Reflections of geological characteristics of Cyprus in soil rare earth element patterns. *Applied Geochemistry, 56*, 80-93.

Rodrigues, S., Urquhart, G., Hossack, I., Pereira, M. E., Duarte, A. C., Davidson, C., Hursthouse, A., Tucker, P., & Roberston, D. (2009). The influence of anthropogenic and natural geochemical factors on urban soil quality variability: a comparison between Glasgow, UK and Aveiro, Portugal. *Environmental Chemistry Letters, 7*, 141-148.

Rogan Šmuc, N., Dolenec, T., Serafimovski, T., Dolenec M., & Vrhovnik, P. (2012). Geochemical characteristics of rare earth elements (REEs) in the paddy soil and rice (*Oryza sativa L.*) system of Kocani Field, Republic of Macedonia. *Geoderma, 183-184*, 1-11.

Sadeghi, M., Morris, G. A., Carranza, E. J. M., Ladenberger, A., & Andersson, M. (2013). Rare earth element distribution and mineralization in Sweden: an application of principle component analysis to FOREGS soil geochemistry. *Journal of Geochemical Exploration, 133*, 160-175.

Shaari, H., Mohamad Azmi, S. N. H., Sultan, K., Bidai, J., & Mohamad, Y. (2015). Spatial distribution of selected heavy metalsin surface sediments of the EEZ of the east coast of Peninsular Malaysia. *International Journal of Oceanography, 618074,* 1-10.

Shamsuddin, S., Sulaiman, A. B., & Che Amat, R. (2012). Urban landscape factors that influenced the character of George Town, Penang UNESCO World Heritage Site. *Procedia- Social and Behavioral Sciences, 50*, 238-253.

Sherameti, I., & Varma, A. (Eds.). (2010). *Soil heavy metals*. Berlin: Springer Verlag.

Shi, J., Wang, H., Xu, J., Wu, J., Liu, X., Zhu, H., & Yu, C. (2007). Spatial distribution of heavy metals in soils: a case study of Changxing, China. *Environmental Geology, 52,* 1-10.

Shi, L. T., Wang, Z. Z., Zhao, H. G., Yu, X. M., Rui, L. P., & Guo, C. L. (2004). Distribution characteristics of rare earth elements in children's scalp hair from a rare earths mining area in southern China. *Journal of Environmental Science and Health, 39*(9), 2517-2532.

Silva, Y. J. A. B., Nascimento, C. W. A., Biondi, C. M., Straaten, P., Souza Júnior, V. S., Silva, Y. J. A. B., Santos, C. A., & Araújo, J. C. T. (2017). Influence of metaluminous granite mineralogy on the rare earth element geochemistry of rocks and soils along a climosequence in Brazil. *Geoderma, 306*, 28-39.

Simasuwannarong, B., Satapanajaru, T., Khuntong, S., & Pengthamkeerati, P. (2012). Spatial distribution and risk assessment of As, Cd, Cu, Pb, and Zn in topsoil at Rayong Province, Thailand. *Water, Air, & Soil Pollution, 223*, 1931-1943.

Skinner, B. J., Porter, S. C., & Park, J. (2004). *Dynamic earth: an introduction to physical geology* (5th ed.). United States: John Wiley & Sons.

Slavkovic´, L., Škrbic´, B., Miljevic´, N., & Onjia, A. (2004). Principle component analysis of trace elements in industrial soils. *Environmental Chemistry Letters, 2,* 105-108.

Sultan, K., & Noor Azhar, S. (2009). Rare earth elements in tropical surface water, soil and sediments of the Terengganu River Basin, Malaysia. *Journal of Rare Earths, 6*(27), 1072-1078.

Suntharalingam, T. (1984). Studies on the quartenary geology of Peninsular Malaysia. *Geological Society of Malaysia Warta Geologi, 10*, 101-110.

Tarbuck, E. J., & Lutgens, F. K. (2009). *Earth Science* (12th ed.). United States: Pearson Prentice Hall.

Tay, L. T., Alkhasawneh, M. S., Ngah, U. K., & Lateh, H. (2014). Landslide hazard mapping with new topographic factors: a study case of Penang Island, Malaysia. *Australian Journal of Basic and Applied Sciences, 8*(4), 387-392.

Town and Country Planning Department of Penang (DTCP). (2015). *Penang Annual Report 2015*. Retrieved from http://jpbd.penang.gov.my/index.php/en/

Turk, G. C., Yu, L. L., Salit, M. L., & Guthrie, W. F. (2001). Using inductively coupled plasma-mass spectrometry for calibration transfer between environmental CRMs. *Fresenius Journal of Analytical Chemistry, 370,* 259-263.

Unguraenu, T., Iancu, G. O., Pintilei, M., & Chicoș, M. M. (2016). Spatial distribution and geochemistry of heavy metals in soils: a case study from the NE area of Vaslui County, Romania. *Journal of Geochemical Exploration, 176*, 20-32.

United States Environmental Protection Agency (USEPA). (2010). *Contract laboratory program for national functional guidelines for inorganic data review*. Retrieved on 18 September 2017, from https://nepis.epa.gov/Exe/ZyNET.exe/ P1006PUX.TXT?ZyActionD=Zy Docum ent&Client=EPA&Index.

Voncken, J. H. L. (2016). *The rare earth elements*. Switzerland: Springer.

Wang, L., & Liang, T. (2015). Geochemical fractions of rare earth elements in soil around a mine tailing in Baotou, China. *Scientific Reports, 5*(12483), 1-11.

Wang, W., Lai, Y., Ma, Y., Liu, Z., Wang, S., & Hong, C. (2016). Heavy metal contamination of urban topsoil in a petrochemical industrial city in Xinjiang, China. *Journal of Arid Land, 8*(6), *871-880.*

Webster, R., & Oliver, M. A. (2001). *Geostatistics for environmental scientists*. United Kingdom: John Wiley & Sons.

Wei, B., & Yang, L. (2010). A review of heavy metal contaminations in urban soils, urban road dusts and agricultural soils from China. *Microchemical. Journal, 94*(2), 99-107.

Wong, C. S. C., Li, X., & Thornton, I. (2006). Urban environmental geochemistry of trace metals. *Environmental Pollution, 142*, 1-16.

Wu, C., & Ishihara, S. (1994). REE geochemistry of the Southern Thailand granites. *Journal of Asian Earth Sciences, 10*(1-2), 81-94.

Wu, C., & Zhang, L. (2010). Heavy metal concentrations and their possible sources in paddy soils of a modern agriculture zone, southeastern China. *Environmental Earth Sciences, 60*, 45-56.

Wubbeke, J. (2015). China's rare earth industry and end-use: supply security and innovation. In R. D. Kiggins (Ed.), *The political economy of REEs* (pp. 20- 42). United Kingdom: Macmillan Publishers Limited.

Yang, G. G., Yan, P. G., & Qin, L. (2016). Contamination, bioaccessibilty and human health risk of heavy metals in exposed-lawn soils from 28 urban parks in southern China's largest city, Guangzhou. *Applied Geochemistry, 67,* 52-58.

Yuan, Y., Cave, M., & Zhang, C. (2017). Using Local Moran's to identify contamination hotspots of rare earth elements in urban soils of London. *Applied Geochemistry, 83*, 1-12.

Yukselen, Y., & Kaya, A. (2008). Suitability of the methylene blue test for surface area, cation exchange capacity and swell potential determination of clayey soils. *Engineering Geology, 102,* 38-45.

Yusoff, Z., Ngwenya, B. T., & Parsons, I. (2013). Mobility and fractionation of REEs during deep weathering of geochemically contrasting granites in a tropical setting, Malaysia. *Chemical Geology, 349-350*, 71-86.

Zarcinas, B. A., Pongsakul, P., McLaughlin, M. J., & Cozens, G. (2004). Heavy metals in soils and crops in Southeast Asia. 2. Thailand. *Environmental Geochemistry and Health, 26*(4), 359-71.

Zhai, M., Kampunzu, H. A. B., Modisi, M. P., & Totolo, O. (2003). Distribution of heavy metals in Gaborone urban soils (Bostwana) and its relationship to soil pollution and bedrock composition. *Environmental Geology, 45*(2), 171-180.

Zhang, C., & McGrath, D. (2004). Geostatistical and GIS analyses on soil organic carbon concentrations in grassland of southeastern Ireland from two different periods. *Geoderma, 119*, 261–275.

Zhang, X., Zhong, T., Chen, D., Cheng, M., Liu, L., Zhang, X., & Li, X. (2016). Assessment of arsenic (As) occurrence in arable soil and its related health risk in China. *Environmental Geochemistry and Health, 38*(3), 691-702.

Zhengyi, H., Haneklaus, S., Sparovek, G., & Schnug, E. (2006). Rare earth elements in soils. *Communications in Soil Science and Plant Analysis, 37*(9-10), 1381-1420.

Zhengyu, B., Shengying, Q., & Yueming, H. (2006). Contamination and distribution of heavy metals in urban soil in Zhangzhou City, Fujian, China. *Chinese Journal of Geochemistry, 25*(1), 4-5.

Zhou, C. Y., Wong, M. K., Koh, L. L., & Wee, Y. C. (1997). Soil lead and other metal levels in industrial, residential and nature reserve areas in Singapore. *Environmental Monitoring and Assessment, 1-3*(44), 605-615.

Zong, Y., Xiao, Q., & Lu, S. (2016). Distribution, bioavailability, and leachability of heavy metals in soil particle size fractions of urban soils (northeastern China). *Environmental Science and Pollution Research, 23*(14), 14600-14607.

APPENDIX A: Soil samples description

Sample	Latitude	Longitude	Place	Land use	Geology (based on map)	color (munsell)	Soil type
1A	5.38611	100.2834	Bdr Baru Air Itam	Residential & business	Tanjung Bunga Granite	Hue 7.5 YR 6/3-4 dull brown to dull orange	granite residual soil
2A	5.37989	100.2621	Bukit Penara	forest	Batu Maung Granite	Hue 7.5 YR 6/3-8 Dull brown, dull orange to orange	granite residual soil
3A	5.39072	100.2624	Bukit Penara	forest	Tanjung Bunga Granite	Hue 7.5 YR 5/6-8 Bright Brown	granite residual soil
6	5.43747	100.2915	Botanical Garden	Residential & business	Tanjung Bunga Granite	Hue 10 YR 5/3-4 dull yellowish brown	granite residual soil
7A	5.45284	100.3037	Tg Tokong	Residential & business	Simpang Form.	Hue 2.5 Y 3/3 Dark olive brown	quartemary sediment
8A	5.45375	100.2923	Tg Bungah-Tg Tokong	Residential & business	Tanjung Bunga Granite	Hue 5YR 7/4 Dull orange	granite residual soil
9A	5.45959	100.2865	Tg Bungah	Residential & business	Beruas Form.	Hue 10 YR 5-7/4 Dull yellowish brown to dull yellow orange	granite residual soil
11A	5.47343	100.2577	Bt Feringghi	Residential & business	Feringghi Granite	Hue 5 YR 6/6 Orange	granite residual soil
12A	5.46742	100.2494	Bt Feringghi	Residential & business	Feringghi Granite	Hue 5 YR 7/3-6 Dull orange to orange	granite residual soil
13A	5.46225	100.2214	Teluk Bahang	Residential & business	Gula Form.	Hue 2.5 Y 4/1-2 Yellowish gray to dark greyish yellow	quartemary sediment
15A	5.44992	100.205	Teluk Bahang	Residential & business	Feringghi Granite	Hue 10YR 5/6-8 yellowish brown	quartemary sediment
16A	5.43328	100.221	Teluk Bahang Dam	forest	Feringghi Granite	Hue 10 YR 5/6 Yellowish Brown	granite residual soil
17A	5.394844	100.2159	Jalan Teluk Bahang	agriculture area	Gula Form.	Hue 7.5 YR 5/3-6 Dull to bright brown	quartemary sediment
18A	5.40952	100.1984	Pantai Acheh	Residential & business	Gula Form.	Hue 10 YR 4/3 dull yellowish brown	quartemary sediment
19A	5.399599	100.2133	Kg Batu Kecil, Balik Pulau	Residential & business	Gula Form.	Hue 10 YR 3/4 dark brown	quartemary sediment
21	5.34261	100.3032	Sg Nibong	Residential & business	Beruas Form.	Hue 5 YR 3/1-3 brownish black to dark reddish brown	quartemary sediment
23	5.31667	100.2679	Bayan Lepas	Residential & business	Batu Maung Granite	Hue 10 YR 5/3 Dull yellowish brown	quartemary sediment
25A	5.33789	100.2651	Bukit Relau	agriculture area	Batu Maung Granite	Hue 10 YR 5/4-8 dull yellowish brown to yellowish brown	granite residual soil
26A	5.33121	100.2773	Relau	Residential & business	Beruas Form.	Hue 10 YR 4-5/2 grayish yellow brown	quartemary sediment
27	5.32478	100.2993	Bayan Lepas	Industrial area	Gula Form.	Hue 10 YR 4/4 brown	quartemary sediment
28A	5.29625	100.2888	Bayan Lepas	Industrial area	undiff fill materials	Hue 10 YR 5-4/4 Dull yellowish brown to brown	quartemary sediment
29A	5.38436	100.3123	Jelutong	Residential & business	Tanjung Bunga Granite	Hue 10 YR 4/2 Grayish yellow brown	quartemary sediment
30A	5.415886	100.3435	Georgetown	Residential & business	Beruas Form.	Hue 7.5 YR 6/6-8 Orange	granite residual soil
33A	5.41	100.3201	Georgetown	Residential & business	Beruas Form.	Hue 10 YR 2/3 brownish black	quartemary sediment
35A	5.34222	100.2238	Lintang Sg Burung 2, Balik Pulau	Residential & business	Beruas Form.	Hue 7.5 YR 5/4-6 Dull to bright brown	granite residual soil
36A	5.346	100.2059	Balik Pulau	agriculture area	Gula Form.	Hue 10 YR 5/4 Dull yellowish brown	quartemary sediment
37A	5.35733	100.1993	Balik Pulau	agriculture area	Gula Form.	Hue 5 Y 4/2 Grayish olive	quartemary sediment
38A	5.31286	100.2949	Bayan Lepas	Industrial area	Gula Form.	Hue 10 YR 4/2 Grayish yellow brown	quartemary sediment
39A	5.29578	100.2681	Bayan Lepas	Airport	Beruas Form.	Hue 10 YR 5/4 dull yellowish brown (clay) & Hue 7.5 YR 2/2 brownish black(sand)	quartemary sediment
40A	5.417323	100.3121	Hosp.P.Pinang,Georgetown	Residential & business	Simpang Form.	Hue 10 YR 2/3 brownish black	quartemary sediment
41A	5.426306	100.2969	Georgetown	Residential & business	Tanjung Bunga Granite	Hue 10 YR 4/2 Grayish yellow brown	quartemary sediment

APPENDIX B: Soil physicochemical properties results.

Sample	pH	CEC (meq/100g)	Organic matter (%)	Clay (%)	Silt(%)	Sand (%)	Mean (phi)	median size (phi)	Kurtosis (phi)	standard deviation (phi)
1A	6.04	3.33	3.73	0.19	0.95	98.86	very coarse grained	sand	very platykurtic	well sorted
2A	8.22	3.32	5.41	0.27	1.14	98.58	very coarse grained	sand	very platykurtic	well sorted
3A	4.4	3.33	3.89	0.15	0.98	98.87	very coarse grained	sand	very platykurtic	well sorted
6	8.07	3.33	1.94	0.14	1.13	98.73	very coarse grained	sand	very platykurtic	well sorted
7A	5.78	3.32	3.31	0.31	2.13	97.56	very coarse grained	sand	very platykurtic	well sorted
8A	5.16	1.25	1.29	1.01	3.15	95.84	very coarse grained	sand	very platykurtic	well sorted
9A	5.52	3.32	2.57	0.29	1.46	98.25	very coarse grained	sand	very platykurtic	well sorted
11A	5.87	3.33	1.88	0.35	1.51	98.14	very coarse grained	sand	very platykurtic	well sorted
12A	7.93	3.32	1.36	0.27	1.34	98.39	very coarse grained	sand	very platykurtic	well sorted
13A	6.51	1.24	1.58	0.05	1.36	98.59	very coarse grained	sand	very platykurtic	well sorted
15A	6.49	3.33	1.9	0.14	0.79	99.07	very coarse grained	sand	very platykurtic	well sorted
16A	4.88	1.25	3.45	0.03	0.09	99.88	very coarse grained	sand	very platykurtic	well sorted
17A	7.15	3.33	4.31	0.24	1.37	98.39	very coarse grained	sand	very platykurtic	well sorted
18A	3.84	13.74	7.22	31.71	68.29	0.00	medium silt	silt	very platykurtic	very poorly sorted
19A	5.93	1.25	4.39	0.35	2.75	96.90	very coarse grained	sand	very platykurtic	well sorted
21	7.75	3.32	3.01	0.22	1.44	98.34	very coarse grained	sand	very platykurtic	well sorted
23	7.69	3.32	1.14	0.62	5.03	94.35	very coarse grained	sand	very platykurtic	well sorted
25A	4.65	2.49	3.57	0.25	1.23	98.52	very coarse grained	sand	very platykurtic	well sorted
26A	7.1	1.25	1.59	0.07	0.45	99.48	very coarse grained	sand	very platykurtic	well sorted
27	6.74	3.32	3.94	0.29	2.32	97.39	very coarse grained	sand	very platykurtic	well sorted
28A	7.12	3.32	1.62	0.16	0.74	99.10	very coarse grained	sand	very platykurtic	well sorted
29A	4.51	1.25	2.87	0.29	1.75	97.96	very coarse grained	sand	very platykurtic	well sorted
30A	7.36	3.33	1.95	0.08	0.47	99.45	very coarse grained	sand	very platykurtic	well sorted
33A	7.23	3.32	5.11	0.16	0.91	98.94	very coarse grained	sand	very platykurtic	well sorted
35A	5.51	1.25	2.48	0.45	1.94	97.61	very coarse grained	sand	very platykurtic	well sorted
36A	6.61	15.81	17.05	32.57	67.43	0.00	medium silt	silt	very platykurtic	very poorly sorted
37A	7.7	19.93	6.1	39.30	60.70	0.00	medium silt	silt	very platykurtic	very poorly sorted
38A	8.3	3.32	2.42	0.19	1.35	98.46	very coarse grained	sand	very platykurtic	well sorted
39A	7.02	3.33	3.14	0.29	1.80	97.91	very coarse grained	sand	very platykurtic	well sorted
40A	7.7	3.32	7.77	0.91	6.72	92.37	very coarse grained	sand	very platykurtic	well sorted
41A	7.72	3.32	1.69	0.41	2.96	96.62	very coarse grained	sand	very platykurtic	well sorted
9A (duplicate)	5.92	-	-	-	-	-				
8A (duplicate)	-	1.24	1.44	1.31	4.81	93.9				

APPENDIX C: Concentration level of heavy metals and REE results.

Sample	Ni (mg/Kg)	As (mg/Kg)	Cd (mg/Kg)	Pb (mg/Kg)	La (mg/Kg)	Ce (mg/Kg)	Nd (mg/Kg)	Eu (mg/Kg)	Tb (mg/Kg)	Dy (mg/Kg)	Er (mg/Kg)
1A	13.6	2942.1	4.6	164.5	49.4	111.0	41.2	5.86	6.23	9.34	6.96
2A	20.0	880.1	2.2	87.9	78.1	134.6	55.3	3.10	3.10	6.67	3.57
3A	13.0	1020.2	1.6	99.5	55.3	172.7	46.8	1.64	2.13	4.93	2.63
6	18.0	1014.9	1.8	141.5	124.8	298.0	115.3	1.82	3.83	14.94	8.01
7A	9.9	476.0	0.7	61.5	95.8	208.9	72.6	0.52	1.39	4.86	2.26
8A	104.5	404.5	4.7	81.2	75.5	252.0	61.5	0.69	1.38	6.56	3.11
9A	17.1	263.1	0.6	66.8	92.6	202.7	78.3	0.32	1.61	8.05	4.19
11A	8.1	312.0	0.6	2933.7	110.7	277.6	94.8	1.04	2.07	10.22	4.59
12A	12.0	225.3	0.3	100.0	85.2	191.4	75.8	0.77	1.54	7.56	3.40
13A	9.0	262.0	0.5	128.7	109.7	264.6	111.8	0.31	2.34	11.06	5.14
15A	12.4	522.6	0.7	62.8	74.9	181.4	75.6	0.14	1.44	6.49	2.60
16A	59.9	265.8	0.7	213.2	153.6	381.2	135.8	0.50	2.48	10.89	4.29
17A	6.5	428.4	0.3	83.6	46.4	120.7	38.9	0.31	0.77	3.70	1.54
18A	16.4	138.7	0.9	86.8	78.0	175.7	69.0	0.90	1.26	5.23	2.16
19A	8.7	150.1	0.5	113.5	128.8	285.8	111.5	0.73	2.19	9.65	4.19
21	10.7	228.8	0.9	107.1	40.8	116.8	36.6	0.60	1.20	6.46	3.75
23	8.7	267.7	0.7	68.2	86.5	186.3	81.3	0.83	2.17	10.83	4.50
25A	14.1	172.6	0.3	72.1	48.1	113.0	38.6	0.49	0.82	3.12	0.99
26A	17.1	190.9	1.7	160.9	78.6	166.4	70.3	0.78	1.56	7.51	3.13
27	12.9	135.4	0.3	134.9	78.2	116.5	70.6	1.41	1.84	9.75	4.66
28A	14.0	122.5	0.3	94.6	100.3	202.6	93.7	1.66	2.71	13.88	6.18
29A	1049.2	76.5	0.4	63.0	68.5	162.6	63.3	0.37	1.30	6.11	2.59
30A	25.8	180.9	0.3	146.2	218.9	602.3	201.9	2.82	4.07	20.50	10.17
33A	11.1	104.0	0.6	120.0	75.8	174.1	65.9	0.81	1.45	7.41	3.54
35A	6.5	76.6	0.3	106.1	100.8	165.3	98.8	2.89	4.26	24.20	12.63
36A	19.6	88.6	3.7	80.4	45.6	94.4	39.3	1.13	1.13	5.31	2.58
37A	19.5	67.9	0.2	42.1	34.0	70.1	28.8	0.94	0.79	3.62	2.04
38A	14.9	85.8	0.8	78.9	60.2	127.1	55.1	0.75	1.51	7.09	3.32
39A	12.6	77.9	0.6	116.0	51.7	144.3	46.1	0.89	1.63	8.59	4.30
40A	29.0	100.5	16.7	7019.6	38.5	88.9	33.3	0.48	0.80	3.69	1.92
41A	8.2	82.5	0.5	274.5	59.5	136.9	52.5	0.49	1.47	7.52	3.92
SRM (1)	39.9	84.9	3.0	185.4	23.8	51.4	25.6	0.99	0.66	3.78	1.97
SRM (2)	34.1	70.4	2.8	170.4	20.3	43.9	21.8	0.92	0.61	3.23	1.69
SRM (3)	39.3	85.7	3.0	183.1	24.2	51.9	25.1	1.07	0.76	3.65	1.98
SRM (4)	43.2	82.8	2.8	190.3	27.4	61.7	28.1	1.20	0.75	4.04	2.24
8A duplicate	76.9	211.4	4.1	141.3	57.2	198.8	47.8	0.52	1.04	5.35	2.42
13A duplicate	7.3	179.7	0.9	125.4	99.7	241.6	104.2	0.16	2.18	10.44	4.83
35A duplicate	5.6	87.1	0.2	103.0	97.6	160.4	96.6	2.74	4.11	23.74	12.18

APPENDIX D: Calibration plot of ICP-MS analysis.

Calibration - d:\sahar\221116.B\SAHA.C

=== Graph Detail ===

Step Mass Element ISTD Unit
(2) 60 Ni --- ppb

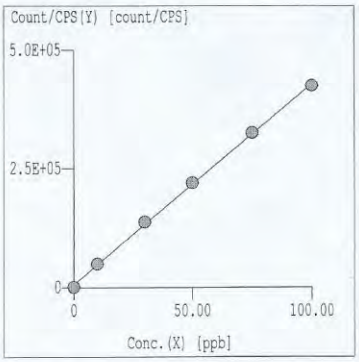

	Rjct	Conc	Calc Conc	CPS/Count	Ratio		RSD [%]
1		0.000	-1.389E+00	169.8	---	P	9.685
2		10.00	10.25	4.927E+04	---	P	5.160E-01
3		30.00	31.08	1.372E+05	---	P	9.564E-01
4		50.00	50.61	2.196E+05	---	P	3.426E-01
5		75.00	75.44	3.244E+05	---	P	9.171E-01
6		100.0	99.02	4.239E+05	---	P	3.157E-01
7		---	---	---	---		---
8		---	---	---	---		---
9		---	---	---	---		---
10		---	---	---	---		---
11		---	---	---	---		---
12		---	---	---	---		---
13		---	---	---	---		---
14		---	---	---	---		---
15		---	---	---	---		---
16		---	---	---	---		---
17		---	---	---	---		---
18		---	---	---	---		---
19		---	---	---	---		---
20		---	---	---	---		---

Curve Fit: Y=aX+b
r = 0.9997
Y = 4.220E+003*X +6.029E+003
X = 2.370E-004*Y -1.429E+000
DL = 1.169E-02 ppb
BEC = 1.429 ppb

Weight: OFF
Min Conc: 0.000

Step Mass Element ISTD Unit
(2) 75 As --- ppb

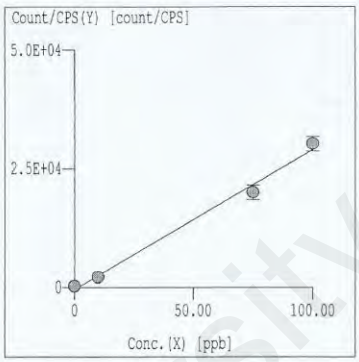

	Rjct	Conc	Calc Conc	CPS/Count	Ratio		RSD [%]
1		0.000	2.356	288.8	---	P	8.731
2		10.00	8.912	2218	---	P	8.338
3	ON	30.00	---	3.579E+04	---	P	1.681
4	ON	50.00	---	1.144E+04	---	P	7.883
5		75.00	69.49	2.005E+04	---	P	7.441
6		100.0	104.2	3.027E+04	---	P	5.045
7		---	---	---	---		---
8		---	---	---	---		---
9		---	---	---	---		---
10		---	---	---	---		---
11		---	---	---	---		---
12		---	---	---	---		---
13		---	---	---	---		---
14		---	---	---	---		---
15		---	---	---	---		---
16		---	---	---	---		---
17		---	---	---	---		---
18		---	---	---	---		---
19		---	---	---	---		---
20		---	---	---	---		---

Curve Fit: Y=aX+b
r = 0.9962
Y = 2.943E+002*X -4.045E+002
X = 3.398E-003*Y +1.375E+000
DL = 2.570E-01 ppb
BEC = -1.375E+00 ppb

Weight: OFF
Min Conc: 0.000

Calibration - d:\sahar\221116.B\SAHA.C

=== Graph Detail ===

Step Mass Element ISTD Unit
(1) 111 Cd --- ppb

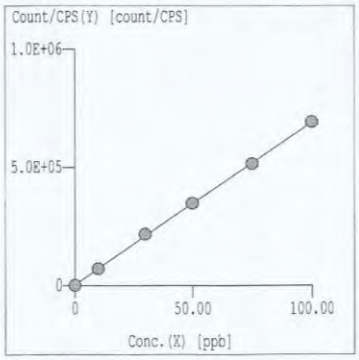

	Rjct	Conc	Calc Conc	CPS/Count	Ratio		RSD [%]
1		0.000	-3.746E-01	59.44	---	P	5.943
2		10.00	9.808	7.023E+04	---	P	4.945
3		30.00	30.95	2.159E+05	---	P	2.427
4		50.00	50.05	3.475E+05	---	P	2.110
5		75.00	74.44	5.156E+05	---	P	2.077
6		100.0	100.1	6.927E+05	---	P	1.664
7		---	---	---	---		---
8		---	---	---	---		---
9		---	---	---	---		---
10		---	---	---	---		---
11		---	---	---	---		---
12		---	---	---	---		---
13		---	---	---	---		---
14		---	---	---	---		---
15		---	---	---	---		---
16		---	---	---	---		---
17		---	---	---	---		---
18		---	---	---	---		---
19		---	---	---	---		---
20		---	---	---	---		---

Curve Fit: Y=aX+b
r = 0.9999
Y = 6.891E+003*X +2.641E+003
X = 1.451E-004*Y -3.832E-001
DL = 1.538E-03 ppb
BEC = 3.832E-01 ppb

Weight: OFF
Min Conc: 0.000

Step Mass Element ISTD Unit
(1) 139 La --- ppb

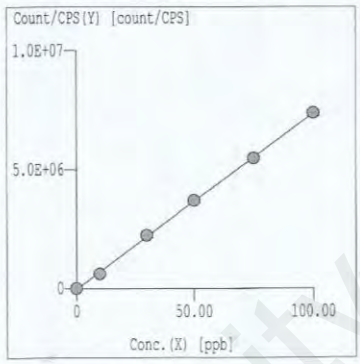

	Rjct	Conc	Calc Conc	CPS/Count	Ratio		RSD [%]
1		0.000	5.421E-01	22.22	---	P	67.64
2		10.00	8.812	6.130E+05	---	P	7.724
3		30.00	30.72	2.237E+06	---	A	4.659
4		50.00	50.32	3.690E+06	---	A	1.938
5		75.00	74.44	5.478E+06	---	A	1.138
6		100.0	100.2	7.383E+06	---	A	1.770
7		---	---	---	---		---
8		---	---	---	---		---
9		---	---	---	---		---
10		---	---	---	---		---
11		---	---	---	---		---
12		---	---	---	---		---
13		---	---	---	---		---
14		---	---	---	---		---
15		---	---	---	---		---
16		---	---	---	---		---
17		---	---	---	---		---
18		---	---	---	---		---
19		---	---	---	---		---
20		---	---	---	---		---

Curve Fit: Y=aX+b
r = 0.9998
Y = 7.412E+004*X -4.016E+004
X = 1.349E-005*Y +5.418E-001
DL = 6.084E-04 ppb
BEC = -5.418E-01 ppb

Weight: OFF
Min Conc: 0.000

Calibration - d:\sahar\221116.B\SAHA.C

=== Graph Detail ===

Step Mass Element (1) 140 Ce | ISTD --- | Unit ppb

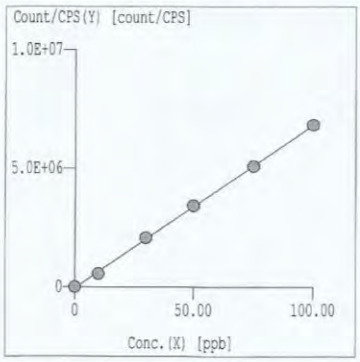

	Rjct	Conc	Calc Conc	CPS/Count	Ratio		RSD [%]
1		0.000	5.957E-01	51.11	---	P	16.41
2		10.00	8.673	5.558E+05	---	P	6.760
3		30.00	30.69	2.070E+06	---	A	4.609
4		50.00	50.41	3.427E+06	---	A	2.325
5		75.00	74.64	5.094E+06	---	A	1.813
6		100.0	99.99	6.838E+06	---	A	1.903
7		---	---	---	---		---
8		---	---	---	---		---
9		---	---	---	---		---
10		---	---	---	---		---
11		---	---	---	---		---
12		---	---	---	---		---
13		---	---	---	---		---
14		---	---	---	---		---
15		---	---	---	---		---
16		---	---	---	---		---
17		---	---	---	---		---
18		---	---	---	---		---
19		---	---	---	---		---
20		---	---	---	---		---

Curve Fit: Y=aX+b
r = 0.9998
Y = 6.880E+004*X -4.093E+004
X = 1.454E-005*Y +5.949E-001
DL = 3.658E-04 ppb
BEC = -5.949E-01 ppb

Weight: OFF
Min Conc: 0.000

Step Mass Element (1) 146 Nd | ISTD --- | Unit ppb

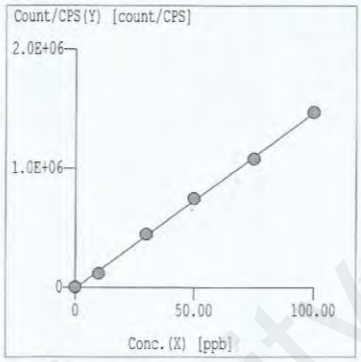

	Rjct	Conc	Calc Conc	CPS/Count	Ratio		RSD [%]
1		0.000	6.097E-01	27.78	---	P	13.86
2		10.00	8.378	1.146E+05	---	P	7.135
3		30.00	30.80	4.455E+05	---	P	3.794
4		50.00	51.15	7.457E+05	---	P	2.319
5		75.00	73.85	1.081E+06	---	A	1.794
6		100.0	100.2	1.470E+06	---	A	1.280
7		---	---	---	---		---
8		---	---	---	---		---
9		---	---	---	---		---
10		---	---	---	---		---
11		---	---	---	---		---
12		---	---	---	---		---
13		---	---	---	---		---
14		---	---	---	---		---
15		---	---	---	---		---
16		---	---	---	---		---
17		---	---	---	---		---
18		---	---	---	---		---
19		---	---	---	---		---
20		---	---	---	---		---

Curve Fit: Y=aX+b
r = 0.9996
Y = 1.475E+004*X -8.968E+003
X = 6.778E-005*Y +6.078E-001
DL = 7.826E-04 ppb
BEC = -6.078E-01 ppb

Weight: OFF
Min Conc: 0.000

Calibration - d:\sahar\221116.B\SAHA.C

=== Graph Detail ===

Step Mass Element (1) 159 Tb | ISTD --- | Unit ppb

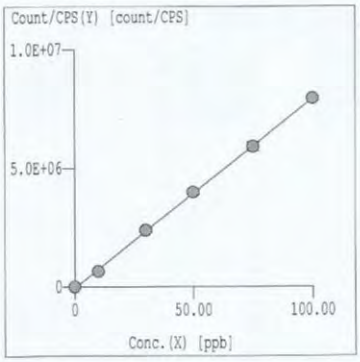

	Rjct	Conc	Calc Conc	CPS/Count	Ratio		RSD [%]
1		0.000	6.592E-01	17.78	---	P	43.30
2		10.00	8.822	6.532E+05	---	P	7.330
3		30.00	30.38	2.378E+06	---	A	3.770
4		50.00	50.45	3.984E+06	---	A	2.334
5		75.00	74.63	5.919E+06	---	A	3.225
6		100.0	100.1	7.953E+06	---	A	1.172
7		---	---	---	---		---
8		---	---	---	---		---
9		---	---	---	---		---
10		---	---	---	---		---
11		---	---	---	---		---
12		---	---	---	---		---
13		---	---	---	---		---
14		---	---	---	---		---
15		---	---	---	---		---
16		---	---	---	---		---
17		---	---	---	---		---
18		---	---	---	---		---
19		---	---	---	---		---
20		---	---	---	---		---

Curve Fit: Y=aX+b
r = 0.9998
Y = 8.001E+004*X -5.272E+004
X = 1.250E-005*Y +6.589E-001
DL = 2.886E-04 ppb
BEC = -6.589E-01 ppb

Weight: OFF
Min Conc: 0.000

Step Mass Element (1) 163 Dy | ISTD --- | Unit ppb

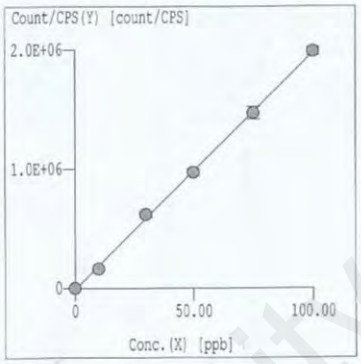

	Rjct	Conc	Calc Conc	CPS/Count	Ratio		RSD [%]
1		0.000	5.487E-01	18.89	---	P	10.19
2		10.00	8.677	1.619E+05	---	P	6.389
3		30.00	31.59	6.183E+05	---	P	3.616
4		50.00	49.33	9.717E+05	---	A	3.197
5		75.00	74.44	1.472E+06	---	A	3.522
6		100.0	100.4	1.989E+06	---	A	1.718
7		---	---	---	---		---
8		---	---	---	---		---
9		---	---	---	---		---
10		---	---	---	---		---
11		---	---	---	---		---
12		---	---	---	---		---
13		---	---	---	---		---
14		---	---	---	---		---
15		---	---	---	---		---
16		---	---	---	---		---
17		---	---	---	---		---
18		---	---	---	---		---
19		---	---	---	---		---
20		---	---	---	---		---

Curve Fit: Y=aX+b
r = 0.9996
Y = 1.992E+004*X -1.091E+004
X = 5.021E-005*Y +5.478E-001
DL = 2.899E-04 ppb
BEC = -5.478E-01 ppb

Weight: OFF
Min Conc: 0.000

Calibration - d:\sahar\221116.B\SAHA.C

=== Graph Detail ===

Step Mass Element ISTD Unit
(1) 166 Er --- ppb

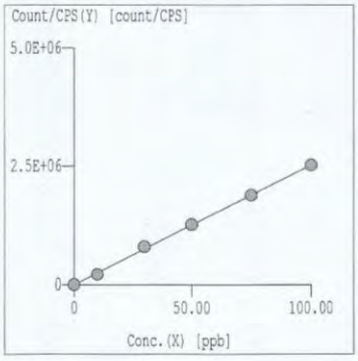

	Rjct	Conc	Calc Conc	CPS/Count	Ratio		RSD [%]
1		0.000	1.297E-01	15.56	---	P	49.49
2		10.00	8.583	2.141E+05	---	P	6.806
3		30.00	31.66	7.986E+05	---	P	4.294
4		50.00	50.08	1.265E+06	---	A	2.167
5		75.00	74.76	1.890E+06	---	A	2.086
6		100.0	99.78	2.523E+06	---	A	1.462
7		---	---	---	---		---
8		---	---	---	---		---
9		---	---	---	---		---
10		---	---	---	---		---
11		---	---	---	---		---
12		---	---	---	---		---
13		---	---	---	---		---
14		---	---	---	---		---
15		---	---	---	---		---
16		---	---	---	---		---
17		---	---	---	---		---
18		---	---	---	---		---
19		---	---	---	---		---
20		---	---	---	---		---

Curve Fit: Y=aX+b
r = 0.9997
Y = 2.532E+004*X -3.270E+003
X = 3.949E-005*Y +1.291E-001
DL = 9.120E-04 ppb
BEC = -1.291E-01 ppb

Weight: OFF
Min Conc: 0.000

Step Mass Element ISTD Unit
(1) 208 Pb --- ppb

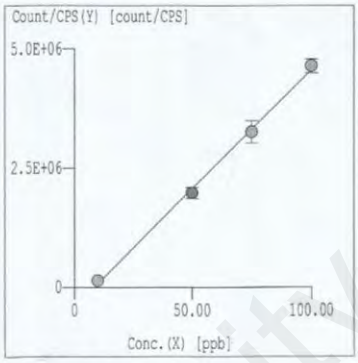

	Rjct	Conc	Calc Conc	CPS/Count	Ratio		RSD [%]
1	ON	0.000	---	1170	---	P	5.136
2		10.00	11.33	1.388E+05	---	P	8.943
3	ON	30.00	---	6.337E+05	---	P	15.36
4		50.00	48.20	1.982E+06	---	M	5.966
5		75.00	73.82	3.262E+06	---	A	7.241
6		100.0	101.7	4.654E+06	---	A	3.140
7		---	---	---	---		---
8		---	---	---	---		---
9		---	---	---	---		---
10		---	---	---	---		---
11		---	---	---	---		---
12		---	---	---	---		---
13		---	---	---	---		---
14		---	---	---	---		---
15		---	---	---	---		---
16		---	---	---	---		---
17		---	---	---	---		---
18		---	---	---	---		---
19		---	---	---	---		---
20		---	---	---	---		---

Curve Fit: Y=aX+b
r = 0.9990
Y = 4.999E+004*X -4.274E+005
X = 2.001E-005*Y +8.550E+000
DL = --- ppb
BEC = -8.550E+00 ppb

Weight: OFF
Min Conc: 0.000

Calibration - d:\sahar\221116.B\SAHA.C

=== Graph Detail ===

Step	Mass	Element	ISTD	Unit
(1)	153	Eu	---	ppb

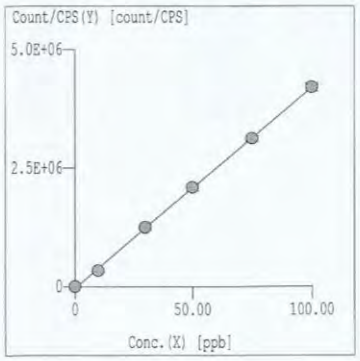

	Rjct	Conc	Calc Conc	CPS/Count	Ratio		RSD [%]
1		0.000	8.980E-01	18.89	---	P	53.91
2		10.00	8.783	3.342E+05	---	P	7.206
3		30.00	30.18	1.241E+06	---	A	4.743
4		50.00	50.27	2.093E+06	---	A	3.323
5		75.00	74.72	3.129E+06	---	A	1.913
6		100.0	100.1	4.206E+06	---	A	2.051
7		---	---	---	---		---
8		---	---	---	---		---
9		---	---	---	---		---
10		---	---	---	---		---
11		---	---	---	---		---
12		---	---	---	---		---
13		---	---	---	---		---
14		---	---	---	---		---
15		---	---	---	---		---
16		---	---	---	---		---
17		---	---	---	---		---
18		---	---	---	---		---
19		---	---	---	---		---
20		---	---	---	---		---

Curve Fit: Y=aX+b
r = 0.9998
Y = 4.238E+004*X -3.804E+004
X = 2.359E-005*Y +8.976E-001
DL = 7.208E-04 ppb
BEC = -8.976E-01 ppb

Weight: OFF
Min Conc: 0.000

APPENDIX E: Contamination factor (CF) assessment results.

Sample	As (mg/Kg)	Pb (mg/Kg)	La (mg/Kg)	Ce (mg/Kg)	Nd (mg/Kg)	Eu (mg/Kg)	Tb (mg/Kg)	Dy (mg/Kg)	Er (mg/Kg)	Ni (mg/Kg)	Cd (mg/Kg)
1A	4.25	0.90	0.37	0.34	0.31	3.01	2.11	0.68	1.08	0.46	1.87
2A	1.27	0.48	0.58	0.41	0.42	1.59	1.05	0.48	0.55	0.68	0.89
3A	1.47	0.55	0.41	0.52	0.35	0.84	0.72	0.36	0.41	0.44	0.67
6A	1.47	0.78	0.92	0.90	0.87	0.93	1.30	1.08	1.24	0.61	0.74
7A	0.69	0.34	0.71	0.63	0.55	0.27	0.47	0.35	0.35	0.34	0.28
8A	0.58	0.45	0.56	0.76	0.47	0.35	0.47	0.48	0.48	3.54	1.90
9A	0.38	0.37	0.69	0.61	0.59	0.17	0.55	0.58	0.65	0.58	0.26
11A	0.45	16.12	0.82	0.84	0.72	0.53	0.70	0.74	0.71	0.28	0.24
12A	0.33	0.55	0.63	0.58	0.57	0.40	0.52	0.55	0.53	0.41	0.13
13A	0.38	0.71	0.81	0.80	0.85	0.16	0.79	0.80	0.80	0.31	0.19
15A	0.76	0.34	0.56	0.55	0.57	0.07	0.49	0.47	0.40	0.42	0.29
16A	0.38	1.17	1.14	1.15	1.03	0.25	0.84	0.79	0.66	2.03	0.27
17A	0.62	0.46	0.34	0.36	0.29	0.16	0.26	0.27	0.24	0.22	0.13
18A	0.20	0.48	0.58	0.53	0.52	0.46	0.43	0.38	0.33	0.56	0.37
19A	0.22	0.62	0.95	0.86	0.85	0.37	0.74	0.70	0.65	0.30	0.22
21A	0.33	0.59	0.30	0.35	0.28	0.31	0.41	0.47	0.58	0.36	0.37
23A	0.39	0.37	0.64	0.56	0.62	0.43	0.73	0.79	0.70	0.29	0.27
25A	0.25	0.40	0.36	0.34	0.29	0.25	0.28	0.23	0.15	0.48	0.13
26A	0.28	0.88	0.58	0.50	0.53	0.40	0.53	0.54	0.48	0.58	0.70
27A	0.20	0.74	0.58	0.35	0.54	0.72	0.62	0.71	0.72	0.44	0.12
28A	0.18	0.52	0.74	0.61	0.71	0.85	0.92	1.01	0.96	0.48	0.12
29A	0.11	0.35	0.51	0.49	0.48	0.19	0.44	0.44	0.40	35.56	0.15
30A	0.26	0.80	1.62	1.82	1.53	1.44	1.38	1.49	1.57	0.87	0.13
33A	0.15	0.66	0.56	0.53	0.50	0.41	0.49	0.54	0.55	0.38	0.26
35A	0.11	0.58	0.75	0.50	0.75	1.48	1.44	1.75	1.96	0.22	0.12
36A	0.13	0.44	0.34	0.28	0.30	0.58	0.38	0.39	0.40	0.67	1.51
37A	0.10	0.23	0.25	0.21	0.22	0.48	0.27	0.26	0.32	0.66	0.06
38A	0.12	0.43	0.45	0.38	0.42	0.39	0.51	0.51	0.51	0.51	0.31
39A	0.11	0.64	0.38	0.44	0.35	0.46	0.55	0.62	0.67	0.43	0.24
40A	0.15	38.58	0.29	0.27	0.25	0.25	0.27	0.27	0.30	0.98	6.80
41A	0.12	1.51	0.44	0.41	0.40	0.25	0.50	0.54	0.61	0.28	0.20

APPENDIX F: Geo-accumulation index (I_{geo}) assessment results.

Sample	As (mg/Kg)	Pb (mg/Kg)	La (mg/Kg)	Ce (mg/Kg)	Nd (mg/Kg)	Eu (mg/Kg)	Tb (mg/Kg)	Dy (mg/Kg)	Er (mg/Kg)	Ni (mg/Kg)	Cd (mg/Kg)
1A	1.50	-0.73	-2.03	-2.16	-2.26	1.00	0.49	-1.15	-0.48	-1.71	0.32
2A	-0.24	-1.63	-1.37	-1.88	-1.84	0.08	-0.51	-1.63	-1.44	-1.15	-0.76
3A	-0.02	-1.46	-1.87	-1.52	-2.08	-0.83	-1.05	-2.07	-1.88	-1.77	-1.16
6A	-0.03	-0.95	-0.70	-0.74	-0.78	-0.68	-0.21	-0.47	-0.27	-1.30	-1.01
7A	-1.12	-2.15	-1.08	-1.25	-1.45	-2.49	-1.67	-2.09	-2.10	-2.16	-2.40
8A	-1.36	-1.75	-1.42	-0.98	-1.69	-2.08	-1.68	-1.66	-1.64	1.24	0.34
9A	-1.98	-2.03	-1.13	-1.29	-1.34	-3.18	-1.46	-1.36	-1.21	-1.37	-2.51
11A	-1.73	3.43	-0.87	-0.84	-1.06	-1.50	-1.09	-1.02	-1.08	-2.44	-2.63
12A	-2.20	-1.45	-1.25	-1.38	-1.38	-1.92	-1.52	-1.45	-1.51	-1.88	-3.57
13A	-1.99	-1.09	-0.88	-0.91	-0.82	-3.23	-0.92	-0.90	-0.91	-2.29	-2.98
15A	-0.99	-2.12	-1.43	-1.45	-1.39	-4.34	-1.62	-1.67	-1.90	-1.83	-2.35
16A	-1.96	-0.36	-0.40	-0.38	-0.54	-2.56	-0.84	-0.93	-1.18	0.44	-2.48
17A	-1.28	-1.71	-2.12	-2.04	-2.35	-3.24	-2.52	-2.48	-2.65	-2.77	-3.57
18A	-2.90	-1.65	-1.37	-1.50	-1.52	-1.70	-1.81	-1.99	-2.16	-1.43	-2.03
19A	-2.79	-1.27	-0.65	-0.80	-0.83	-2.01	-1.02	-1.10	-1.21	-2.34	-2.75
21A	-2.18	-1.35	-2.31	-2.09	-2.43	-2.28	-1.88	-1.68	-1.37	-2.05	-2.03
23A	-1.95	-2.00	-1.23	-1.41	-1.28	-1.81	-1.03	-0.93	-1.11	-2.35	-2.46
25A	-2.59	-1.92	-2.07	-2.14	-2.36	-2.57	-2.43	-2.73	-3.30	-1.65	-3.48
26A	-2.44	-0.76	-1.37	-1.58	-1.49	-1.90	-1.50	-1.46	-1.63	-1.38	-1.09
27A	-2.94	-1.02	-1.37	-2.09	-1.49	-1.05	-1.27	-1.09	-1.06	-1.78	-3.70
28A	-3.08	-1.53	-1.01	-1.29	-1.08	-0.82	-0.70	-0.58	-0.65	-1.66	-3.61
29A	-3.76	-2.12	-1.56	-1.61	-1.64	-2.98	-1.77	-1.76	-1.90	4.57	-3.31
30A	-2.52	-0.90	0.11	0.28	0.03	-0.05	-0.12	-0.01	0.07	-0.78	-3.55
33A	-3.32	-1.19	-1.42	-1.51	-1.59	-1.86	-1.61	-1.48	-1.45	-1.99	-2.51
35A	-3.76	-1.36	-1.01	-1.59	-1.00	-0.02	-0.05	0.23	0.38	-2.76	-3.59
36A	-3.55	-1.76	-2.15	-2.40	-2.33	-1.38	-1.97	-1.96	-1.91	-1.17	0.01
37A	-3.93	-2.70	-2.57	-2.82	-2.78	-1.63	-2.49	-2.52	-2.25	-1.18	-4.55
38A	-3.60	-1.79	-1.75	-1.97	-1.84	-1.96	-1.55	-1.55	-1.55	-1.57	-2.28
39A	-3.74	-1.23	-1.97	-1.78	-2.10	-1.72	-1.44	-1.27	-1.17	-1.81	-2.63
40A	-3.37	4.68	-2.40	-2.48	-2.57	-2.61	-2.47	-2.49	-2.33	-0.61	2.18
41A	-3.65	0.01	-1.77	-1.86	-1.91	-2.58	-1.59	-1.46	-1.31	-2.44	-2.91

APPENDIX G: Contamination index (CI) assessment results.

Sample	As (mg/Kg)	Pb (mg/Kg)	La (mg/Kg)	Ce (mg/Kg)	Nd (mg/Kg)	Eu (mg/Kg)	Tb (mg/Kg)	Dy (mg/Kg)	Er (mg/Kg)	Ni (mg/Kg)	Cd (mg/Kg)
1A	5.76	0.17	-1.67	-1.83	-1.95	4.01	2.60	-0.47	0.60	-1.25	2.19
2A	1.03	-1.15	-0.79	-1.48	-1.42	1.67	0.54	-1.15	-0.89	-0.47	0.13
3A	1.45	-0.91	-1.46	-1.00	-1.72	0.01	-0.33	-1.71	-1.48	-1.33	-0.49
6A	1.43	-0.17	0.23	0.16	0.10	0.25	1.09	0.61	0.97	-0.68	-0.27
7A	-0.44	-1.81	-0.37	-0.62	-0.90	-2.22	-1.20	-1.74	-1.75	-1.83	-2.12
8A	-0.77	-1.30	-0.86	-0.22	-1.22	-1.73	-1.21	-1.18	-1.16	4.78	2.25
9A	-1.60	-1.66	-0.44	-0.68	-0.74	-3.02	-0.91	-0.78	-0.56	-0.80	-2.25
11A	-1.28	19.55	-0.05	0.00	-0.34	-0.96	-0.39	-0.28	-0.37	-2.17	-2.39
12A	-1.88	-0.90	-0.62	-0.80	-0.81	-1.53	-1.00	-0.90	-0.99	-1.47	-3.45
13A	-1.61	-0.38	-0.07	-0.11	0.03	-3.07	-0.13	-0.10	-0.12	-1.99	-2.78
15A	-0.23	-1.78	-0.88	-0.91	-0.81	-4.27	-1.13	-1.20	-1.50	-1.41	-2.05
16A	-1.58	0.82	0.74	0.77	0.49	-2.31	0.00	-0.14	-0.51	2.47	-2.21
17A	-0.66	-1.25	-1.78	-1.68	-2.05	-3.09	-2.26	-2.21	-2.41	-2.55	-3.45
18A	-2.70	-1.17	-0.80	-0.97	-1.00	-1.24	-1.38	-1.61	-1.83	-0.88	-1.66
19A	-2.57	-0.64	0.30	0.07	0.02	-1.63	-0.28	-0.40	-0.56	-2.04	-2.53
21A	-1.85	-0.76	-2.01	-1.74	-2.15	-1.98	-1.47	-1.21	-0.79	-1.69	-1.66
23A	-1.57	-1.63	-0.58	-0.85	-0.66	-1.38	-0.30	-0.15	-0.41	-2.06	-2.19
25A	-2.34	-1.52	-1.72	-1.80	-2.06	-2.32	-2.15	-2.50	-3.15	-1.17	-3.35
26A	-2.17	0.12	-0.78	-1.08	-0.96	-1.50	-0.97	-0.92	-1.15	-0.80	-0.39
27A	-2.74	-0.28	-0.79	-1.74	-0.95	-0.33	-0.65	-0.38	-0.33	-1.35	-3.59
28A	-2.91	-1.01	-0.27	-0.68	-0.37	0.03	0.22	0.43	0.31	-1.18	-3.48
29A	-3.65	-1.77	-1.05	-1.12	-1.16	-2.79	-1.33	-1.32	-1.50	40.12	-3.16
30A	-2.26	-0.10	1.74	2.10	1.56	1.39	1.26	1.47	1.64	0.10	-3.43
33A	-3.17	-0.53	-0.85	-0.99	-1.09	-1.45	-1.12	-0.95	-0.90	-1.62	-2.25
35A	-3.65	-0.78	-0.26	-1.09	-0.25	1.47	1.39	1.98	2.34	-2.54	-3.47
36A	-3.42	-1.32	-1.81	-2.11	-2.03	-0.80	-1.59	-1.58	-1.51	-0.51	1.52
37A	-3.84	-2.46	-2.32	-2.61	-2.56	-1.15	-2.23	-2.25	-1.93	-0.52	-4.48
38A	-3.47	-1.36	-1.30	-1.58	-1.43	-1.57	-1.04	-1.03	-1.03	-1.06	-1.98
39A	-3.62	-0.60	-1.59	-1.35	-1.75	-1.26	-0.89	-0.65	-0.51	-1.39	-2.39
40A	-3.22	43.26	-2.11	-2.21	-2.32	-2.36	-2.19	-2.22	-2.04	0.37	8.98
41A	-3.53	1.52	-1.33	-1.45	-1.52	-2.33	-1.09	-0.92	-0.70	-2.16	-2.71